

Nelms, Mark “Power Electronics”
The Electric Power Engineering Handbook
Ed. L.L. Grigsby
Boca Raton: CRC Press LLC, 2001

14

Power Electronics

Mark Nelms

Auburn University

14.1 Power Semiconductor Devices *Kaushik Rajashekara*

14.2 Uncontrolled and Controlled Rectifiers *Mahesh M. Swamy*

14.3 Inverters *Michael Giesselmann*

14.4 Active Filters for Power Conditioning *Hirofumi Akagi*

14

Power Electronics

Kaushik Rajashekara
Delphi Automotive Systems

Mahesh M. Swamy
Yaskawa Electric America

Michael Giesselmann
Texas Tech University

Hirofumi Akagi
Tokyo Institute of Technology

14.1 Power Semiconductor Devices

Thyristor and Triac • Gate Turn-Off Thyristor (GTO) • Reverse-Conducting Thyristor (RCT) and Asymmetrical Silicon-Controlled Rectifier (ASCR) • Power Transistor • Power MOSFET • Insulated-Gate Bipolar Transistor • MOS-Controlled Thyristor (MCT)

14.2 Uncontrolled and Controlled Rectifiers

Uncontrolled Rectifiers • Controlled Rectifiers • Conclusion

14.3 Inverters

Fundamental Issues • Single Phase Inverters • Three Phase Inverters • Multilevel Inverters • Line Commutated Inverters

14.4 Active Filters for Power Conditioning

Harmonic-Producing Loads • Theoretical Approach to Active Filters for Power Conditioning • Classification of Active Filters • Integrated Series Active Filters • Practical Applications of Active Filters for Power Conditioning

14.1 Power Semiconductor Devices

Kaushik Rajashekara

The modern age of power electronics began with the introduction of thyristors in the late 1950s. Now there are several types of power devices available for high-power and high-frequency applications. The most notable power devices are gate turn-off thyristors, power Darlington transistors, power MOSFETs, and insulated-gate bipolar transistors (IGBTs). Power semiconductor devices are the most important functional elements in all power conversion applications. The power devices are mainly used as switches to convert power from one form to another. They are used in motor control systems, uninterrupted power supplies, high-voltage DC transmission, power supplies, induction heating, and in many other power conversion applications. A review of the basic characteristics of these power devices is presented in this section.

Thyristor and Triac

The thyristor, also called a silicon-controlled rectifier (SCR), is basically a four-layer three-junction *pnpn* device. It has three terminals: anode, cathode, and gate. The device is turned on by applying a short pulse across the gate and cathode. Once the device turns on, the gate loses its control to turn off the device. The turn-off is achieved by applying a reverse voltage across the anode and cathode. The thyristor symbol and its volt-ampere characteristics are shown in Fig. 14.1. There are basically two classifications of thyristors: converter grade and inverter grade. The difference between a converter-grade and an inverter-grade thyristor is the low turn-off time (on the order of a few microseconds) for the latter. The converter-grade thyristors are slow type and are used in natural commutation (or phase-controlled) applications. Inverter-grade thyristors are used in forced commutation applications such as DC-DC choppers and

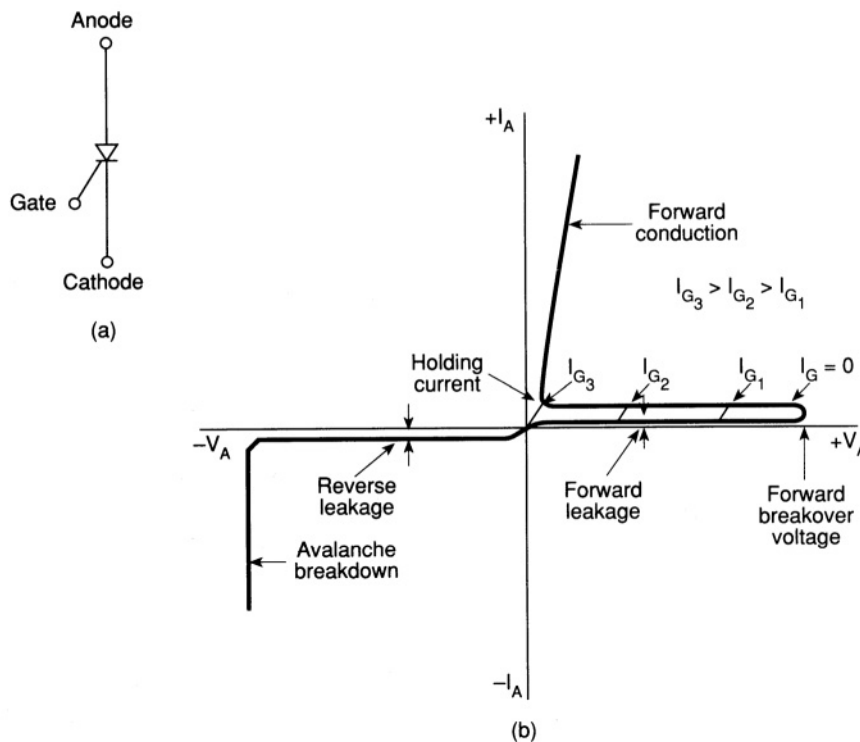


FIGURE 14.1 (a) Thyristor symbol and (b) volt-ampere characteristics. (Source: B.K. Bose, *Modern Power Electronics: Evaluation, Technology, and Applications*, p. 5. © 1992 IEEE.)

DC-AC inverters. The inverter-grade thyristors are turned off by forcing the current to zero using an external commutation circuit. This requires additional commutating components, thus resulting in additional losses in the inverter.

Thyristors are highly rugged devices in terms of transient currents, di/dt , and dv/dt capability. The forward voltage drop in thyristors is about 1.5 to 2 V, and even at higher currents of the order of 1000 A, it seldom exceeds 3 V. While the forward voltage determines the on-state power loss of the device at any given current, the switching power loss becomes a dominating factor affecting the device junction temperature at high operating frequencies. Because of this, the maximum switching frequencies possible using thyristors are limited in comparison with other power devices considered in this section.

Thyristors have I^2t withstand capability and can be protected by fuses. The nonrepetitive surge current capability for thyristors is about 10 times their rated root mean square (rms) current. They must be protected by snubber networks for dv/dt and di/dt effects. If the specified dv/dt is exceeded, thyristors may start conducting without applying a gate pulse. In DC-to-AC conversion applications, it is necessary to use an antiparallel diode of similar rating across each main thyristor. Thyristors are available up to 6000 V, 3500 A.

A triac is functionally a pair of converter-grade thyristors connected in antiparallel. The triac symbol and volt-ampere characteristics are shown in Fig. 14.2. Because of the integration, the triac has poor reapplied dv/dt , poor gate current sensitivity at turn-on, and longer turn-off time. Triacs are mainly used in phase control applications such as in AC regulators for lighting and fan control and in solid-state AC relays.

Gate Turn-Off Thyristor (GTO)

The GTO is a power switching device that can be turned on by a short pulse of gate current and turned off by a reverse gate pulse. This reverse gate current amplitude is dependent on the anode current to be turned off. Hence there is no need for an external commutation circuit to turn it off. Because turn-off

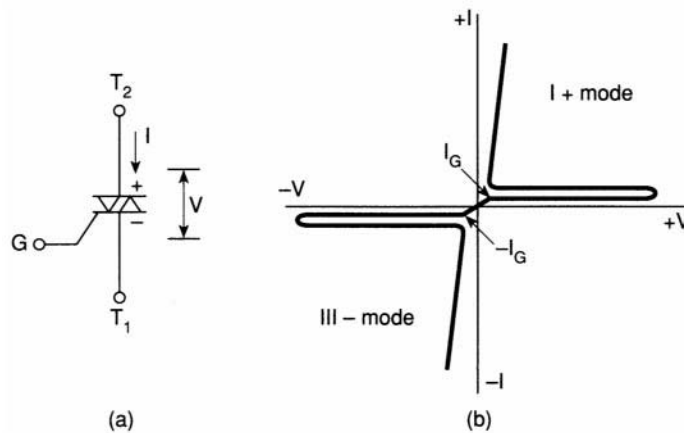


FIGURE 14.2 (a) Triac symbol and (b) volt-ampere characteristics. (Source: B.K. Bose, *Modern Power Electronics: Evaluation, Technology, and Applications*, p. 5. © 1992 IEEE.)

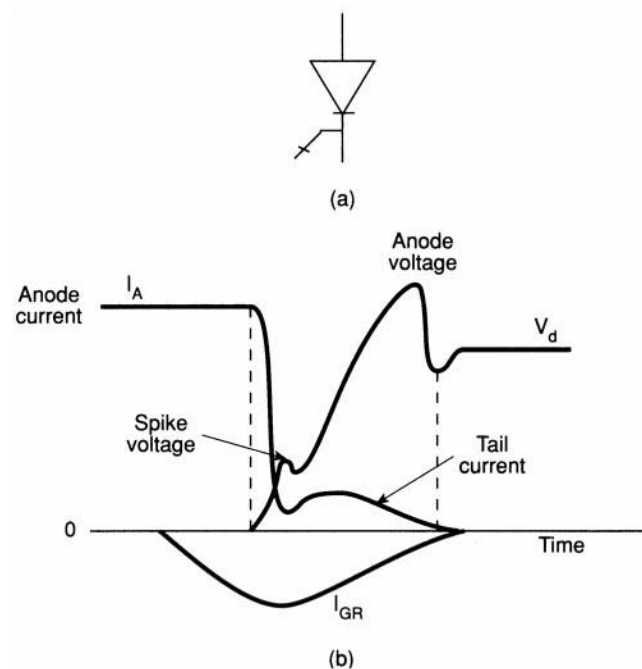


FIGURE 14.3 (a) GTO symbol and (b) turn-off characteristics. (Source: B.K. Bose, *Modern Power Electronics: Evaluation, Technology, and Applications*, p. 5. © 1992 IEEE.)

is provided by bypassing carriers directly to the gate circuit, its turn-off time is short, thus giving it more capability for high-frequency operation than thyristors. The GTO symbol and turn-off characteristics are shown in Fig. 14.3.

GTOs have the Pt withstand capability and hence can be protected by semiconductor fuses. For reliable operation of GTOs, the critical aspects are proper design of the gate turn-off circuit and the snubber circuit. A GTO has a poor turn-off current gain of the order of 4 to 5. For example, a 2000-A peak current GTO may require as high as 500 A of reverse gate current. Also, a GTO has the tendency to latch at temperatures above 125°C. GTOs are available up to about 4500 V, 2500 A.

Reverse-Conducting Thyristor (RCT) and Asymmetrical Silicon-Controlled Rectifier (ASCR)

Normally in inverter applications, a diode in antiparallel is connected to the thyristor for commutation/freewheeling purposes. In RCTs, the diode is integrated with a fast switching thyristor in a single silicon chip. Thus, the number of power devices could be reduced. This integration brings forth a substantial improvement of the static and dynamic characteristics as well as its overall circuit performance.

The RCTs are designed mainly for specific applications such as traction drives. The antiparallel diode limits the reverse voltage across the thyristor to 1 to 2 V. Also, because of the reverse recovery behavior of the diodes, the thyristor may see very high reapplied dv/dt when the diode recovers from its reverse voltage. This necessitates use of large RC snubber networks to suppress voltage transients. As the range of application of thyristors and diodes extends into higher frequencies, their reverse recovery charge becomes increasingly important. High reverse recovery charge results in high power dissipation during switching.

The ASCR has similar forward blocking capability to an inverter-grade thyristor, but it has a limited reverse blocking (about 20–30 V) capability. It has an on-state voltage drop of about 25% less than an inverter-grade thyristor of a similar rating. The ASCR features a fast turn-off time; thus it can work at a higher frequency than an SCR. Since the turn-off time is down by a factor of nearly 2, the size of the commutating components can be halved. Because of this, the switching losses will also be low.

Gate-assisted turn-off techniques are used to even further reduce the turn-off time of an ASCR. The application of a negative voltage to the gate during turn-off helps to evacuate stored charge in the device and aids the recovery mechanisms. This will, in effect, reduce the turn-off time by a factor of up to 2 over the conventional device.

Power Transistor

Power transistors are used in applications ranging from a few to several hundred kilowatts and switching frequencies up to about 10 kHz. Power transistors used in power conversion applications are generally npn type. The power transistor is turned on by supplying sufficient base current, and this base drive has to be maintained throughout its conduction period. It is turned off by removing the base drive and making the base voltage slightly negative (within $-V_{BE(max)}$). The saturation voltage of the device is normally 0.5 to 2.5 V and increases as the current increases. Hence, the on-state losses increase more than proportionately with current. The transistor off-state losses are much lower than the on-state losses because the leakage current of the device is of the order of a few milliamperes. Because of relatively larger switching times, the switching loss significantly increases with switching frequency. Power transistors can block only forward voltages. The reverse peak voltage rating of these devices is as low as 5 to 10 V.

Power transistors do not have Pt withstand capability. In other words, they can absorb only very little energy before breakdown. Therefore, they cannot be protected by semiconductor fuses, and thus an electronic protection method has to be used.

To eliminate high base current requirements, Darlington configurations are commonly used. They are available in monolithic or in isolated packages. The basic Darlington configuration is shown schematically in Fig. 14.4. The Darlington configuration presents a specific advantage in that it can considerably increase the current switched by the transistor for a given base drive. The $V_{CE(sat)}$ for the Darlington is generally more than that of a single transistor of similar rating with corresponding increase in on-state power loss. During switching, the reverse-biased collector junction may show hot-spot breakdown effects that are specified by reverse-bias safe operating area (RBSOA) and

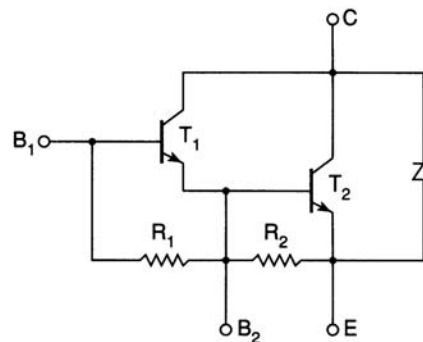


FIGURE 14.4 A two-stage Darlington transistor with bypass diode. (Source: B.K. Bose, *Modern Power Electronics: Evaluation, Technology, and Applications*, p. 6. © 1992 IEEE.)

forward-bias safe operating area (FBSOA). Modern devices with highly interdigitated emitter base geometry force more uniform current distribution and therefore considerably improve secondary breakdown effects. Normally, a well-designed switching aid network constrains the device operation well within the SOAs.

Power MOSFET

Power MOSFETs are marketed by different manufacturers with differences in internal geometry and with different names such as MegaMOS, HEXFET, SIPMOS, and TMOS. They have unique features that make them potentially attractive for switching applications. They are essentially voltage-driven rather than current-driven devices, unlike bipolar transistors.

The gate of a MOSFET is isolated electrically from the source by a layer of silicon oxide. The gate draws only a minute leakage current on the order of nanoamperes. Hence, the gate drive circuit is simple and power loss in the gate control circuit is practically negligible. Although in steady state the gate draws virtually no current, this is not so under transient conditions. The gate-to-source and gate-to-drain capacitances have to be charged and discharged appropriately to obtain the desired switching speed, and the drive circuit must have a sufficiently low output impedance to supply the required charging and discharging currents. The circuit symbol of a power MOSFET is shown in Fig. 14.5.

Power MOSFETs are majority carrier devices, and there is no minority carrier storage time. Hence, they have exceptionally fast rise and fall times. They are essentially resistive devices when turned on, while bipolar transistors present a more or less constant $V_{CE(sat)}$ over the normal operating range. Power dissipation in MOSFETs is $I_d^2 R_{DS(on)}$, and in bipolars it is $I_C V_{CE(sat)}$. At low currents, therefore, a power MOSFET may have a lower conduction loss than a comparable bipolar device, but at higher currents, the conduction loss will exceed that of bipolars. Also, the $R_{DS(on)}$ increases with temperature.

An important feature of a power MOSFET is the absence of a secondary breakdown effect, which is present in a bipolar transistor, and as a result, it has an extremely rugged switching performance. In MOSFETs, $R_{DS(on)}$ increases with temperature, and thus the current is automatically diverted away from the hot spot. The drain body junction appears as an antiparallel diode between source and drain. Thus, power MOSFETs will not support voltage in the reverse direction. Although this inverse diode is relatively fast, it is slow by comparison with the MOSFET. Recent devices have the diode recovery time as low as 100 ns. Since MOSFETs cannot be protected by fuses, an electronic protection technique has to be used.

With the advancement in MOS technology, ruggedized MOSFETs are replacing the conventional MOSFETs. The need to ruggedize power MOSFETs is related to device reliability. If a MOSFET is operating within its specification range at all times, its chances for failing catastrophically are minimal. However, if its absolute maximum rating is exceeded, failure probability increases dramatically. Under actual operating conditions, a MOSFET may be subjected to transients — either externally from the power bus supplying the circuit or from the circuit itself due, for example, to inductive kicks going beyond the absolute maximum ratings. Such conditions are likely in almost every application, and in most cases are beyond a designer's control. Rugged devices are made to be more tolerant for over-voltage transients. Ruggedness is the ability of a MOSFET to operate in an environment of dynamic electrical stresses, without activating any of the parasitic bipolar junction transistors. The rugged device can withstand higher levels of diode recovery dv/dt and static dv/dt .

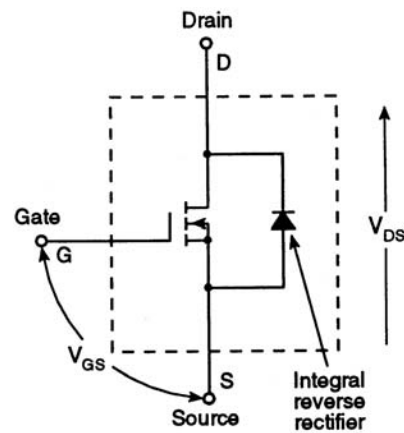


FIGURE 14.5 Power MOSFET circuit symbol.
(Source: B.K. Bose, *Modern Power Electronics: Evaluation, Technology, and Applications*, p. 7.
© 1992 IEEE.)

Insulated-Gate Bipolar Transistor (IGBT)

The IGBT has the high input impedance and high-speed characteristics of a MOSFET with the conductivity characteristic (low saturation voltage) of a bipolar transistor. The IGBT is turned on by applying a positive voltage between the gate and emitter and, as in the MOSFET, it is turned off by making the gate signal zero or slightly negative. The IGBT has a much lower voltage drop than a MOSFET of similar ratings. The structure of an IGBT is more like a thyristor and MOSFET. For a given IGBT, there is a critical value of collector current that will cause a large enough voltage drop to activate the thyristor. Hence, the device manufacturer specifies the peak allowable collector current that can flow without latch-up occurring. There is also a corresponding gate source voltage that permits this current to flow that should not be exceeded.

Like the power MOSFET, the IGBT does not exhibit the secondary breakdown phenomenon common to bipolar transistors. However, care should be taken not to exceed the maximum power dissipation and specified maximum junction temperature of the device under all conditions for guaranteed reliable operation. The on-state voltage of the IGBT is heavily dependent on the gate voltage. To obtain a low on-state voltage, a sufficiently high gate voltage must be applied.

In general, IGBTs can be classified as punch-through (PT) and nonpunch-through (NPT) structures, as shown in Fig. 14.6. In the PT IGBT, an N^+ buffer layer is normally introduced between the P^+ substrate and the N^- epitaxial layer, so that the whole N^- drift region is depleted when the device is blocking the off-state voltage, and the electrical field shape inside the N^- drift region is close to a rectangular shape. Because a shorter N^- region can be used in the punch-through IGBT, a better trade-off between the forward voltage drop and turn-off time can be achieved. PT IGBTs are available up to about 1200 V.

High voltage IGBTs are realized through a nonpunch-through process. The devices are built on an N^- wafer substrate which serves as the N^- base drift region. Experimental NPT IGBTs of up to about 4 kV have been reported in the literature. NPT IGBTs are more robust than PT IGBTs, particularly under short circuit conditions. But NPT IGBTs have a higher forward voltage drop than the PT IGBTs.

The PT IGBTs cannot be as easily paralleled as MOSFETs. The factors that inhibit current sharing of parallel-connected IGBTs are (1) on-state current unbalance, caused by $V_{CE(sat)}$ distribution and main circuit wiring resistance distribution, and (2) current unbalance at turn-on and turn-off, caused by the switching time difference of the parallel connected devices and circuit wiring inductance distribution. The NPT IGBTs can be paralleled because of their positive temperature coefficient property.

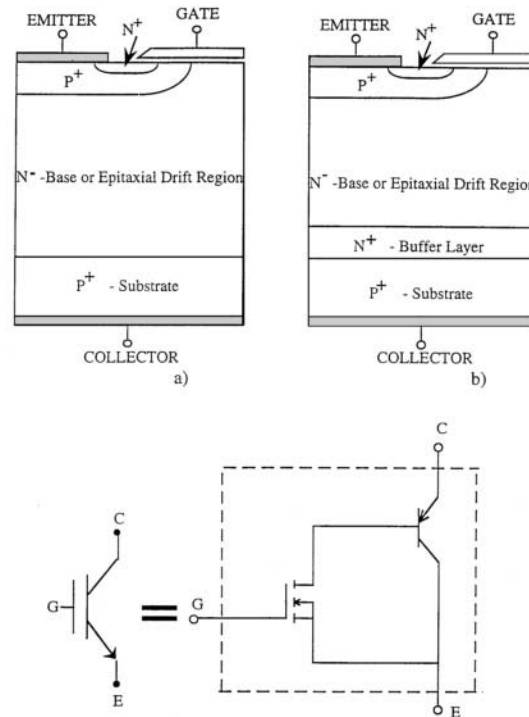


FIGURE 14.6 (a) Nonpunch-through IGBT, (b) punch-through IGBT, (c) IGBT equivalent circuit.

MOS-Controlled Thyristor (MCT)

The MCT is a new type of power semiconductor device that combines the capabilities of thyristor voltage and current with MOS gated turn-on and turn-off. It is a high power, high frequency, low conduction

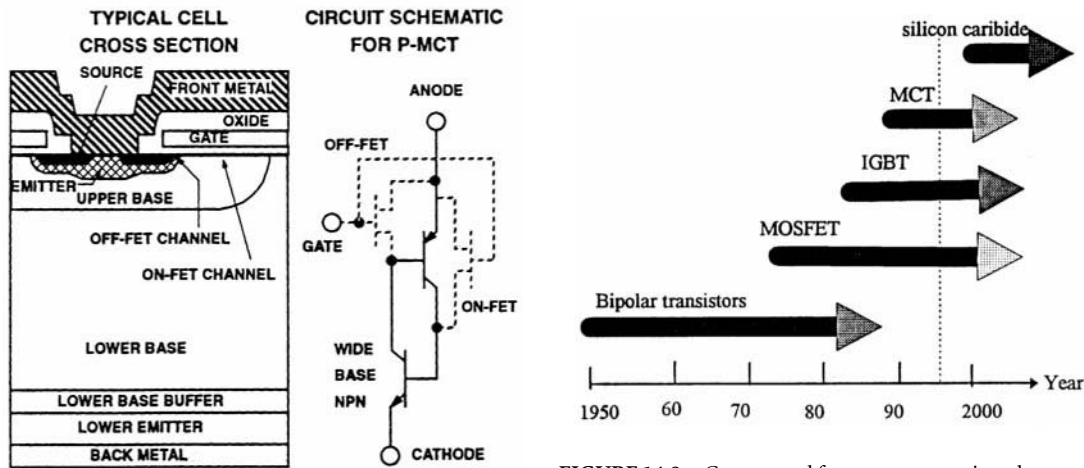


FIGURE 14.7 (Source: Harris Semiconductor, *User's Guide of MOS Controlled Thyristor*. With permission.)

FIGURE 14.8 Current and future power semiconductor devices development direction. (Source: A.Q. Huang, *Recent Developments of Power Semiconductor Devices, VPEC Seminar Proceedings*, pp. 1–9. With permission.)

drop and a rugged device, which is more likely to be used in the future for medium and high power applications. A cross-sectional structure of a p -type MCT with its circuit schematic is shown in Fig. 14.7. The MCT has a thyristor type structure with three junctions and PNP layers between the anode and cathode. In a practical MCT, about 100,000 cells similar to the one shown are paralleled to achieve the desired current rating. MCT is turned on by a negative voltage pulse at the gate with respect to the anode, and is turned off by a positive voltage pulse.

The MCT was announced by the General Electric R & D Center on November 30, 1988. Harris Semiconductor Corporation has developed two generations of p -MCTs. Gen-1 p -MCTs are available at 65 A/1000 V and 75 A/600 V with peak controllable current of 120 A. Gen-2 p -MCTs are being developed at similar current and voltage ratings, with much improved turn-on capability and switching speed. The reason for developing a p -MCT is the fact that the current density that can be turned off is 2 or 3 times higher than that of an n -MCT; but n -MCTs are the ones needed for many practical applications. Harris Semiconductor Corporation is in the process of developing n -MCTs, which are expected to be commercially available during the next one to two years.

The advantage of an MCT over IGBT is its low forward voltage drop. N -type MCTs will be expected to have a similar forward voltage drop, but with an improved reverse bias safe operating area and switching speed. MCTs have relatively low switching times and storage time. The MCT is capable of high current densities and blocking voltages in both directions. Since the power gain of an MCT is extremely high, it could be driven directly from logic gates. An MCT has high di/dt (of the order of 2500 A/ μ s) and high dv/dt (of the order of 20,000 V/ μ s) capability.

The MCT, because of its superior characteristics, shows a tremendous possibility for applications such as motor drives, uninterrupted power supplies, static VAR compensators, and high power active power line conditioners.

The current and future power semiconductor devices developmental direction is shown in Fig. 14.8. High-temperature operation capability and low forward voltage drop operation can be obtained if silicon is replaced by silicon carbide material for producing power devices. The silicon carbide has a higher band gap than silicon. Hence, higher breakdown voltage devices could be developed. Silicon carbide devices have excellent switching characteristics and stable blocking voltages at higher temperatures. But the silicon carbide devices are still in the very early stages of development.

References

- B.K. Bose, *Modern Power Electronics: Evaluation, Technology, and Applications*, New York: IEEE Press, 1992.
- Harris Semiconductor, *User's Guide of MOS Controlled Thyristor*.
- A.Q. Huang, Recent Developments of Power Semiconductor Devices, in *VPEC Seminar Proceedings*, September 1995, 1–9.
- N. Mohan and T. Undeland, *Power Electronics: Converters, Applications, and Design*, John Wiley & Sons, New York, 1995.
- J. Wojcik, Ruggedized transistors emerging as power MOSFET standard-bearers, *Power Technics Magazine*, January 1988, 29–32.

Further Information

- B.M. Bird and K.G. King, *An Introduction to Power Electronics*, Wiley-Interscience, New York, 1984.
- R. Sittig and P. Roggwiller, *Semiconductor Devices for Power Conditioning*, Plenum, New York, 1982.
- V.A.K. Temple, Advances in MOS controlled thyristor technology and capability, *Power Conversion*, 544–554, Oct. 1989.
- B.W. Williams, *Power Electronics, Devices, Drivers and Applications*, John Wiley, New York, 1987.

14.2 Uncontrolled and Controlled Rectifiers

Mahesh M. Swamy

Rectifiers are electronic circuits that convert bidirectional voltage to unidirectional voltage. This process can be accomplished either by mechanical means like in the case of DC machines employing commutators or by static means employing semiconductor devices. Static rectification is more efficient and reliable compared to rotating commutators. This section covers rectification of electric power for industrial and commercial use. In other words, we will not be discussing small signal rectification that generally involves low power and low voltage signals. Static power rectifiers can be classified into two broad groups. They are (1) uncontrolled rectifiers and (2) controlled rectifiers. Uncontrolled rectifiers make use of power semiconductor diodes while controlled rectifiers make use of thyristors (SCRs), gate turn-off thyristors (GTOs), and MOSFET-controlled thyristors (MCTs).

Rectifiers, in general, are widely used in power electronics to rectify single-phase as well as three-phase voltages. DC power supplies used in computers, consumer electronics, and a host of other applications typically make use of single-phase rectifiers. Industrial applications include, but are not limited to, industrial drives, metal extraction processes, industrial heating, power generation and transmission, etc. Most industrial applications of large power rating typically employ three-phase rectification processes.

Uncontrolled rectifiers in single-phase as well as in three-phase circuits will be discussed, as will controlled rectifiers. Application issues regarding uncontrolled and controlled rectifiers will be briefly discussed within each section.

Uncontrolled Rectifiers

The simplest uncontrolled rectifier use can be found in single-phase circuits. There are two types of uncontrolled rectification. They are (1) half-wave rectification and (2) full-wave rectification. Half-wave and full-wave rectification techniques have been used in single-phase as well as in three-phase circuits. As mentioned earlier, uncontrolled rectifiers make use of diodes. Diodes are two-terminal semiconductor devices that allow flow of current in only one direction. The two terminals of a diode are known as the anode and the cathode.

Mechanics of Diode Conduction

The anode is formed when a pure semiconductor material, typically silicon, is doped with impurities that have fewer valence electrons than silicon. Silicon has an atomic number of 14, which according to Bohr's atomic model means that the *K* and *L* shells are completely filled by 10 electrons and the remaining 4 electrons occupy the *M* shell. The *M* shell can hold a maximum of 18 electrons. In a silicon crystal, every atom is bound to four other atoms, which are placed at the corners of a regular tetrahedron. The bonding, which involves sharing of a valence electron with a neighboring atom is known as covalent bonding. When a Group 3 element (typically boron, aluminum, gallium, and indium) is doped into the silicon lattice structure, three of the four covalent bonds are made. However, one bonding site is vacant in the silicon lattice structure. This creates vacancies or *holes* in the semiconductor. In the presence of either a thermal field or an electrical field, electrons from a neighboring lattice or from an external agency tend to migrate to fill this vacancy. The vacancy or *hole* can also be said to move toward the approaching electron, thereby creating a mobile hole and hence current flow. Such a semiconductor material is also known as lightly doped semiconductor material or *p type*. Similarly, the cathode is formed when silicon is doped with impurities that have higher valence electrons than silicon. This would mean elements belonging to Group 5. Typical doping impurities of this group are phosphorus, arsenic, and antimony. When a Group 5 element is doped into the silicon lattice structure, it oversatisfies the covalent bonding sites available in the silicon lattice structure, creating excess or loose electrons in the valence shell. In the presence of either a thermal field or an electrical field, these loose electrons easily get detached from the lattice structure and are free to conduct electricity. Such a semiconductor material is also known as heavily doped semiconductor material or *n type*.

The structure of the final doped crystal even after the addition of *acceptor* impurities (Group 3) or *donor* impurities (Group 5), remains electrically neutral. The available electrons balance the net positive charge and there is no charge imbalance.

When a *p*-type material is joined with an *n*-type material, a *p-n* junction is formed. Some loose electrons from the *n*-type material migrate to fill the holes in the *p*-type material and some holes in the *p*-type migrate to meet with the loose electrons in the *n*-type material. Such a movement causes the *p*-type structure to develop a slight negative charge and the *n*-type structure to develop some positive charge. These slight positive and negative charges in the *n*-type and *p*-type areas, respectively, prevent further migration of electrons from *n*-type to *p*-type and holes from *p*-type to *n*-type areas. In other words, an energy barrier is automatically created due to the movement of charges within the crystalline lattice structure. Keep in mind that the combined material is still electrically neutral and no charge imbalance exists.

When a positive potential greater than the barrier potential is applied across the *p-n* junction, then electrons from the *n*-type area migrate to combine with the holes in the *p*-type area, and vice versa. The *p-n* junction is said to be *forward-biased*. Movement of charge particles constitutes current flow. Current is said to flow from the anode to the cathode when the potential at the anode is higher than the potential at the cathode by a minimum threshold voltage also known as the junction barrier voltage. The magnitude of current flow is high when the externally applied positive potential across the *p-n* junction is high.

When the polarity of the applied voltage across the *p-n* junction is reversed compared to the case described above, then the flow of current ceases. The holes in the *p*-type area move away from the *n*-type area and the electrons in the *n*-type area move away from the *p*-type area. The *p-n* junction is said to be *reverse-biased*. In fact, the holes in the *p*-type area get attracted to the negative external potential and similarly the electrons in the *n*-type area get attracted to the positive external potential. This creates a depletion region at the *p-n* junction and there are almost no charge carriers flowing in the depletion region. This phenomenon brings us to the important observation that a *p-n* junction can be utilized to force current to flow only in one direction, depending on the polarity of the applied voltage across it. Such a semiconductor device is known as a *diode*. Electrical circuits employing diodes for the purpose of making the current flow in a unidirectional manner through a load are known as *rectifiers*. The voltage-current characteristic of a typical power semiconductor diode along with its symbol is shown in [Fig. 14.9](#).

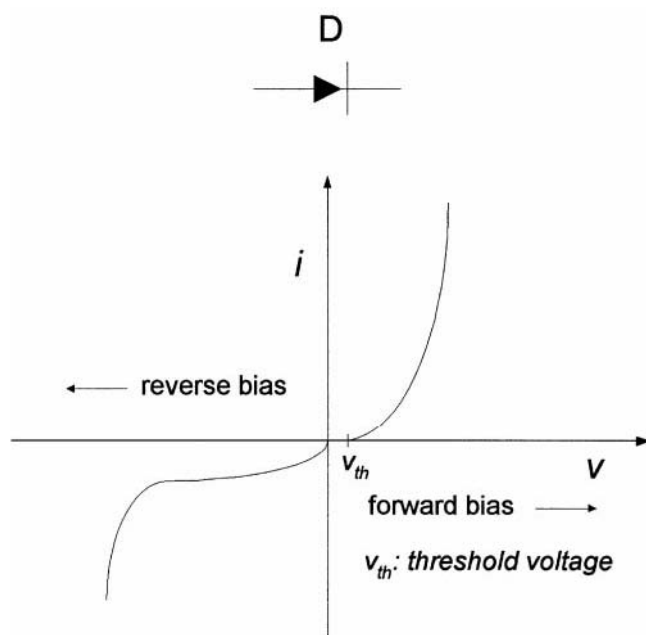


FIGURE 14.9 Typical v - i characteristic of a semiconductor diode and its symbol.

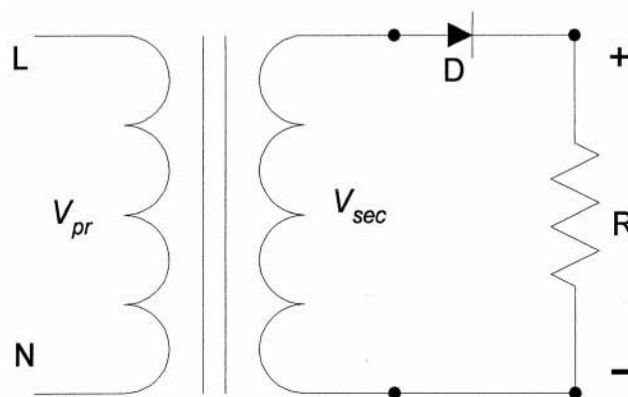


FIGURE 14.10 Electrical schematic of a single-phase half-wave rectifier circuit feeding a resistive load. Average output voltage is V_o .

Single-Phase Half-Wave Rectifier Circuits

A single-phase half-wave rectifier circuit employs one diode. A typical circuit, which makes use of a half-wave rectifier, is shown in [Fig. 14.10](#).

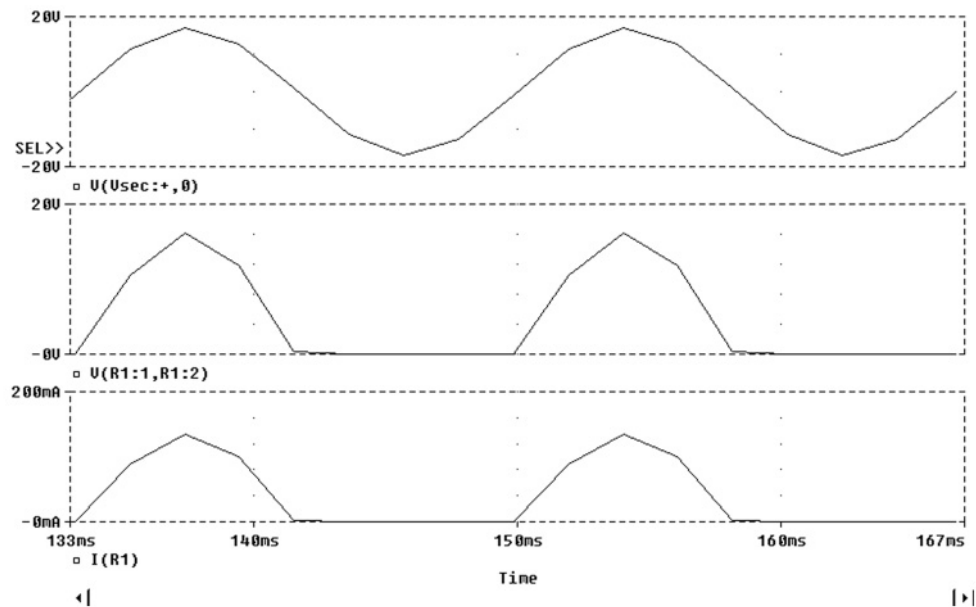


FIGURE 14.11 Typical waveforms at various points in the circuit of Fig. 14.10. For a purely resistive load, $V_o = \sqrt{2} * V_{sec} / \pi$.

A single-phase AC source is applied across the primary windings of a transformer. The secondary of the transformer consists of a diode and a resistive load. This is typical since many consumer electronic items including computers utilize single-phase power.

Typically, the primary side is connected to a single-phase AC source, which could be 120 V, 60 Hz, 100 V, 50 Hz, 220 V, 50 Hz, or any other utility source. The secondary side voltage is generally stepped down and rectified to achieve low DC voltage for consumer applications. The secondary voltage, the voltage across the load resistor, and the current through it is shown in Fig. 14.11.

As one can see, when the voltage across the anode-cathode of diode D1 in Fig. 14.10 goes negative, the diode does not conduct and no voltage appears across the load resistor R. The current through R follows the voltage across it. The value of the secondary voltage is chosen to be 12 VAC and the value of R is chosen to be 120 Ω . Since, only one-half of the input voltage waveform is allowed to pass onto the output, such a rectifier is known as a *half-wave* rectifier. The voltage ripple across the load resistor is rather large and, in typical power supplies, such ripples are unacceptable. The current through the load is discontinuous and the current through the secondary of the transformer is unidirectional. The AC component in the secondary of the transformer is balanced by a corresponding AC component in the primary winding. However, the DC component in the secondary does not induce any voltage on the primary side and hence is not compensated for. This DC current component through the transformer secondary can cause the transformer to saturate and is not advisable for large power applications. In order to smooth the output voltage across the load resistor R and to make the load current continuous, a smoothing filter circuit comprised of either a large DC capacitor or a combination of a series inductor and shunt DC capacitor is employed. Such a circuit is shown in Fig. 14.12.

The resulting waveforms are shown in Fig. 14.13. It is interesting to see that the voltage across the load resistor has very little ripple and the current through it is smooth. However, the value of the filter components employed is large and is generally not economically feasible. For example, in order to get a voltage waveform across the load resistor R, which has less than 6% peak-peak voltage ripple, the value of inductance that had to be used is 100 mH and the value of the capacitor is 1000 μ F. In order to improve the performance without adding bulky filter components, it is a good practice to employ full-wave

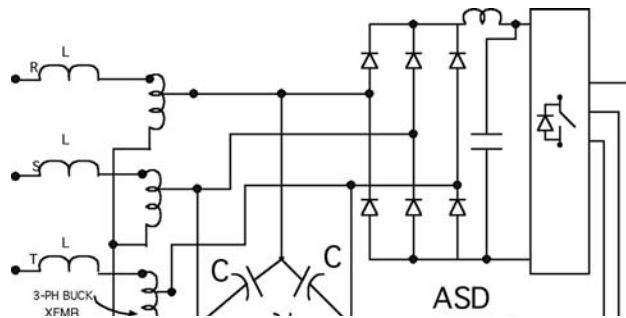


FIGURE 14.12 Modified circuit of Fig. 14.10 employing smoothing filters.

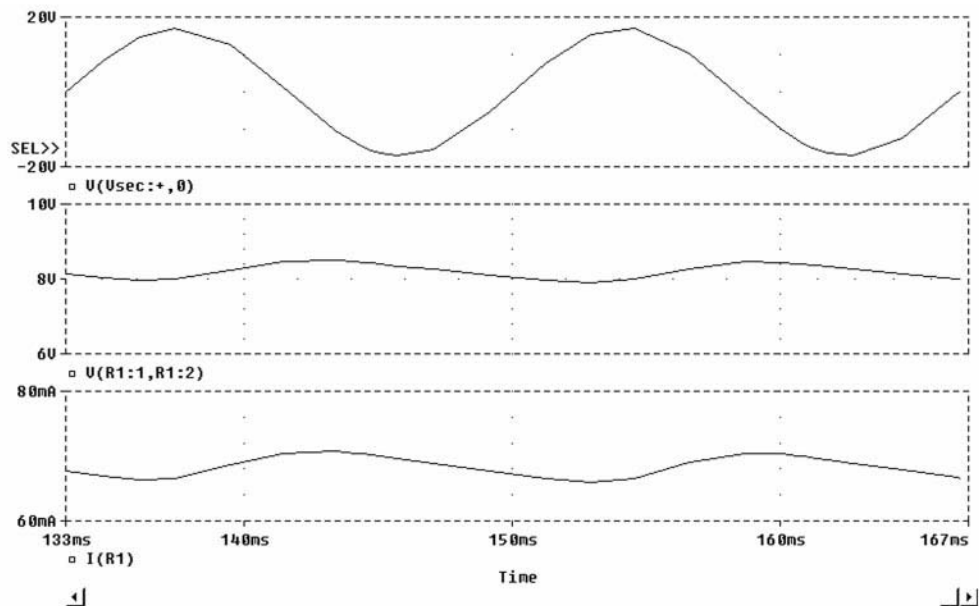


FIGURE 14.13 Voltage across load resistor R and current through it for the circuit in Fig. 14.12.

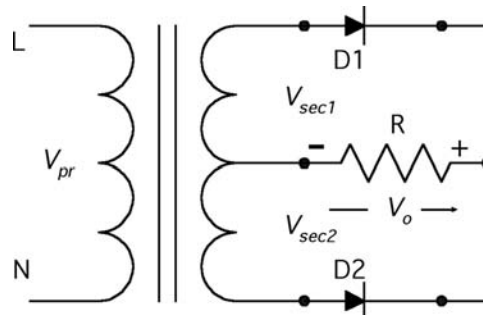


FIGURE 14.14 Electrical schematic of a single-phase full-wave rectifier circuit. Average output voltage is V_o .

rectifiers. The circuit in Fig. 14.10 can be easily modified into a full-wave rectifier. The transformer is changed from a single secondary winding to a center-tapped secondary winding. Two diodes are now employed instead of one. The new circuit is shown in Fig. 14.14.

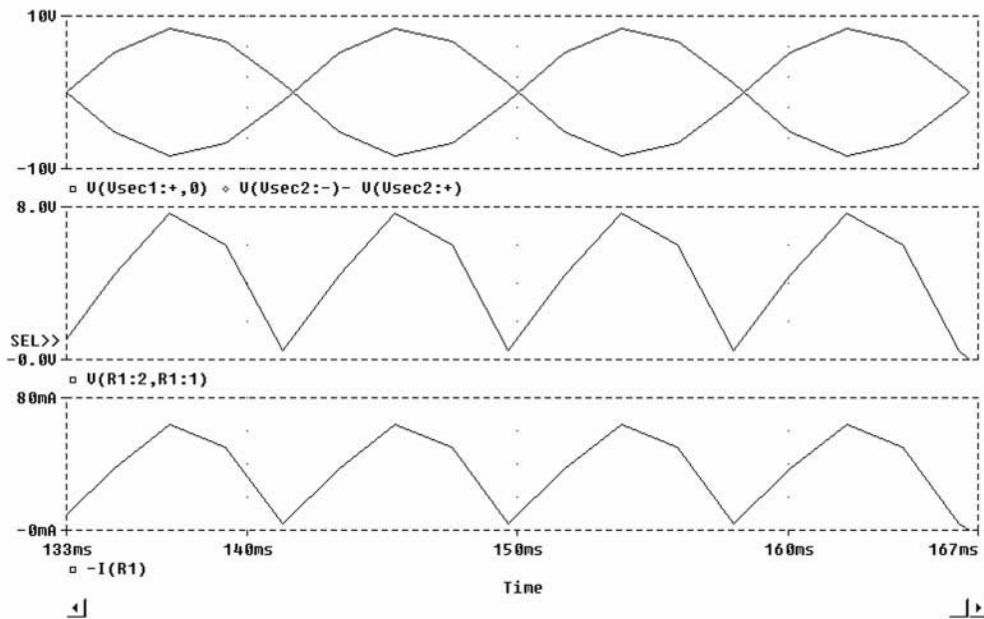


FIGURE 14.15 Typical waveforms at various points in the circuit of Fig. 14.14. For a purely resistive load, $V_o = 2\sqrt{2} \cdot V_{sec}/\pi$.

Full Wave Rectifiers

The waveforms for the circuit of Fig. 14.14 are shown in Fig. 14.15. The voltage across the load resistor is a full-wave rectified voltage. The current has subtle discontinuities but can be improved by employing smaller size filter components. A typical filter for the circuit of Fig. 14.14 may include only a capacitor. The waveforms obtained are shown in Fig. 14.16.

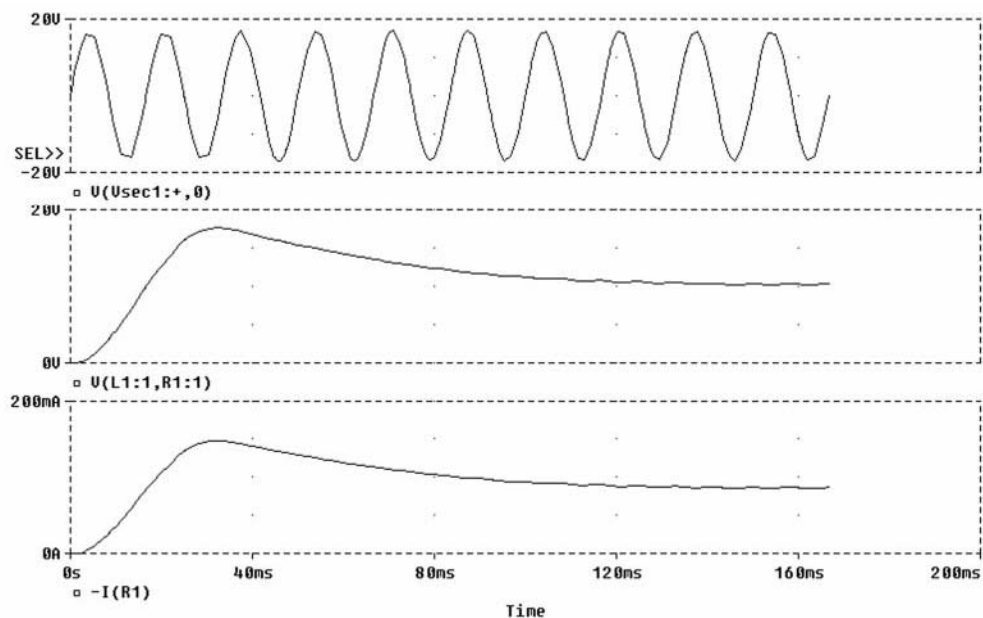


FIGURE 14.16 Voltage across the load resistor and current through it with the same filter components as in Fig. 14.12. Notice the conspicuous reduction in ripple across R.

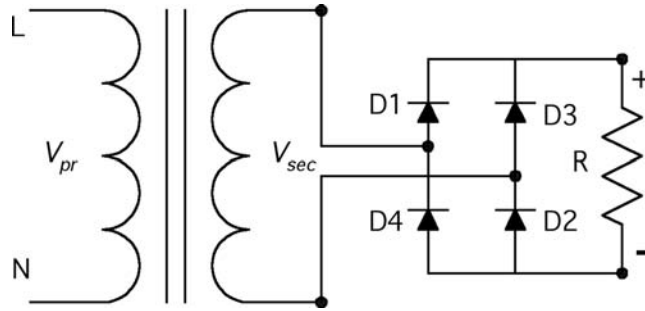


FIGURE 14.17 Schematic representation of a single-phase full-wave H-bridge rectifier.

Yet another way of reducing the size of the filter components is to increase the frequency of the supply. In many power supply applications similar to the one used in computers, a high frequency AC supply is achieved by means of switching. The high frequency AC is then level translated via a ferrite core transformer with multiple secondary windings. The secondary voltages are then rectified employing a simple circuit as shown in Fig. 14.10 or Fig. 14.12 with much smaller filters. The resulting voltage across the load resistor is then maintained to have a peak-peak voltage ripple of less than 1%.

Full-wave rectification can be achieved without the use of center-tap transformers. Such circuits make use of 4 diodes in single-phase circuits and 6 diodes in three-phase circuits. The circuit configuration is typically referred to as the *H-bridge* circuit. A single-phase full-wave H-bridge topology is shown in Fig. 14.17. The main difference between the circuit topology shown in Figs. 14.14 and 14.17 is that the H-bridge circuit employs 4 diodes while the topology of Fig. 14.14 utilizes only two diodes. However, a center-tap transformer of a higher power rating is needed for the circuit of Fig. 14.14. The voltage and current stresses in the diodes in Fig. 14.14 are also greater than that occurring in the diodes of Fig. 14.17.

In order to comprehend the basic difference in the two topologies, it is interesting to compare the component ratings for the same power output. To make the comparison easy, let both topologies employ very large filter inductors such that the current through R is constant and ripple-free. Let this current through R be denoted by I_{dc} . Let the power being supplied to the load be denoted by P_{dc} . The output power and the load current are then related by the following expression:

$$P_{dc} = I_{dc}^2 * R.$$

The rms current flowing through the first secondary winding in the topology in Fig. 14.14 will be $I_{dc}/\sqrt{2}$. This is because the current through a secondary winding flows only when the corresponding diode is forward biased. This means that the current through the secondary winding will flow only for one half cycle. If the voltage at the secondary is assumed to be V , the VA rating of the secondary winding of the transformer in Fig. 14.14 will be given by:

$$VA_1 = V * I_{dc} / \sqrt{2}$$

$$VA_2 = V * I_{dc} / \sqrt{2}$$

$$VA = VA_1 + VA_2 = \sqrt{2} * V * I_{dc}$$

This is the secondary-side VA rating for the transformer shown in Fig. 14.14.

For the isolation transformer shown in Fig. 14.17, let the secondary voltage be V and the load current be of a constant value I_{dc} . Since, in the topology of Fig. 14.17, the secondary winding carries the current I_{dc} when diodes D1 and D2 conduct and as well as when diodes D3 and D4 conduct, the rms value of

the secondary winding current is I_{dc} . Hence, the VA rating of the secondary winding of the transformer shown in Fig. 14.17 is V^*I_{dc} , which is less than that needed in the topology of Fig. 14.14. Note that the primary VA rating for both cases remains the same since in both cases the power being transferred from the source to the load remains the same.

When diode D2 in the circuit of Fig. 14.14 conducts, the secondary voltage of the second winding V_{sec2} ($=V$) appears at the cathode of diode D1. The voltage being blocked by diode D1 can thus reach 2 times the peak secondary voltage ($=2*V_{pk}$) (Fig. 14.15). In the topology of Fig. 14.17, when diodes D1 and D2 conduct, the voltage V_{sec} ($=V$), which is same as V_{sec2} appears across D3 as well as across D4. This means that the diodes have to withstand only one times the peak of the secondary voltage, V_{pk} . The rms value of the current flowing through the diodes in both topologies is the same. Hence, from the diode voltage rating as well as from the secondary VA rating points of view, the topology of Fig. 14.17 is better than that of Fig. 14.14. Further, the topology in Fig. 14.17 can be directly connected to a single-phase AC source and does not need a center-tapped transformer. The voltage waveform across the load resistor is similar to that shown in Figs. 14.15 and 14.16.

In many industrial applications, the topology shown in Fig. 14.17 is used along with a DC filter capacitor to smooth the ripples across the load resistor. The load resistor is simply a representative of a load. It could be an inverter system or a high-frequency resonant link. In any case, the diode rectifier-bridge would see a representative load resistor. The DC filter capacitor will be large in size compared to an H-bridge configuration based on three-phase supply system. When the rectified power is large, it is advisable to add a DC link inductor. This can reduce the size of the capacitor to some extent and reduce the current ripple through the load. When the rectifier is turned on initially with the capacitor at zero voltage, a large amplitude of charging current will flow into the filter capacitor through a pair of conducting diodes. The diodes D1~D4 should be rated to handle this large surge current. In order to limit the high inrush current, it is a normal practice to add a charging resistor in series with the filter capacitor. The charging resistor limits the inrush current but creates a significant power loss if it is left in the circuit under normal operation. Typically, a contactor is used to short-circuit the charging resistor after the capacitor is charged to a desired level. The resistor is thus electrically nonfunctional during normal operating conditions. A typical arrangement showing a single-phase full-wave H-bridge rectifier system for an inverter application is shown in Fig. 14.18.

The charging current at time of turn-on is shown in a simulated waveform in Fig. 14.19. Note that the contacts across the soft-charge resistor are closed under normal operation. The contacts across the soft-charge resistor are initiated by various means. The coil for the contacts could be powered from the input AC supply and a timer or it could be powered on by a logic controller that senses the level of voltage across the DC bus capacitor or senses the rate of change in voltage across the DC bus capacitor. A simulated waveform depicting the inrush with and without a soft-charge resistor is shown in Figs. 14.19(a) and (b), respectively.

For larger power applications, typically above 1.5 kW, it is advisable to use a higher power supply. In some applications, two of the three phases of a three-phase power system are used as the source powering

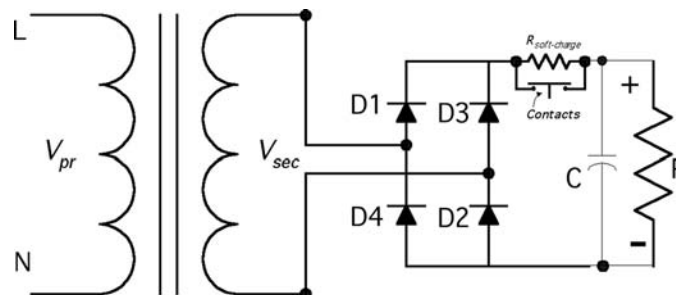


FIGURE 14.18 Single-phase H-bridge circuit for use with power electronic circuits.

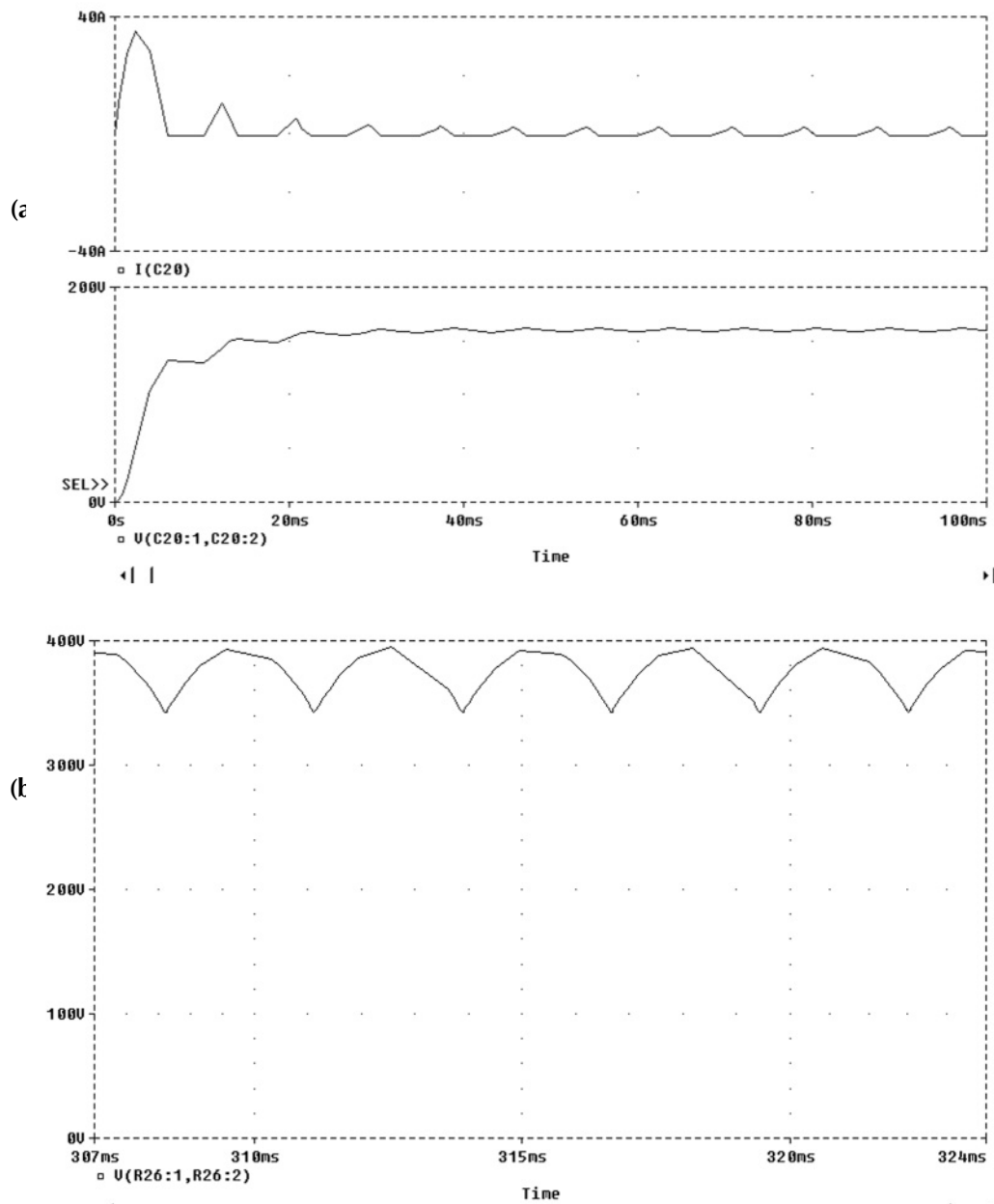


FIGURE 14.19 (a) Charging current and voltage across capacitor for a typical value of soft-charge resistor of 2Ω . The DC bus capacitor is about $1000\mu F$. The load is approximately 200Ω . (b) Charging current and voltage across capacitor for no soft charge resistor. The current is limited by the system impedance and by the diode forward resistance. The DC bus capacitor is about $1000\mu F$. The load is approximately 200Ω .

the rectifier of Fig. 14.17. The line-line voltage could be either 240 VAC or 480 VAC. Under those circumstances, one may go up to 10 kW of load power before adopting a full three-phase H-bridge configuration. Beyond 10 kW, the size of the capacitor becomes too large to achieve a peak-peak voltage ripple of less than 5%. Hence, it is advisable then to employ three-phase rectifier configurations.

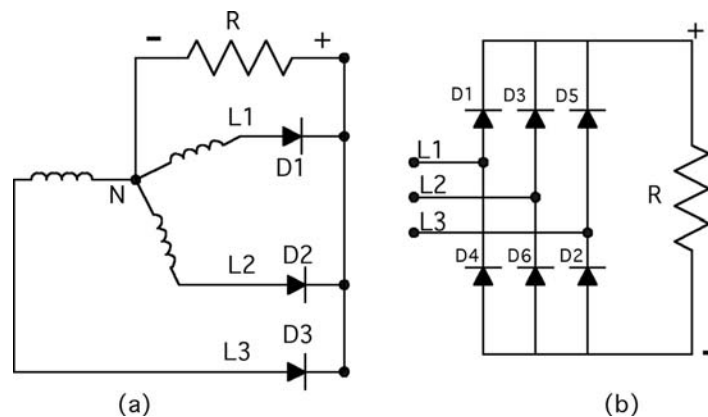


FIGURE 14.20 Schematic representation of three-phase rectifier configurations: (a) half-wave rectifier needing a neutral point, N; and (b) full-wave rectifier.

Three-Phase Rectifiers (Half-Wave and Full-Wave)

Similar to the single-phase case, there exist half-wave and full-wave three-phase rectifier circuits. Again, similar to the single-phase case, the half-wave rectifier in the three-phase case also yields DC components in the source current. The source has to be large enough to handle this. Therefore, it is not advisable to use three-phase half-wave rectifier topology for large power applications. The three-phase half-wave rectifier employs three diodes while the full-wave H-bridge configuration employs six diodes. Typical three-phase half-wave and full-wave topologies are shown in Fig. 14.20.

In the half-wave rectifier shown in Fig. 14.20(a), the shape of the output voltage and current through the resistive load is dictated by the instantaneous value of the source voltages, L1, L2, and L3. These source voltages are phase shifted in time by 120 electrical degrees, which corresponds to approximately 5.55 msec for a 60 Hz system. This means that if one considers the L1 phase to reach its peak value at time t_1 , the L2 phase will achieve its peak 120 electrical degrees later ($t_1 + 5.55$ msec), and L3 will achieve its peak 120 electrical degrees later than L2 ($t_1 + 5.55$ msec + 5.55 msec). Since all three phases are connected to the same output resistor R, the phase that provides the highest instantaneous voltage is the phase that appears across R. In other words, the phase with the highest instantaneous voltage reverse biases the diodes of the other two phases and prevents them from conducting, which consequently prevents those phase voltages from appearing across R. Since a particular phase is connected to only one diode in Fig. 14.20(a), only three pulses, each of 120° duration, appear across the load resistor, R. Typical output voltage across R for the circuit of Fig. 14.20(a) is shown in Fig. 14.21(a).

A similar explanation can be provided to explain the voltage waveform across a purely resistive load in the case of the three-phase full-wave rectifier shown in Fig. 14.20(b). The output voltage that appears across R is the highest instantaneous line-line voltage and not simply the phase voltage. Since there are six such intervals, each of 60 electrical degrees duration in a given cycle, the output voltage waveform will have six pulses in one cycle [Fig. 14.21(b)]. Since a phase is connected to two diodes (diode pair), each phase conducts current out and into itself, thereby eliminating the DC component in one complete cycle.

The waveform for a three-phase full-wave rectifier with a purely resistive load is shown in Fig. 14.21(b). Note that the number of humps in Fig. 14.21(a) is only three in one AC cycle, while the number of humps in Fig. 14.21(b) is six in one AC cycle.

In both the configurations shown in Fig. 14.20, the load current does not become discontinuous due to three-phase operation. Comparing this to the single-phase half-wave and full-wave rectifier, one can say that the output voltage ripple is much lower in three-phase rectifier systems compared to single-phase rectifier systems. Hence, with the use of moderately sized filters, three-phase full-wave rectifiers

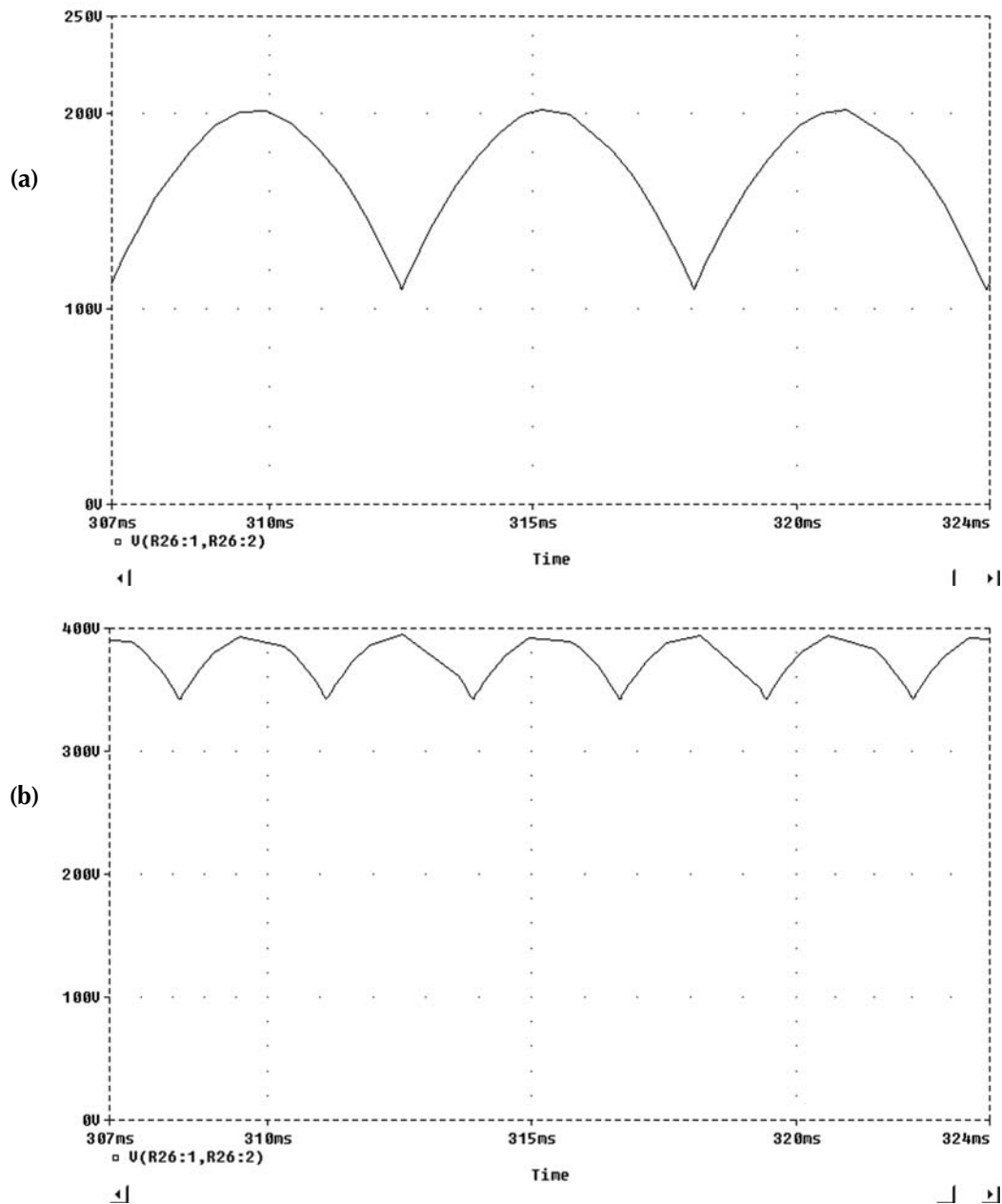


FIGURE 14.21 (a) Typical output voltage across a purely resistive network for the half-wave rectifier shown in Fig. 14.12(a). (b) Typical output voltage across a purely resistive network for the full-wave rectifier shown in Fig. 14.12(b).

can be operated at hundred to thousands of kilowatts. The only limitation would be the size of the diodes used and power system harmonics, which will be discussed next. Since there are six humps in the output voltage waveform per electrical cycle, the three-phase full-wave rectifier shown in Fig. 14.20(b) is also known as a six-pulse rectifier system.

Average Output Voltage

In order to evaluate the average value of the output voltage for the two rectifiers shown in Fig. 14.20, the output voltages in Figs. 14.21(a) and (b) have to be integrated over a cycle. For the circuit shown in Fig. 14.20(a), the integration yields the following:

$$V_o = \frac{3}{2\pi} \int_{\pi/6}^{5\pi/6} \sqrt{2} V_{L-N} \sin(wt) d(wt)$$
$$V_o = \frac{3 * \sqrt{3} * \sqrt{2} * V_{L-N}}{2 * \pi}$$

Similar operations can be performed to obtain the average output voltage for the circuit shown in Fig. 14.20(b). This yields:

$$V_o = \frac{3}{\pi} \int_{\pi/3}^{2\pi/3} \sqrt{2} V_{L-L} \sin(wt) d(wt)$$
$$V_o = \frac{3 * \sqrt{2} * V_{L-L}}{\pi} = \frac{3 * \sqrt{2} * \sqrt{3} * V_{L-N}}{\pi}$$

In other words, the average output voltage for the circuit in Fig. 14.20(b) is twice that for the circuit in Fig. 14.20(a).

Influence of Three-Phase Rectification on the Power System

Events over the last several years have focused attention on certain types of loads on the electrical system that result in power quality problems for the user and utility alike. When the input current into the electrical equipment does not follow the impressed voltage across the equipment, then the equipment is said to have a nonlinear relationship between the input voltage and input current. All equipment that employs some sort of rectification (either 1-ph or 3-ph) are examples of nonlinear loads. Nonlinear loads generate voltage and current harmonics that can have adverse effects on equipment designed for operation as linear loads. Transformers that bring power into an industrial environment are subject to higher heating losses due to harmonic generating sources (nonlinear loads) to which they are connected. Harmonics can have a detrimental effect on emergency generators, telephones, and other electrical equipment. When reactive power compensation (in the form of passive power factor improving capacitors) is used with nonlinear loads, resonance conditions can occur that may result in even higher levels of harmonic voltage and current distortion, thereby causing equipment failure, disruption of power service, and fire hazards in extreme conditions.

The electrical environment has absorbed most of these problems in the past. However, the problem has now reached a magnitude where Europe, the U.S., and other countries have proposed standards to responsibly engineer systems considering the electrical environment. IEEE 519-1992 and IEC 1000 have evolved to become a common requirement cited when specifying equipment on newly engineered projects.

Why Diode Rectifiers Generate Harmonics

The current waveform at the inputs of a three-phase full-wave rectifier is not continuous. It has multiple zero crossings in one electrical cycle. The current harmonics generated by rectifiers having DC bus capacitors are caused by the pulsed current pattern at the input. The DC bus capacitor draws charging current only when it gets discharged due to the load. The charging current flows into the capacitor when the input rectifier is forward biased, which occurs when the instantaneous input voltage is higher than

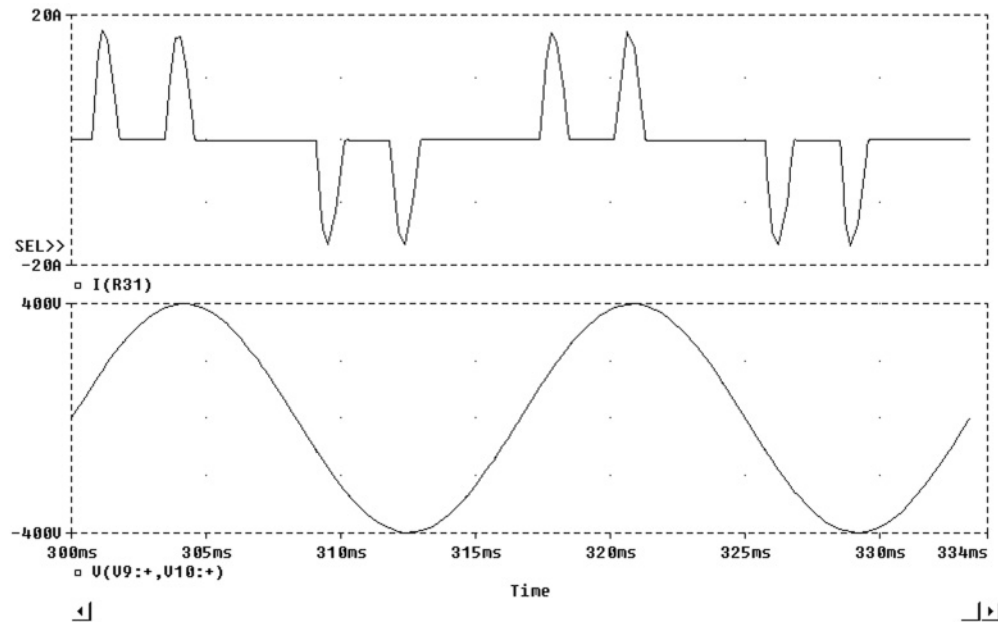


FIGURE 14.22 Typical pulsed-current waveform as seen at input of a three-phase diode rectifier with DC capacitor filter. The lower trace is input line-line voltage.

the steady-state DC voltage across the DC bus capacitor. The pulsed current drawn by the DC bus capacitor is rich in harmonics due to the fact that it is discontinuous as shown in Fig. 14.22. Sometimes there are also voltage harmonics that are associated with three-phase rectifier systems. The voltage harmonics generated by three-phase rectifiers are due to the flat-topping effect caused by a weak AC source charging the DC bus capacitor without any intervening impedance. The distorted voltage waveform gives rise to voltage harmonics that could lead to possible network resonance.

The order of current harmonics produced by a semiconductor converter during normal operation is termed characteristic harmonics. In a three-phase, six-pulse rectifier with **no DC bus capacitor**, the characteristic harmonics are nontriplen odd harmonics (e.g., 5th, 7th, 11th, etc.). In general, the characteristic harmonics generated by a semiconductor rectifier are given by:

$$h = kq \pm 1$$

where h is the order of harmonics; k is any integer, and q is the pulse number of the semiconductor rectifier (six for a six-pulse rectifier). When operating a six-pulse rectifier system with a DC bus capacitor (as in voltage source inverters, or VSI), one may start observing harmonics of orders other than those given by the above equation. Such harmonics are called *noncharacteristic* harmonics. Though of lower magnitude, these also contribute to the overall harmonic distortion of the input current. The per-unit value of the characteristic harmonics present in the theoretical current waveform at the input of the semiconductor converter is given by $1/h$, where h is the order of the harmonics. In practice, the observed per-unit value of the harmonics is much greater than $1/h$. This is because the theoretical current waveform is a rectangular pattern made up of equal positive and negative halves, each occupying 120 electrical degrees. The pulsed discontinuous waveform observed commonly at the input of a three-phase full-wave rectifier system depends greatly on the impedance of the power system, the size of the DC bus capacitors, and the level of loading of the DC bus capacitors. Total harmonic current distortion is defined as:

$$THD_I = \frac{\sqrt{\sum_{n=2}^{n=\infty} I_n^2}}{I_1}$$

where I_1 is the rms value of the fundamental component of current; and I_n is the rms value of the n^{th} harmonic component of current.

Harmonic Limits Based on IEEE Std. 519-1992

The IEEE Std. 519-1992 relies strongly on the definition of the point of common coupling or PCC. The PCC from the utility viewpoint will usually be the point where power comes into the establishment (i.e., point of metering). However, IEEE Std. 519-1992 also suggests that **“within an industrial plant, the point of common coupling (PCC) is the point between the nonlinear load and other loads”** (IEEE Std. 519-1992). This suggestion is crucial since many plant managers and building supervisors feel that it is equally, if not more important to keep the harmonic levels at or below acceptable guidelines within their facility. In view of the many recently reported problems associated with harmonics within industrial plants, it is important to recognize the need for mitigating harmonics at the point where the offending equipment is connected to the power system. This approach would minimize harmonic problems, thereby reducing costly downtime and improving the life of electrical equipment. If one is successful in mitigating individual load current harmonics, then the total harmonics at the point of the utility connection will in most cases meet or exceed the IEEE recommended guidelines. In view of this, it is becoming increasingly common for specifiers to require nonlinear equipment suppliers to adopt the procedure outlined in IEEE Std. 519-1992 to mitigate the harmonics to acceptable levels at the point of the offending equipment. For this to be interpreted equally by different suppliers, the intended PCC must be identified. If the PCC is not defined clearly, many suppliers of offending equipment would likely adopt the PCC at the utility metering point, which would not benefit the plant or the building, but rather the utility.

Having established that it is beneficial to adopt the PCC to be the point where the nonlinear equipment connects to the power system, the next step is to establish the short circuit ratio. Short circuit ratio calculations are key in establishing the allowable current harmonic distortion levels. For calculating the short circuit ratio, one has to determine the available short circuit current at the input terminals of the nonlinear equipment. The short-circuit current available at the input of nonlinear equipment can be calculated by knowing the value of the short-circuit current available at the secondary of the utility transformer supplying power to the establishment (building) and the series impedance in the electrical circuit between the secondary of the transformer and the nonlinear equipment. **In practice, it is common to assume the same short circuit current level as at the secondary of the utility transformer feeding the nonlinear equipment.** The next step is to compute the fundamental value of the rated input current into the nonlinear equipment (three-phase full-wave rectifier in this case). An example is presented here to recap the above procedure. A widely used industrial equipment item that employs a three-phase full-wave rectifier is the voltage source inverter (VSI). These are used for controlling speed and torque of induction motors. Such equipment is also known as an Adjustable Speed Drive (ASD) or Variable Frequency Drive (VFD).

A 100-hp ASD/motor combination connected to a 480-V system being fed from a 1500-kVA, three-phase transformer with impedance of 4% is required to meet IEEE Std. 519-1992 at its input terminals. The rated current of the transformer is $1500 \times 1000 / (\sqrt{3} \times 480)$, and is calculated to be 1804.2 A. The short circuit current available at the secondary of the transformer is equal to the rated current divided by the per unit impedance of the transformer. This is calculated to be: 45,105.5 A. The short circuit ratio, which is defined as the ratio of the short circuit current at the PCC to the fundamental value of the nonlinear current is computed next. NEC amps for 100-hp, 460-V is 124 A. Assuming that the short circuit current at the ASD input is practically the same as that at the secondary of the utility transformer, the short-circuit

TABLE 14.1 Current Distortion Limits for General Distribution Systems

(120 V through 69,000 V)						
Maximum Harmonic Current Distortion in percent of I_L						
Individual Harmonic Order (Odd Harmonics) ^a						
I_{sc}/I_L	<11	$11 \leq h \leq 17$	$17 \leq h \leq 23$	$23 \leq h \leq 35$	$35 \leq h$	TDD ^b
<20 ^c	4.0	2.0	1.5	0.6	0.3	5.0
20 < 50	7.0	3.5	2.5	1.0	0.5	8.0
50 < 100	10.0	4.5	4.0	1.5	0.7	12.0
100 < 1000	12.0	5.5	5.0	2.0	1.0	15.0
>1000	15.0	7.0	6.0	2.5	1.4	20.0

^a Even harmonics are limited to 25% of the odd harmonic limits above.

^b TDD is Total Demand Distortion and is defined as the harmonic current distortion in % of maximum demand load current. The maximum demand current could either be a 15-minute or a 30-minute demand interval.

^c All power generation equipment is limited to these values of current distortion, regardless of actual I_{sc}/I_L ; where I_{sc} is the maximum short circuit current at PCC and I_L is the maximum demand load current (fundamental frequency) at PCC.

Source: IEEE Std. 519-1992.

ratio is calculated to be: $45,105.5/124$, which equals 363.75. On referring to IEEE Std. 519-1992, Table 10.3 (IEEE Std. 519-1992), the short circuit ratio falls in the 100–1000 category. For this ratio, the total demand distortion (TDD) at the point of ASD connection to the power system network is recommended to be 15% or less. For reference, see [Table 14.1](#).

Harmonic Mitigating Techniques

Various techniques of improving the input current waveform are discussed below. The intent of all techniques is to make the input current more continuous so as to reduce the overall current harmonic distortion. The different techniques can be classified into four broad categories:

1. Introduction of line reactors and/or DC link chokes
2. Passive filters (series, shunt, and low pass broadband filters)
3. Phase multiplication (12-pulse, 18-pulse rectifier systems)
4. Active harmonic compensation

The following paragraphs will briefly discuss the available technologies and their relative advantages and disadvantages. The term three-phase line reactor or just reactor is used in the following paragraphs to denote three-phase line inductors.

Three-Phase Line Reactors

Line reactors offer a significant magnitude of inductance that can alter the way the current is drawn by a nonlinear load such as a rectifier bridge. The reactor makes the current waveform less discontinuous, resulting in lower current harmonics. Since the reactor impedance increases with frequency, it offers larger impedance to the flow of higher order harmonic currents. Therefore, it is instrumental in impeding higher frequency current components while allowing the fundamental frequency component to pass through with relative ease.

On knowing the input reactance value, one can estimate the expected current harmonic distortion. A table illustrating the typically expected input current harmonics for various amounts of input reactance is shown in [Table 14.2](#).

Input reactance is determined by the accumulated impedance of the AC reactor, DC link choke (if used), input transformer, and cable impedance. To maximize the input reactance while minimizing AC voltage drop, one can combine the use of both AC-input reactors and DC link chokes. One can approximate the total effective reactance and view the expected harmonic current distortion from [Table 14.2](#). The effective impedance value in percent is based on the actual loading and is:

TABLE 14.2 Percent Harmonics vs. Total Line Impedance

Harmonic	Total Input Impedance							
	3%	4%	5%	6%	7%	8%	9%	10%
5th	40	34	32	30	28	26	24	23
7th	16	13	12	11	10	9	8.3	7.5
11th	7.3	6.3	5.8	5.2	5	4.3	4.2	4
13th	4.9	4.2	3.9	3.6	3.3	3.15	3	2.8
17th	3	2.4	2.2	2.1	0.9	0.7	0.5	0.4
19th	2.2	2	0.8	0.7	0.4	0.3	0.25	0.2
%THID	44	37	35	33	30	28	26	25
True rms	1.09	1.07	1.06	1.05	1.05	1.04	1.03	1.03

$$Z_{eff} = \frac{\sqrt{3} * 2 * \pi * f * L * I_{act(fnd.)}}{V_{L-L}} * 100$$

where $I_{act(fnd.)}$ is the fundamental value of the actual load current and V_{L-L} is the line-line voltage. The effective impedance of the transformer as seen from the nonlinear load is:

$$Z_{eff, x-mer} = \frac{Z_{eff, x-mer} * I_{act(fnd.)}}{I_r}$$

where $Z_{eff, x-mer}$ is the effective impedance of the transformer as viewed from the nonlinear load end; Z_{x-mer} is the nameplate impedance of the transformer; and I_r is the nameplate rated current of the transformer.

On observing one conducting period of a diode pair, it is interesting to see that the diodes conduct only when the instantaneous value of the input AC waveform is higher than the DC bus voltage by at least 3 V. Introducing a three-phase AC reactor in between the AC source and the DC bus makes the current waveform less pulsating because the reactor impedes sudden change in current. The reactor also electrically differentiates the DC bus voltage from the AC source so that the AC source is not clamped to the DC bus voltage during diode conduction. This feature practically eliminates flat topping of the AC voltage waveform caused by many ASDs when operated with weak AC systems.

DC Link Choke

Based on the above discussion, it can be noted that any inductor of adequate value placed between the AC source and the DC bus capacitor of the ASD will help in improving the current waveform. These observations lead to the introduction of a DC link choke, which is electrically present after the diode rectifier and before the DC bus capacitor. The DC link choke performs very similar to the three-phase line inductance. The ripple frequency that the DC link choke has to handle is six times the input AC frequency for a six-pulse ASD. However, the magnitude of the ripple current is small. One can show that the effective impedance offered by a DC link choke is approximately half of that offered by a three-phase AC inductor. In other words, a 6% DC link choke is equivalent to a 3% AC inductor from an impedance viewpoint. This can be mathematically derived equating AC side power flow to DC side power flow as follows:

$$P_{ac} = \frac{3 * V_{L-N}^2}{R_{ac}}; \quad P_{ac} = P_{dc}$$

V_{L-N} is the line-neutral voltage at the input to the three-phase rectifier.

$$P_{dc} = \frac{V_{dc}^2}{R_{dc}}; \quad V_{dc} = \frac{3 * \sqrt{3} * \sqrt{2} * V_{L-N}}{\pi}; \quad \text{Hence, } R_{dc} = 2 * \left(\frac{9}{\pi^2} \right) R_{ac}$$

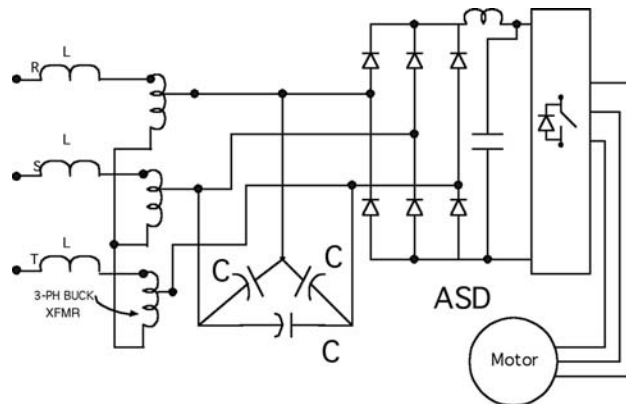


FIGURE 14.23 Schematic representation of a low-pass broadband harmonic filter connected to an ASD with diode rectifier front end. U.S. Patent 5,444,609.

Since $9/\pi^2$ is approximately equal to 1, the ratio of DC impedance to AC impedance can be said to be approximately 1:2. The DC link choke is less expensive and smaller than a three-phase line reactor and is often included inside an ASD. However, as the derivation shows, one has to keep in mind that the effective impedance offered by a DC link choke is only half its numerical impedance value when referred to the AC side. DC link chokes are electrically after the diode bridge and so they do not offer any significant spike or overvoltage surge protection to the diode bridge rectifiers. It is a good engineering practice to incorporate both a DC link choke and a three-phase line reactor in an ASD for better overall performance.

Passive Filters

Passive filters consist of passive components like inductors, capacitors, and resistors arranged in a pre-determined fashion either to attenuate the flow of harmonic components through them or to shunt the harmonic component into them. Passive filters can be of many types. Some popular ones are series passive filters, shunt passive filters, and low-pass broadband passive filters. Series and shunt passive filters are effective only in the narrow proximity of the frequency at which they are tuned. Low-pass broadband passive filters have a broader bandwidth and attenuate almost all harmonics above their cutoff frequency. However, applying passive filters requires good knowledge of the power system because passive filter components can interact with existing transformers and power factor correcting capacitors and could create electrical instability by introducing resonance into the system. Some forms of low-pass broadband passive filters do not contribute to resonance but they are bulky, expensive, and occupy space. A typical low-pass broadband filter structure popularly employed by users of ASDs is shown in [Fig. 14.23](#).

Phase Multiplication

As discussed previously, the characteristic harmonics generated by a full-wave rectifier bridge converter is a function of the pulse number for that converter. A 12-pulse converter will have the lowest harmonic order of 11. In other words, the 5th, and the 7th harmonic orders are theoretically nonexistent in a 12-pulse converter. Similarly, an 18-pulse converter will have harmonic spectrum starting from the 17th harmonic and upwards. The lowest harmonic order in a 24-pulse converter will be the 23rd. The size of the passive harmonic filter needed to filter out the harmonics reduces as the order of the lowest harmonic in the current spectrum increases. Hence, the size of the filter needed to filter the harmonics out of a 12-pulse converter is much smaller than that needed to filter out the harmonics of a 6-pulse converter. However, a 12-pulse converter needs two 6-pulse bridges and two sets of 30° phase shifted AC inputs. The phase shift is achieved either by using an isolation transformer with one primary and two phase-shifted secondary windings or by using an autotransformer that provides phase-shifted outputs. Many different autotransformer topologies exist and the choice of a topology over the other involves a compromise between ease of construction, performance, and cost. An 18-pulse converter would need three 6-pulse diode bridges and three sets of 20° phase shifted inputs; similarly, a 24-pulse converter

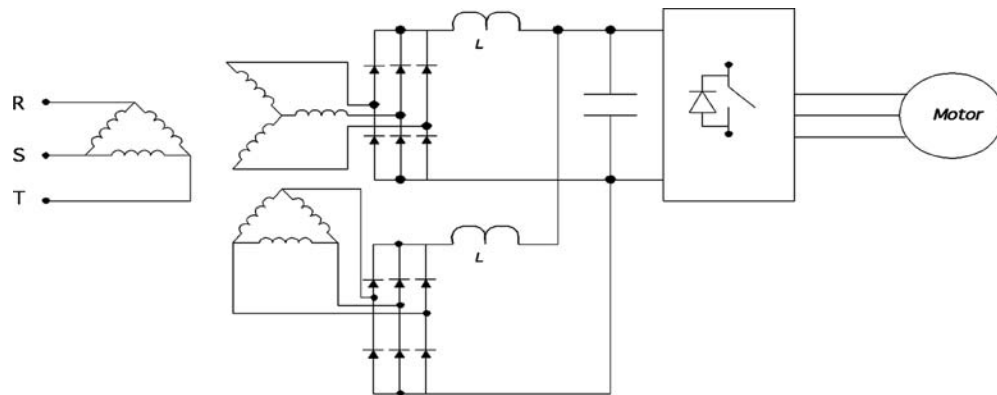


FIGURE 14.24 Schematic of a 12-pulse converter employing a three-winding transformer. Note that the input transformer has to be sized for rated power operation.

would need four 6-pulse diode bridges and four sets of 15° phase-shifted inputs. The transformers providing the phase-shifted outputs for multipulse converters have to be properly designed to handle circulating harmonic flux.

A typical 12-pulse structure is shown in Fig. 14.24. In one electrical cycle, the DC voltage will have 12 humps and hence the name 12-pulse rectifier.

Active Harmonic Compensation

Most passive techniques discussed above aim to cure the harmonic problems once nonlinear loads have created them. However, motor-drive manufacturers are developing rectification techniques that do not generate low-order harmonics. These drives use active front ends. Instead of using diodes as rectifiers, the active front-end ASDs make use of active switches like IGBTs along with parallel diodes. Power flow through a switch becomes bidirectional and can be manipulated to recreate a current waveform that linearly follows the applied voltage waveform.

Apart from the active front ends, there also exist shunt active filters used for actively introducing a current waveform into the AC network, which, when combined with the harmonic current, results in an almost perfect sinusoidal waveform.

One of the most interesting active filter topologies for use in retrofit applications is the combination of a series active filter along with shunt tuned passive filters. This combination is also known as the hybrid structure.

Most active filter topologies are complicated and require active switches and control algorithms that are implemented using digital signal processing (DSP) chips. The active filter topology also needs current and voltage sensors and corresponding analog-to-digital (A/D) converters. This extra hardware increases the cost and component count, reducing the overall reliability and robustness of the design. Manufacturers of smaller power equipment like computer power supplies, lighting ballast, etc. have successfully employed active circuits, employing boost converter topologies.

Controlled Rectifiers

Controlled rectifier circuits make use of devices known as “thyristors.” A thyristor is a four-layer ($p-n-p-n$), three-junction device that conducts current only in one direction similar to a diode. The last (third) junction is utilized as the control junction and consequently the rectification process can be initiated at will provided the device is favorably biased and the load is of favorable magnitude. The operation of a thyristor can be explained by assuming it to be made up of two transistors connected back-to-back as shown in Fig. 14.25.

Let α_1 and α_2 be the ratio of collector to emitter currents of transistors Q1 and Q2, respectively. In other words:

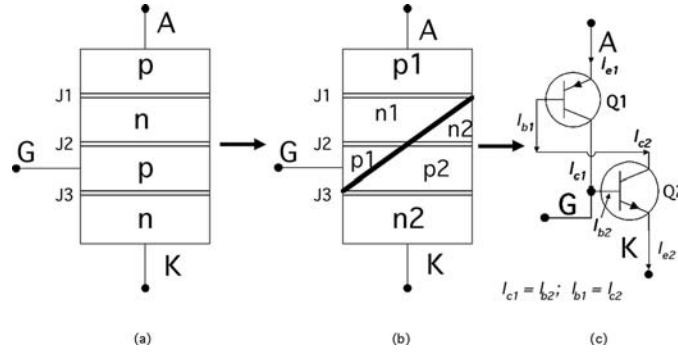


FIGURE 14.25 Virtual representation of a thyristor to explain its operation.

$$\alpha_1 = \frac{I_{c1}}{I_{e1}}; \quad \alpha_2 = \frac{I_{c2}}{I_{e2}};$$

Also, from Fig. 14.25: $I_{e1} = I_{e2} = I_A$ where I_A is the anode current flowing through the thyristor. From transistor theory, the value of I_{e2} is equal to $I_{c2} + I_{b2} + I_{lkg}$; where I_{lkg} is the leakage current crossing the $n1$ - $p2$ junction. From Fig. 14.25, $I_{b2} = I_{c1}$. Hence, the anode current can be rewritten as:

$$I_A = I_{c1} + I_{c2} + I_{lkg}$$

Substituting the collector currents by the product of ratio α and emitter current, the anode current becomes:

$$I_A = (\alpha_1 * I_{e1}) + (\alpha_2 * I_{e2}) + I_{lkg}$$

$$I_A = (\alpha_1 + \alpha_2) I_A + I_{lkg}$$

$$I_A = \frac{I_{lkg}}{1 - (\alpha_1 + \alpha_2)}$$

If the ratios of the collector current to base current (gain) of the transistors are assumed to be β_1 and β_2 , respectively, then the relationship between β_1 , β_2 and α_1 , α_2 can be written as:

$$\alpha_1 = \frac{\beta_1}{1 + \beta_1}; \quad \alpha_2 = \frac{\beta_2}{1 + \beta_2}$$

Substituting for α_1 and α_2 in the expression for I_A yields the following expression:

$$I_A = \frac{(1 + \beta_1)(1 + \beta_2) I_{lkg}}{1 - \beta_1 \beta_2}.$$

If the values of α_1 and α_2 are low (low gains), then the anode current is low and comparable to the leakage current. Under this condition, the thyristor is said to be in its OFF state. However, if the effective gain of the transistor is such that the product of the gains are close to 1 (i.e., sum of the ratios of α_1 and

α_2 are close to 1), then there is a large increase in anode current and the thyristor is said to be in conduction. External circuit conditions can be changed to influence the product of the gains ($\beta_1\beta_2$). Some techniques of achieving this are briefly discussed next.

Increasing applied voltage: On applying a voltage across the anode to cathode terminals of the thyristor (anode being more positive than the cathode), one can see that junctions J1 and J3 in Fig. 14.25 are forward biased while junction J2 is reverse biased. The thyristor does not conduct any current and is said to be in a blocking state. On increasing the applied voltage, minority carriers in junction J2 (i.e., holes in $n1$, $n2$ and electrons in $p1$, $p2$) start acquiring more energy and hence start to migrate. In the process, these holes could dislodge more holes. Recombination of the electrons and holes also occur, which creates more motion. If the voltage is increased beyond a particular level, the movement of holes and electrons becomes great and junction J2 ceases to exist. The product of the gains of the two transistors in the two-transistor model is said to achieve values close to unity. This method of forcing current to flow through the thyristor is not recommended since junction J2 gets permanently damaged and the thyristor ceases to block forward voltage. Hence, this method is a destructive method.

High dv/dt : As explained earlier, junction J2 is the forward blocking junction when a forward voltage is applied across anode to cathode of a thyristor. Any p - n junction behaves like a depletion region when it is reverse-biased. Since J2 is reverse-biased, this junction behaves like a depletion region. Another way of looking at a depletion region is that the boundary of the depletion region has abundant holes and electrons while the region itself is depleted of charged carriers. This characteristic is similar to that of a capacitor. If the voltage across the junction (J2) changes very abruptly, then there will be rapid movement of charged carriers through the depleted region. If the rate of change of voltage across this junction (J2) exceeds a predetermined value, then the movement of charged carriers through the depleted region is so high that junction J2 is again annihilated. After this event, the thyristor is said to have lost its capability to block forward voltage and even a small amount of forward voltage will result in significant current flow, limited only by the load impedance. This method is destructive too, and is hence not recommended.

Temperature: Temperature affects the movement of holes and electrons in any semiconductor device. Increasing the temperature of junction J2 will have a very similar effect. More holes and electrons will begin to move, causing more dislodging of electrons and holes from neighboring lattice. If a high temperature is maintained, this could lead to an avalanche breakdown of junction J2 and again render the thyristor useless since it would no longer be able to block forward voltage. Increasing temperature is yet another destructive method of forcing the thyristor to conduct.

Gate current injection: If a positive voltage is applied across the gate to cathode of a thyristor, then one would be forward biasing junction J3. Charged carriers will start moving. The movement of charged carriers in junction J3 will attract electrons from $n2$ region of the thyristor (Fig. 14.25). Some of these electrons will flow out of the gate terminal but there would be ample of electrons that could start crossing junction J2. Since electrons in $p2$ region of junction J2 are minority carriers, these can cause rapid recombination and help increase movement of minority carriers in junction J2. By steadily increasing the forward biasing potential of junction J3, one could potentially control the depletion width of junction J2. If a forward biasing voltage is applied across anode to cathode of the thyristor with its gate to cathode favorably biased at the same time, then the thyristor can be made to conduct current. This method achieves conduction by increasing the leakage current in a controlled manner. The gain product in the two-transistor equivalent is made to achieve a value of unity in a controlled manner and the thyristor is said to turn ON. This is the only recommended way of turning ON a thyristor. When the gate-cathode junction is sufficiently forward biased, the current through the thyristor depends on the applied voltage across the anode-cathode and the load impedance. The load impedance and the externally applied anode-cathode voltage should be such that the current through the thyristor is greater than a minimum current known as *latching current*, I_L . Under such a condition, the thyristor is said to have *latched ON*. Once it has latched ON, the thyristor remains ON. In other words, even if the forward biasing voltage across the gate-cathode terminals is removed, the thyristor continues to conduct. Junction J2 does not exist during the ON condition. The thyristor reverts to its blocking state only when the current through it falls below a minimum threshold value known as *holding current*, I_H . Typically, holding current is lower than latching

current ($I_h < I_l$). There are two ways of achieving this. They are either (1) increase the load impedance to such a value that the thyristor current falls below I_h or (2) apply reverse-biasing voltage across the anode-cathode of the thyristor.

An approximate v - i characteristic of a typical thyristor and its symbol are shown in Fig. 14.26.

Since the thyristor allows flow of current only in one direction like a diode and the instant at which it is turned ON can be controlled, the device is a key component in building a controlled rectifier unit. One can replace the diode in all the circuits discussed so far with the thyristor. Because of its controllability, the instant at which the thyristor conducts can be delayed to alter the average and rms output voltages. By doing so, one can choose to control the output voltage and power of a rectifier circuit. Hence, rectifiers that employ thyristors are also known as silicon controlled rectifiers or SCR.

A typical single-phase, R-L rectifier circuit with one thyristor as the rectifier is shown in Fig. 14.27. The figure also shows the relevant circuit waveforms. The greatest difference between this circuit and its diode counterpart is also shown for comparison. Both circuits conduct beyond π radians due to the presence of the inductor L since the average voltage across an inductor is zero. If the value of the circuit components and the input supply voltage are the same in both cases, the duration for which the current flows into the output R-L load depends on the values of R and L . In the case of the diode circuit, it does not depend on anything else; while in the case of the thyristor circuit, it also depends on the instant the thyristor is given a gate trigger.

From Fig. 14.27, it is interesting to note that the energy stored in the inductor during the conduction interval can be controlled in the case of a thyristor in such a manner so as to reduce the conduction interval and thereby alter (reduce) the output power. Both the diode and the thyristor show reverse recovery phenomenon. The thyristor, like the diode, can block reverse voltage applied across it repeatedly, provided the voltage is less than its breakdown voltage.

Gate Circuit Requirements

The trigger signal should have voltage amplitude greater than the minimum gate trigger voltage of the thyristor being turned ON. It should not be greater than the maximum gate trigger voltage, either. The gate current should likewise be in between the minimum and maximum values specified by the thyristor manufacturer. Low gate current driver circuits can fail to turn ON the thyristor. The thyristor is a current controlled switch and so the gate circuit should be able to provide the needed turn ON gate current into the thyristor. Unlike the bipolar transistor, the thyristor is not an amplifier and so the gate current requirement does not absolutely depend on the voltage and current rating of the thyristor. Sufficient gate trigger current will turn ON the thyristor and current will flow from the anode to the cathode provided that the thyristor is favorably biased and the load is such that the current flowing is higher than the latching current of the thyristor. In other words, in single phase AC to DC rectifier circuits, the gate trigger will turn ON the thyristor only if it occurs during the positive part of the AC cycle (Fig. 14.27). Any trigger signal during the negative part of the AC cycle will not turn ON the thyristor and the thyristor will remain in blocking state. Keeping the gate signal ON during the negative part of the AC cycle does not typically damage a thyristor.

Single-Phase H-bridge Rectifier Circuits with Thyristors

Similar to the diode H-bridge rectifier topology, there exist SCR-based rectifier topologies. Because of their unique ability to be controlled, the output voltage and hence the power can be controlled to desired levels. Since the triggering of the thyristor has to be synchronized with the input sinusoidal voltage in

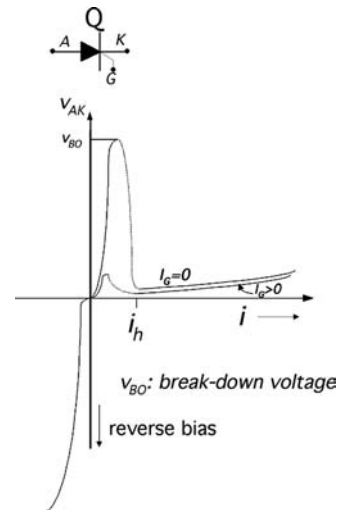


FIGURE 14.26 v - i characteristic of a thyristor along with its symbol.

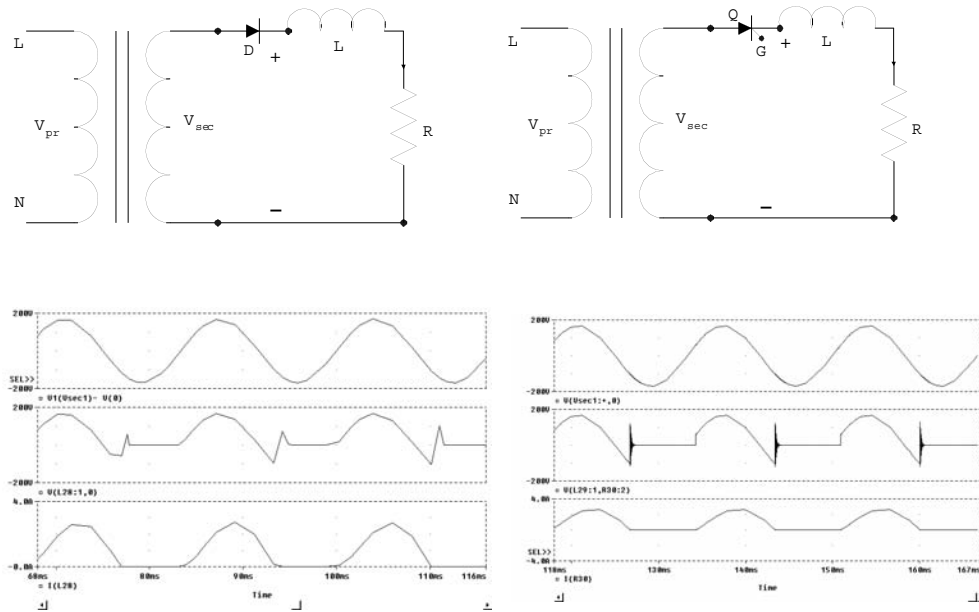


FIGURE 14.27 Comparing a single diode rectifier circuit with a single thyristor rectifier circuit. Note that the thyristor conduction is delayed deliberately to bring out the differences.

an AC to DC rectifier circuit, one can achieve a soft-charge characteristic of the filter capacitor. In other words, there is no need for employing soft-charge resistor and contactor combination as is required in single-phase and three-phase AC to DC rectifier circuits with DC bus capacitors.

In controlled AC to DC rectifier circuits, it is important to discuss control of resistive, inductive, and resistive-inductive load circuits. DC motor control falls into the resistive-inductive load circuit. DC motors are still an important part of the industry. However, the use of DC motors in industrial applications is declining rapidly. Control of DC motors are typically achieved by controlled rectifier circuits employing thyristors. Small motors of less than 3 kW (approximately 5 hp) rating can be controlled by single-phase SCR circuits while larger ratings require three-phase versions. A typical single-phase H-bridge SCR-based circuit for the control of a DC motor is shown in Fig. 14.28. Typical output waveforms are shown in Fig. 14.29. The current in the load side can be assumed continuous due to the large inductance of the armature of the DC motor.

In Fig. 14.28, V_f is the field voltage, which is applied externally and generally is independent of the applied armature voltage. Such a DC motor is known as a separately excited motor. I_a is the armature current while I_f is the field current. The output of the controlled rectifier is applied across the armature. Since the output voltage can be controlled, one can effectively control the armature current. Since the

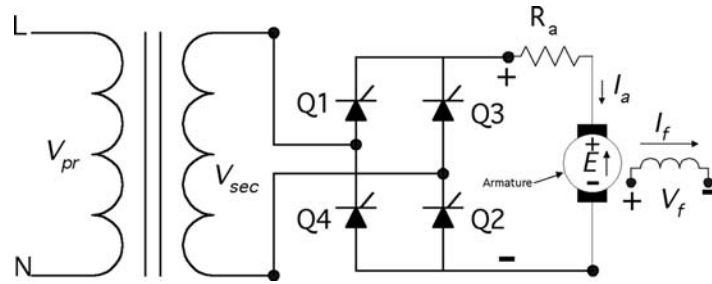


FIGURE 14.28 Single-phase DC motor control circuit for controlling a separately excited DC motor. R_a indicates equivalent armature resistance and E is the back emf.

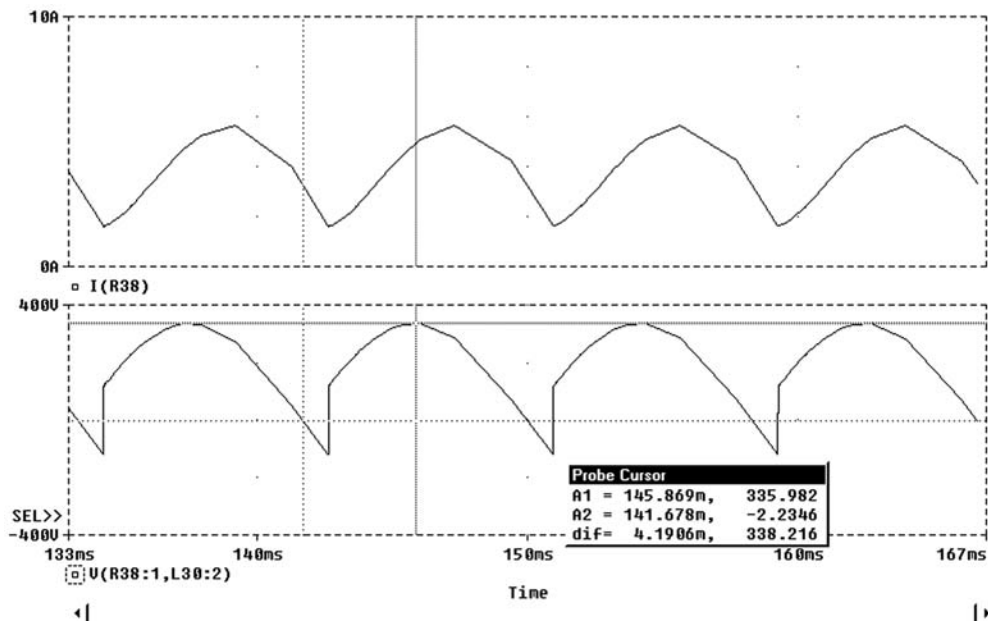


FIGURE 14.29 Armature current and output voltage of AC to DC rectifier employed to control a DC motor.

torque produced by a DC motor is directly proportional to the armature current, the torque developed can thus be controlled.

$$T = K\phi I_a;$$

where K is the motor constant and depends on the number of armature conductors, number of poles, and type of winding employed in the DC machine. ϕ is flux produced by the field and is proportional to the field current, I_f . Hence, the torque produced by a DC machine can be rewritten as $T = K(K_f I_f) I_a$. By keeping the field current constant, the torque then becomes directly proportional to the armature current, which is controlled by controlling the output voltage of the AC to DC controlled rectifier. In the circuit shown in Fig. 14.28, it is interesting to note that the current I_a cannot flow in the opposite direction. Hence, the motor cannot generate negative torque. In order to make the motor run in the opposite direction, the direction of the field has to be changed. Speed control within the base speed can also be accomplished by controlling the armature voltage as is shown below.

$$E = K\phi\omega = K(K_f I_f)\omega;$$

ω is the speed of the armature in radians/sec. The back emf, E , is the difference between the output DC voltage of the AC to DC controlled rectifier and the drop across the equivalent armature resistance. Hence, E can be rewritten as:

$$E = V_a - (I_a R_a); \quad \omega = \frac{V_a - (I_a R_a)}{KK_1 I_f}$$

For control of speed beyond base speed, the field current has to be altered. Hence, it can be shown that controlling the armature current can control the speed and torque produced by a DC machine. Controlling the output DC voltage can control the armature current. Because of the large inductance of the armature circuit, the current through it can be assumed to be continuous for a practical operating region. The average output voltage of a single-phase AC to DC rectifier circuit for continuous current operation is given by (referring to Fig. 14.29):

$$V_o = \frac{1}{\pi} \int_{\alpha}^{\pi+\alpha} (\sqrt{2} * V_{rms}) d(\omega t) = \frac{2 * \sqrt{2} * V_{rms} * \cos(\alpha)}{\pi};$$

for continuous current condition. By controlling the triggering angle, α , one can control the average value of the output voltage, V_o . If armature current control is the main objective (to control output torque), then one can configure the controller of Fig. 14.28 with a feedback loop. The measured current can be compared with a set reference and the error can be used to control the triggering angle, α . Since the output voltage and hence the armature current are not directly proportional to α but to $\cos(\alpha)$, the above method will yield a nonlinear (co-sinusoidal) relationship between the output voltage and control angle, α . However, one could choose to use the error signal to control $\cos(\alpha)$ instead of α . This would then yield a linear relationship between the output voltage and \cos of control angle, α .

It is interesting to note from the equation for the output average voltage that the output average voltage can become negative if the triggering angle is greater than 90 electrical degrees. This leads us to the topic of regeneration. AC to DC controlled rectifiers employing thyristors and having large inductance on the DC side can be made to operate in the regeneration mode by simply delaying the trigger angle. This is quite beneficial in overhauling loads like cranes. When the load on a hook of the crane has to be lifted up, electrical energy is supplied to the motor. The voltage across the motor is positive and the current through the armature is positive. Positive torque is generated and hence the load moves up. When the load is to be brought down, the load starts to rotate the motor in the opposite direction due to gravity. The voltage at the terminals becomes negative since speed is negative. The thyristors are gated at an angle greater than 90 electrical degrees to match the generated (negative) voltage of the DC motor. Since current through the thyristors cannot go negative, current is forced to flow into the DC motor in the positive direction. The large inductance of the motor helps to maintain the positive direction of current through the armature. Positive torque is still produced since the direction of current is still positive and the field remains unchanged. In other words, the motor develops positive torque and tries to move the load up against gravity but the gravity is pushing the motor down. The product of current through the motor and the voltage across it is negative, meaning that the motor is not consuming energy, and on the contrary, is producing electrical energy — the kinetic energy due to the motor's downward motion is partly converted to electrical energy by the field and armature. This energy produced by the motor is routed out to the supply via the appropriately gated thyristors. Conversion of kinetic energy to electrical energy acts like a **dynamic-brake** and slows the rapid downward descent of the load.

A typical crane is required to operate in all four quadrants (Fig. 14.30). In the first quadrant, the motor develops positive torque and the motor runs in the positive direction, meaning its speed is positive — the product of torque and speed is power, and so positive electric power is supplied to the motor from the AC to DC rectifier. When the crane with a load is racing upward, close to the end of its travel, the

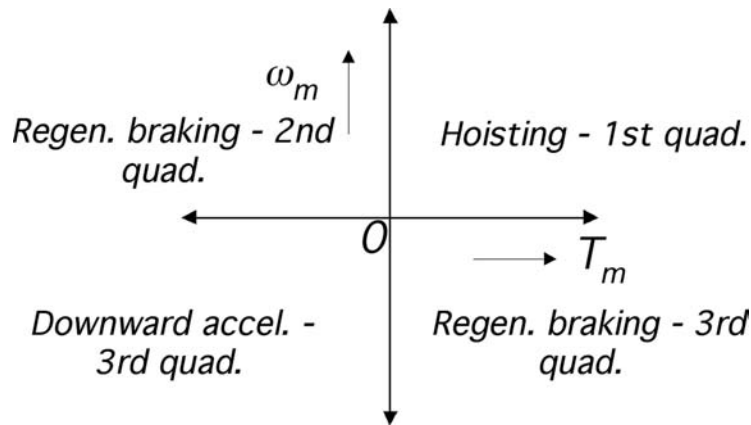


FIGURE 14.30 Four-quadrant operation of a crane or hoist.

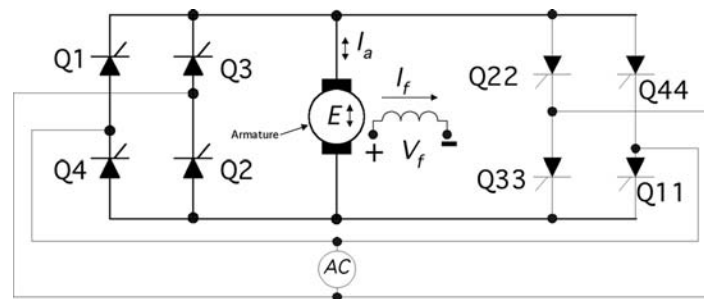


FIGURE 14.31 Two rectifier-bridge arrangements for four-quadrant operation of DC motor.

AC to DC controlled rectifier is made to stop powering the motor. The rectifier generates practically no voltage. The inertia of the load moving upward generates a voltage in the form of a back emf. This voltage is fed into a second rectifier bridge arranged in the opposite direction as shown in Fig. 14.31. The second bridge is turned ON to let the generated voltage across the still upwardly mobile motor flow into the utility, thereby converting the inertial motion to electric power. In the second quadrant, speed remains positive but torque becomes negative, since the current through the motor flows in the opposite direction into the second rectifier bridge arrangement (Fig. 14.31). The product of speed and torque is negative, meaning that the motor behaves like a generator during this part of the travel.

The third quadrant, as explained earlier, occurs at the beginning of the lowering action. Both torque and speed are negative and so the product of torque and speed is positive. Power is applied to the motor to overcome static friction and accelerate the rotating parts of the mechanism to move the load downward. In this case, the direction of armature current through the motor is opposite to that in quadrant 1, and the electrical power needed by the motor is supplied by the second rectifier bridge arrangement (Fig. 14.31).

The mechanical load and motor arrangement goes into the fourth quadrant of operation for the larger part of the downward motion. This is the period during which the motor resists the tendency of the load to accelerate downward by developing positive torque. Since motion is downward, speed is negative and the product of torque and speed is negative. This means the motor behaves like a generator as explained earlier.

Since the thyristors cannot conduct in the opposite direction, a new inverter section had to be provided to enable the four-quadrant operation needed in cranes and hoists. The method by which unidirectional electrical power was routed to the bidirectional AC utility lines is known as inversion (opposite of rectification). Since no external means of switching OFF the thyristors was employed, the process of inversion was achieved by natural commutation. Such an inverter is also known as a line commutated inverter.

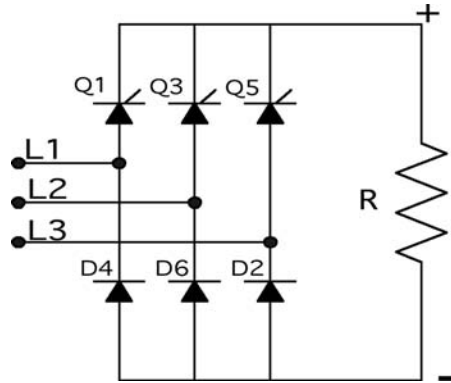


FIGURE 14.32 A typical three-phase semiconverter. Rarely employed in modern industry.

Three-Phase Controlled AC to DC Rectifier Systems

The observations made so far for the single-phase controlled AC to DC rectifiers can be easily extended to three-phase versions. An important controlled rectification scheme that was not mentioned in the single-phase case is the semiconverter circuit. In Fig. 14.28, if the thyristors Q2 and Q4 are replaced by diodes (D2 and D4), then the circuit of Fig. 14.28 is converted into a semiconverter circuit. Such a circuit does not have the potential to provide regeneration capability and hence is of limited use. However, in dual converter applications, especially in three-phase versions, there are a few instances where a semiconverter can be employed to reduce cost. A typical three-phase semiconverter circuit will consist of three thyristors and three diodes arranged in an H-bridge configuration as shown in Fig. 14.32.

Three-phase dual converter schemes similar to the one shown in Fig. 14.31 are still employed to operate large steel mills, hoists, and cranes. However, the advent of vector controlled AC drives has drastically changed the electrical landscape of the modern industry. Most DC motor applications are being rapidly replaced by AC motors with field-oriented control schemes. DC motor application in railway traction has also seen significant reduction due to the less expensive and more robust AC motors.

However, there are still a few important applications where three-phase controlled rectification (inversion) is the most cost-effective solution. One such application is the regenerative converter module that many inverter-drive manufacturers provide as optional equipment to customers with overhauling loads. Under normal circumstances, during the motoring mode of operation of an AC drive, the regenerative unit does not come into the circuit. However, when the DC bus voltage tends to go higher than a predetermined level due to overhauling of the load, the kinetic energy of the load is converted into electrical energy and is fed back into the AC system via a six-pulse thyristor-based inverter-bridge. One such scheme is shown in Fig. 14.33.

Average Output Voltage

In order to evaluate the average value of the output voltage for a three-phase full-bridge converter, the process of integrating the output voltage similar to the one in Fig. 14.21(b) has to be undertaken. For the circuit shown in Fig. 14.20(b), where the diodes are replaced by thyristors, the integration yields the following:

$$V_o = \frac{3}{\pi} \int_{\alpha + (\pi/3)}^{\alpha + (2\pi/3)} \sqrt{2} V_{L-L} \sin(\omega t) d(\omega t)$$

$$V_o = \frac{3 * \sqrt{2} * V_{L-L} * \cos(\alpha)}{\pi} = \frac{3 * \sqrt{2} * \sqrt{3} * V_{L-N} * \cos(\alpha)}{\pi}$$

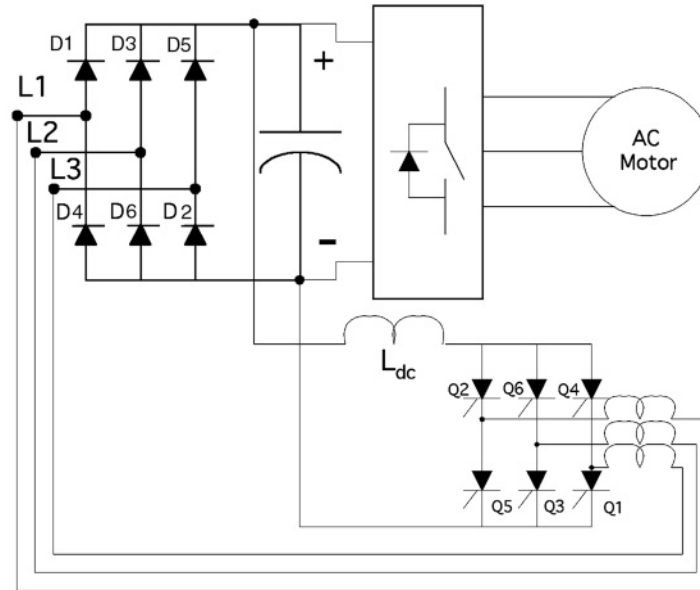


FIGURE 14.33 Use of six-pulse thyristor bridge in the inverter mode to provide regeneration capability to an existing AC drive system.

The average output voltage for the circuit in Fig. 14.20(b) with the diodes being replaced by thyristors is only different in the *cosine* of the triggering angle, α . If the triggering angle is zero, the circuit performs similar to a three-phase diode rectifier and the average output voltages become the same.

HVDC Transmission Systems

One area where it is difficult to replace the use of high voltage, high current carrying thyristors is high voltage DC (HVDC) transmission systems. When a large amount of power is to be transported over long distances, or under water, it has been found that high voltage DC transmission is more economical. HVDC systems are in reality back-to-back rectifier systems. The sending end rectifier system consists typically of 12- or 24-pulse thyristor bridges while the receiving end consists of a similar configuration but in the opposite direction. The receiving end 12- or 24-pulse bridge operates in the inverter mode while the sending end operates in the rectifier mode. 12-pulse configuration is achieved by cascading two 6-pulse bridges in series while 24-pulse configuration needs four 6-pulse bridges cascaded in series. Typical advantages of high voltage DC transmission over high voltage AC transmission is briefly listed below:

1. No stability problems due to transmission line length since no reactive power needs to be transmitted.
2. No limitation of cable lengths for underground cable or submarine cable transmission due to the fact that no charging power compensation need be done.
3. AC power systems can be interconnected employing a DC tie without reference to system frequencies, short circuit power, etc.
4. High-speed control of DC power transmission is possible due to the fact that the control angle, α , has a relatively short time constant.
5. Fault isolation between receiving end and sending end can be dynamically achieved due to fast efficient control of the high voltage DC link.
6. Employing simple control logic can change energy flow direction very fast. This can help in meeting peak demands at either the sending or the receiving station.
7. High reliability of thyristor converter and inverter stations makes this mode of transmission a viable solution for transmission lengths typically over 500 km.
8. The right-of-way needed for high voltage DC transmission is much lower than that of AC transmission of the same power capacity.

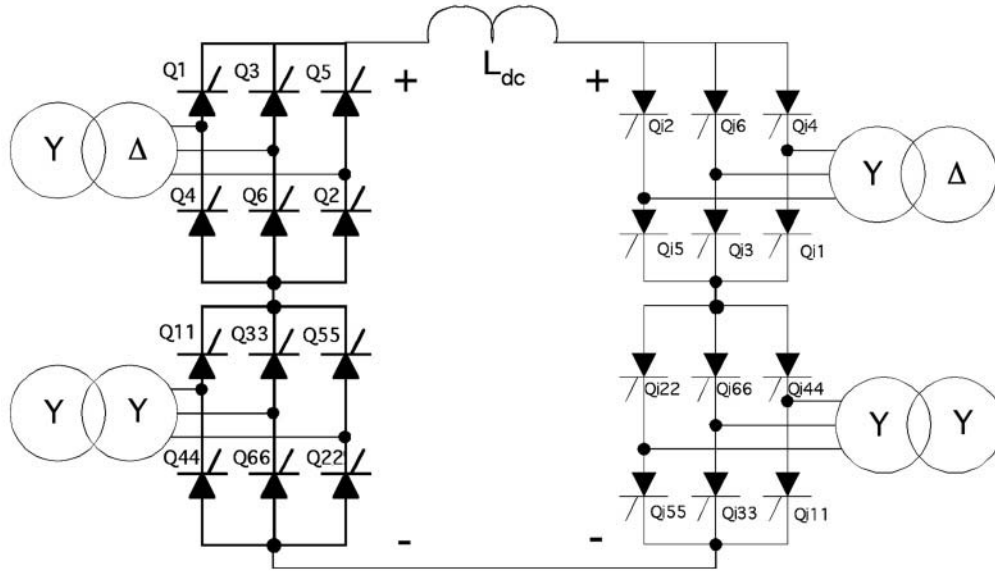


FIGURE 14.34 Schematic representation of a bipolar HVDC system employing 12-pulse rectification/inversion scheme.

The advantages of DC transmission over AC should not be misunderstood and DC should not be considered as a general substitute for AC power transmission. In a power system, it is generally believed that both AC and DC should be considered as complementary to each other, so as to bring about the integration of their salient features to the best advantage in realizing a power network that ensures high quality and reliability of power supply. A typical rectifier-inverter system employing a 12-pulse scheme is shown in Fig. 14.34.

Typical DC link voltage can be as high as 400 kV to 600 kV. Higher voltage systems are also in use. Typical operating power levels are over 1000 MW. There are a few systems transmitting close to 3500 MW of power through two bipolar systems. Most thyristors employed in large HVDC transmission systems are liquid cooled to improve their performance.

Power System Interaction with Three-phase Thyristor AC to DC Rectifier Systems

Similar to the diode rectifiers, the thyristor based AC to DC rectifiers also suffer from low order current harmonics. In addition to current harmonics, there is a voltage notching phenomenon occurring at the input terminals of an AC to DC thyristor based rectifier system. The voltage notching is a very serious problem. Since thyristors are generally slower to turn ON and turn OFF compared to power semiconductor diodes, there are nontrivial durations during which an outgoing thyristor and an incoming thyristor remain in conduction, thereby creating a short-circuit across the power supply phases feeding the corresponding thyristors. Thyristors used in rectifiers are generally known as phase control type thyristors and have typical turn OFF times of 50 to 100 μsec . Thyristors employed in inverter circuits typically are faster and have turn OFF times in the 10 to 50 μsec range.

Notching can create major disturbances in sensitive electronic equipment that rely on the zero-crossing of the voltage for satisfactory operation. Multiple pseudo zero-crossings of the voltage waveform can occur due to the notching effect of thyristor based rectifier systems. Notching can create large magnitudes of currents to flow into power-factor correcting capacitors, thereby potentially causing permanent damage to them. IEEE Std. 519-1992 in the U.S. has strict regulations regarding the depth of the notch as well as the duration of the notch. AC line inductors in series with the supply feeding power to the three-phase bridge help to minimize the notching effect on the power system. The theory behind this phenomenon is discussed next.

When an external inductance is added in front of a three-phase AC to DC rectifier employing thyristors, the duration of commutation increases. In other words, the time period for which the outgoing thyristor remains in conduction along with the incoming thyristor increases. This overlap period causes the average output voltage to reduce because during this period, the output voltage is composed of two shorted phases and a healthy phase. The extent of reduction in the output voltage depends on the duration of overlap in electrical degrees. The duration of overlap in electrical degrees is commonly represented by μ . The overlap duration is directly proportional to the value of the external inductance used. If no external line inductor is used, then this duration will depend on the existing inductance of the system including the wiring inductance. In order to compute the factors influencing the overlap duration, a simple model can be assumed. Assume that the line is comprised of inductance L in each phase. Let the DC load current be I_{dc} and let it be assumed that this current does not change during the overlap interval. The current in the incoming thyristor is zero at start and by the end of the overlap interval, it rises to I_{dc} . Based on this assumption, the relationship between current and voltage can be expressed as:

$$v_{ab} = \sqrt{2} * V_{L-L} * \sin(\omega t) = 2 * L * (di/dt)$$

$$\sqrt{2} * V_{L-L} * \int_{\alpha + (\pi/3)}^{\alpha + (\pi/3) + \mu} \sin(\omega t) d(t) = 2 * L * \int_0^{I_{dc}} di$$

$$I_{dc} = \frac{\sqrt{2} * V_{L-L} * (\cos(\alpha + \pi/3) - \cos(\alpha + \pi/3 + \mu))}{2\omega L} = \frac{\sqrt{2} * V_{L-L} * \sin(\alpha + \pi/3 + \mu/2) * \sin(\mu/2)}{\omega L}$$

For small values of overlap angle μ , $\sin(\mu/2) = \mu/2$ and $\sin(\alpha + \pi/3 + (\mu/2)) = \sin(\alpha + \pi/3)$. Rearranging the above equation yields:

$$\mu = \frac{2\omega L * I_{dc}}{\sqrt{2} * V_{L-L} * \sin(\alpha + \pi/3)}.$$

From the above expression, it is interesting to note the following:

1. If the inductance L in the form of either external inductance or leakage inductance of transformer or lead length is large, the overlap duration will be large.
2. If the load current, I_{dc} is large, the overlap duration will be large.
3. If the delay angle is small, then the inductance will store more energy and so the duration of overlap will be large. The minimum value of delay angle α is 0° and the maximum value typically is 60° .

The average output voltage will reduce due to the overlap angle as mentioned before. In order to compute the average output voltage with a certain overlap angle, the limits of integration have to be changed. This exercise yields the following:

$$V_o = \frac{3}{\pi} \int_{\alpha + \mu + (\pi/3)}^{\alpha + \mu + (2\pi/3)} \sqrt{2} V_{L-L} \sin(\omega t) d(\omega t)$$

$$V_o = \frac{3 * \sqrt{2} * V_{L-L} * \cos(\alpha + \mu)}{\pi} = \frac{3 * \sqrt{2} * \sqrt{3} * V_{L-N} * \cos(\alpha + \mu)}{\pi}$$

Thus, it can be seen that the overlap angle has an equivalent effect of advancing the delay angle, thereby reducing the average output voltage. From the discussions in the previous paragraphs on notching, it is

interesting to note that adding external inductance increases the duration of the overlap and reduces the average value of the output DC voltage. However, when viewed from the AC source side, the notching effect is conspicuously reduced and in some cases not observable. Since all other electrical equipment in the system will be connected to the line side of the AC inductor (in front of a thyristor based AC to DC rectifier), these equipment will not be affected by the notching phenomenon of thyristors. The external inductance also helps limit the circulating current between the two thyristors during the overlap duration.

Conclusion

Uncontrolled and controlled rectifier circuits have been discussed in this chapter. An introduction to the theory of diode and thyristor conduction has been presented to explain the important operating characteristics of these devices. Rectifier topologies employing both diodes and thyristors and their relative advantages and disadvantages have been discussed. Use of a dual thyristor bridge converter to achieve four-quadrant operation of a DC motor has been discussed. The topic of high-voltage DC (HVDC) transmission has been briefly introduced. Power quality issues relating to diode and thyristor-based rectifier topologies has also been addressed. To probe further into the various topics briefly discussed in this section, the reader is encouraged to refer to the references listed below.

References

- Dewan, S. B. and Straughen, A., *Power Semiconductor Circuits*, John Wiley & Sons, New York, 1975.
Hoft, R. G., *Semiconductor Power Electronics*, Van Nostrand Reinhold Company, New York, 1986.
IEEE Recommended Practices and Requirements for Harmonic Control in Electrical Power Systems, IEEE Std. 519-1992.
Laughton M. A. and Say, M. G., Eds., *Electrical Engineer's Reference Book –14th edition*, Butterworths, 1985.
Sen, P. C., *Principles of Electric Machines and Power Electronics*, John Wiley & Sons, New York, 1997.
Passive Harmonic Filter Systems for Variable Frequency Drives, U.S. Patent 5,444,609, 1995.

14.3 Inverters

Michael Giesselmann

Inverters are used to create single or polyphase AC voltages from a DC supply. In the class of polyphase inverters, three-phase inverters are by far the largest group. A very large number of inverters are used for adjustable speed motor drives. The typical inverter for this application is a “hard-switched” voltage source inverter producing **Pulse-Width Modulated (PWM)** signals with a sinusoidal fundamental (Holtz, 1992). Recently research has shown detrimental effects on the windings and the bearings resulting from unfiltered PWM waveforms and recommend the use of filters (Cash and Habetler, 1998; Von Jouanne et al., 1996). A very common application for single-phase inverters are so-called “Uninterruptable Power Supplies” (UPS) for computers and other critical loads. Here, the output waveforms range from square wave to almost ideal sinusoids. UPS designs are classified as either “off-line” or “on-line”. An off-line UPS will connect the load to the utility for most of the time and quickly switch over to the inverter if the utility fails. An online UPS will always feed the load from the inverter and switch the supply of the DC bus instead. Since the DC bus is heavily buffered with capacitors, the load sees virtually no disturbance if the power fails.

In addition to the very common hard-switched inverters, active research is being conducted on soft-switching techniques. Hard-switched inverters use controllable power semiconductors to connect an output terminal to a stable DC-bus. On the other hand, soft switching inverters have an oscillating intermediate circuit and attempt to open and close the power switches under zero-voltage and or zero-current conditions.

A separate class of inverters are the line commutated inverters for multimewatt power ratings, that use Thyristors (also called Silicon Controlled Rectifiers, SCRs). SCRs can only be turned “on” on command. After being turned on, the current in the device must approach zero in order to turn the device off. All other inverters are self commutated, meaning that the power control devices can be turned on and off. Line commutated inverters need the presence of a stable utility voltage to function. They are used for DC links between utilities, ultra long distance energy transport, and very large motor drives (Ahmed, 1999; Barton, 1994; Mohan et al., 1995; Rashid, 1993; Tarter, 1993). However, the latter application is more and more taken over by modern hard-switched inverters including multilevel inverters (Brumsickle et al., 1998; Tolbert et al., 1999).

Modern inverters use **I**solated **G**ate **B**ipolar **T**ransistors (IGBTs) as the main power control devices (Mohan et al., 1995). Besides IGBTs, power MOSFETs are also used especially for lower voltages, power ratings, and applications that require high efficiency and high switching frequency. In recent years, IGBTs, MOSFETs, and their control and protection circuitry have made remarkable progress. IGBTs are now available with voltage ratings of up to 3300 V and current ratings up to 1200 A. MOSFETs have achieved on-state resistances approaching a few milliohms. In addition to the devices, manufacturers today offer customized control circuitry that provides for electrical isolation, proper operation of the devices under normal operating conditions, and protection from a variety of fault conditions (Mohan et al., 1995). In addition, the industry provides good support for specialized passive devices such as capacitors and mechanical components such as low inductance bus-bar assemblies to facilitate the design of reliable inverters. In addition to the aforementioned inverters, a large number of special topologies are used. A good overview is given by Gottlieb (1984).

Fundamental Issues

Inverters fall in the class of power electronics circuits. The most widely accepted definition of a power electronics circuit is that the circuit is actually processing electric energy rather than information. The actual power level is not very important for the classification of a circuit as a power electronics circuit. One of the most important performance considerations of power electronics circuits, like inverters, is their energy conversion efficiency. The most important reason for demanding high efficiency is the problem of removing large amounts of heat from the power devices. Of course, the judicious use of energy is also paramount, especially if the inverter is fed from batteries such as in electric cars. For these reasons, inverters operate the power devices, which control the flow of energy, as switches. In the ideal case of a switching event, there would be no power loss in the switch since either the current in the switch is zero (switch open) or the voltage across the switch is zero (switch closed) and the power loss is computed as the product of both. In reality, there are two mechanisms that do create some losses, however; these are on-state losses and switching losses (Bird et al., 1993; Kassakian et al., 1991; Mohan et al., 1995; Rashid, 1993). On-state losses are due to the fact that the voltage across the switch in the on state is not zero, but typically in the range of 1–2 V for IGBTs. For power MOSFETs, the on-state voltage is often in the same range, but it can be substantially below 0.5 V due to the fact that these devices have a purely resistive conduction channel and no fixed minimum saturation voltage like bipolar junction devices (IGBTs). The switching losses are the second major loss mechanism and are due to the fact that, during the turn on and turn off transition, current is flowing while voltage is present across the device. In order to minimize the switching losses, the individual transitions have to be rapid (tens to hundreds of nanoseconds) and the maximum switching frequency needs to be carefully considered.

In order to avoid audible noise being radiated from motor windings or transformers, most modern inverters operate at switching frequencies substantially above 10 kHz (Bose, 1992; 1996).

Single Phase Inverters

Figure 14.35 shows the basic topology of a full bridge inverter with single-phase output. This configuration is often called an H-bridge, due to the arrangement of the power switches and the load. The inverter can deliver and accept both real and reactive power. The inverter has two legs, left and right. Each leg

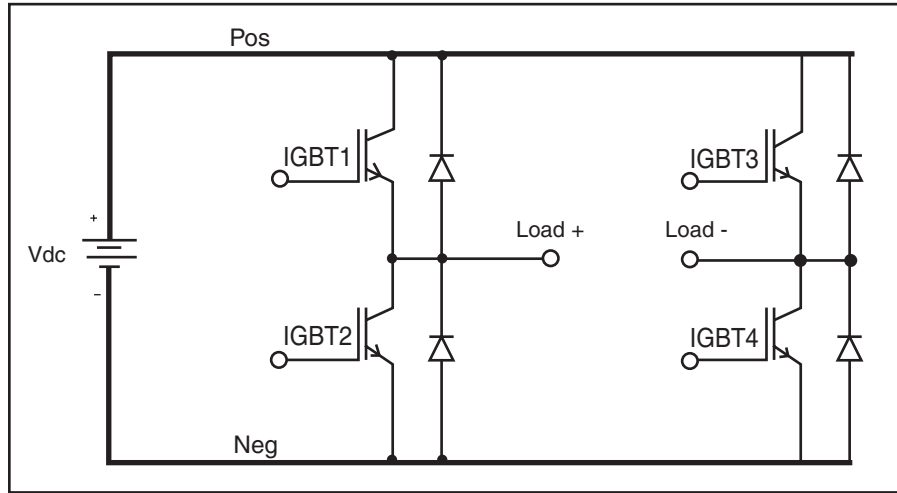


FIGURE 14.35 Topology of a single-phase, full bridge inverter.

consists of two power control devices (here IGBTs) connected in series. The load is connected between the mid-points of the two phase legs. Each power control device has a diode connected in antiparallel to it. The diodes provide an alternate path for the load current if the power switches are turned off. For example, if the lower IGBT in the left leg is conducting and carrying current toward the negative DC bus, this current would “commutate” into the diode across the upper IGBT of the left leg, if the lower IGBT is turned off. Control of the circuit is accomplished by varying the turn on time of the upper and lower IGBT of each inverter leg, with the provision of never turning on both at the same time, to avoid a short circuit of the DC bus. In fact, modern drivers will not allow this to happen, even if the controller would erroneously command both devices to be turned on. The controller will therefore alternate the turn on commands for the upper and lower switch, i.e., turn the upper switch on and the lower switch off, and vice versa. The driver circuit will typically add some additional blanking time (typically 500–1000 ns) during the switch transitions to avoid any overlap in the conduction intervals.

The controller will hereby control the duty cycle of the conduction phase of the switches. The average potential of the center-point of each leg will be given by the DC bus voltage multiplied by the duty cycle of the upper switch, if the negative side of the DC bus is used as a reference. If this duty cycle is modulated with a sinusoidal signal with a frequency that is much smaller than the switching frequency, the short-term average of the center-point potential will follow the modulation signal. “Short-term” in this context means a small fraction of the period of the fundamental output frequency to be produced by the inverter. For the single phase inverter, the modulation of the two legs are inverse of each other such that if the left leg has a large duty cycle for the upper switch, the right leg has a small one, etc. The output voltage is then given by Eq. (14.1) in which m_a is the modulation factor. The boundaries for m_a are for linear modulation. Values greater than 1 cause overmodulation and a noticeable increase in output voltage distortion.

$$V_{ac1}(t) = m_a \cdot V_{dc} \cdot \sin(\omega_1 \cdot t) \quad 0 \leq m_a \leq 1 \quad (14.1)$$

This voltage can be filtered using a LC low pass filter. The voltage on the output of the filter will closely resemble the shape and frequency of the modulation signal. This means that the frequency, wave-shape, and amplitude of the inverter output voltage can all be controlled as long as the switching frequency is at least 25–100 times higher than the fundamental output frequency of the inverter (Holtz, 1992). The actual generation of the PWM signals is mostly done using microcontrollers and Digital Signal Processors (DSPs) (Bose, 1987).

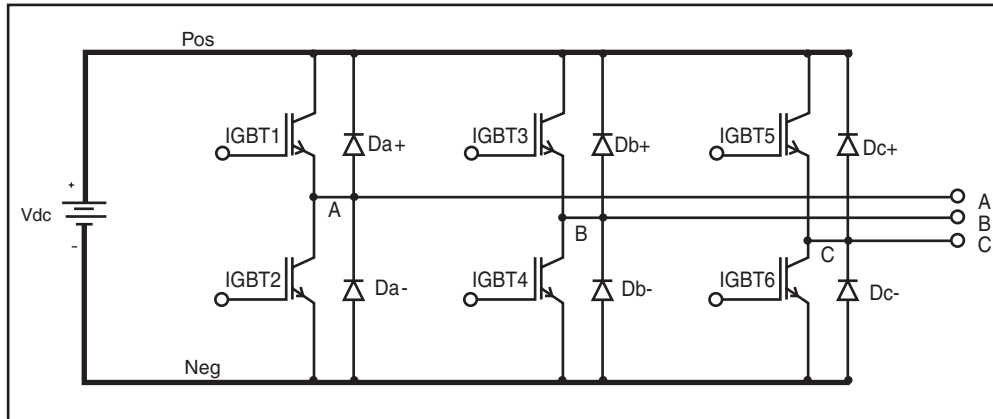


FIGURE 14.36 Topology of a three-phase inverter.

Three Phase Inverters

Figure 14.36 shows a three-phase inverter, which is the most commonly used topology in today's motor drives. The circuit is basically an extension of the H-bridge style single-phase inverter, by an additional leg. The control strategy is similar to the control of the single-phase inverter, except that the reference signals for the different legs have a phase shift of 120° instead of 180° for the single-phase inverter. Due to this phase shift, the odd triplen harmonics (3rd, 9th, 15th, etc.) of the reference waveform for each leg are eliminated from the line-to-line output voltage (Mohan et al., 1995; Novotny and Lipo, 1996; Rashid, 1993; Shepherd and Zand, 1979). The even numbered harmonics are canceled as well if the waveforms are pure AC, which is usually the case. For linear modulation, the amplitude of the output voltage is reduced with respect to the input voltage of a three phase rectifier feeding the DC bus by a factor given by Eq. (14.2).

$$\frac{3}{(2 \cdot \pi)} \cdot \sqrt{3} = 82.7\% \quad (14.2)$$

To compensate for this voltage reduction, the fact of the harmonics cancellation is sometimes used to boost the amplitudes of the output voltages by intentionally injecting a 3rd harmonic component into the reference waveform of each phase leg (Mohan et al., 1995).

Figure 14.37 shows the typical output of a three-phase inverter during a startup transient into a typical motor load. This figure was created using circuit simulation. The upper graph shows the pulse-width modulated waveform between phases A and B, whereas the lower graph shows the currents in all three phases. It is obvious that the motor acts as a low-pass filter for the applied PWM voltage and the current assumes the waveshape of the fundamental modulation signal with very small amounts of switching ripple.

Like the single-phase inverter based on the H-bridge topology, the inverter can deliver and accept both real and reactive power. In many cases, the DC bus is fed by a diode rectifier from the utility, which cannot pass power back to the AC input. The topology of a three-phase rectifier would be the same as shown in Fig. 14.36 with all IGBTs deleted.

A reversal of power flow in an inverter with a rectifier front end would lead to a steady rise of the DC bus voltage beyond permissible levels. If the power flow to the load is only reversing for brief periods of time, such as to brake a motor occasionally, the DC bus voltage could be limited by dissipating the power in a so-called brake resistor. To accommodate a brake resistor, inverter modules with an additional 7th IGBT (called "brake-chopper") are offered. This is shown in Fig. 14.38. For long-term regeneration, the

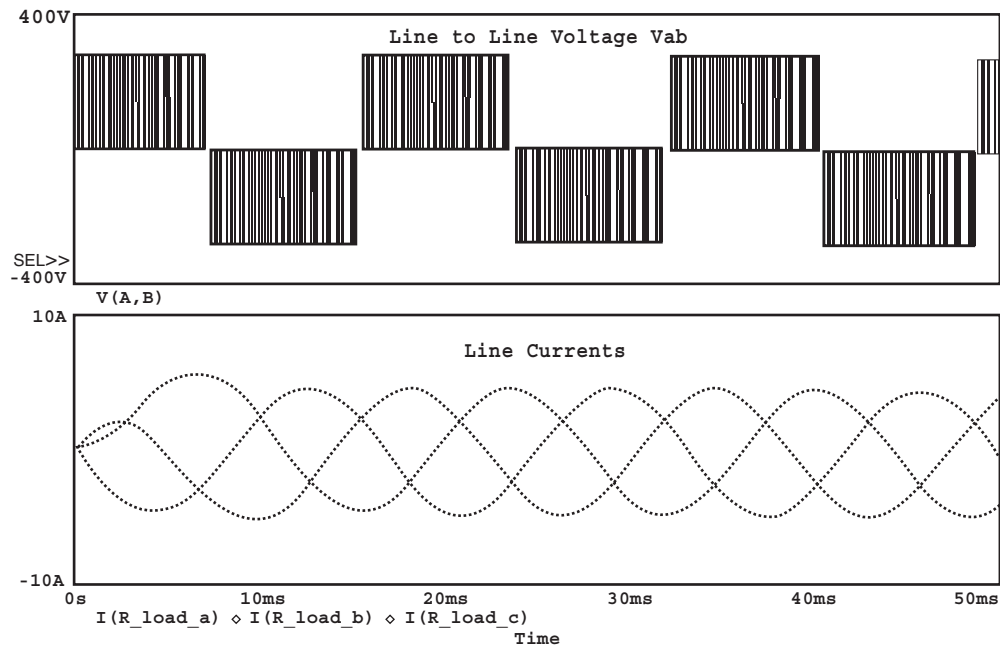


FIGURE 14.37 Typical waveforms of inverter voltages and currents.

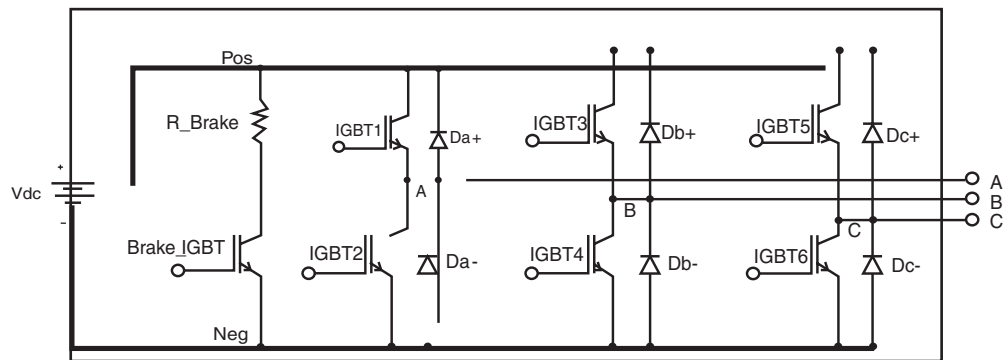


FIGURE 14.38 Topology of a three-phase inverter with brake-chopper IGBT.

rectifier can be replaced by an additional three-phase converter (Mohan et al., 1995). This additional converter is often called a controlled synchronous rectifier. The additional converter including its controller is of course much more expensive than a simple rectifier, but with this arrangement bidirectional power flow can be achieved. In addition, the interface toward the utility system can be managed such that the real and reactive power that is drawn from or delivered to the utility can be independently controlled. Also, the harmonics content of the current in the utility link can be reduced to almost zero. The topology for an arrangement like this is shown in Fig. 14.39.

The inverter shown in Fig. 14.36 provides a three-phase voltage without a neutral point. A fourth leg can be added to provide a four-wire system with a neutral point. Likewise four, five, or n -phase inverters can be realized by simply adding the appropriate number of phase legs.

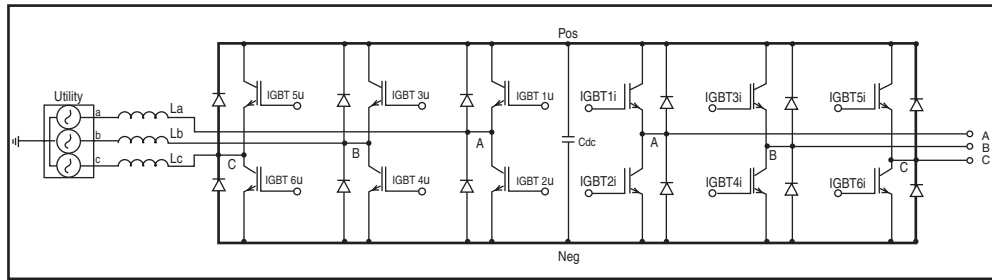


FIGURE 14.39 Topology of a three-phase inverter system for bidirectional power flow.

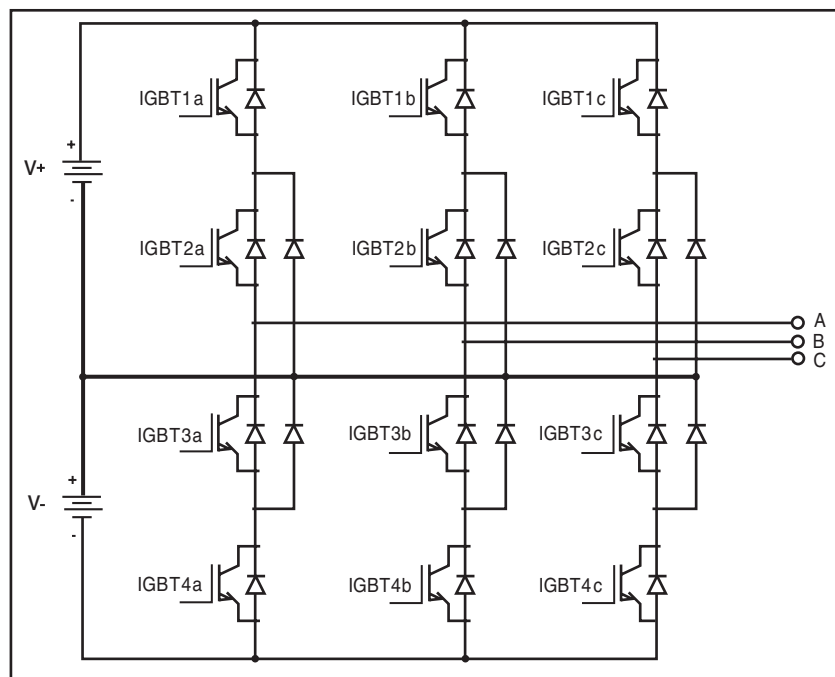


FIGURE 14.40 Topology of a three-level inverter.

As in single-phase inverters, the generation of the PWM control signals is done using modern micro-controllers and DSPs. These digital controllers are typically not only controlling just the inverter, but through the controlled synthesis of the appropriate voltages, motors and attached loads are controlled for high-performance dynamic response. The most commonly used control principle for superior dynamic response is called field-oriented or vector control (Bose, 1987; Bose, 1996; DeDonker and Novotny, 1988; Lorenz and Divan, 1990; Trzynadlowski, 1994).

Multilevel Inverters

Multilevel inverters are a class of inverters where a DC source with several tabs between the positive and negative terminal is present. The two main advantages of multilevel inverters are the higher voltage capability and the reduced harmonics content of the output waveform due to the multiple DC levels. The higher voltage capability is due to the fact that clamping diodes are used to limit the voltage stress

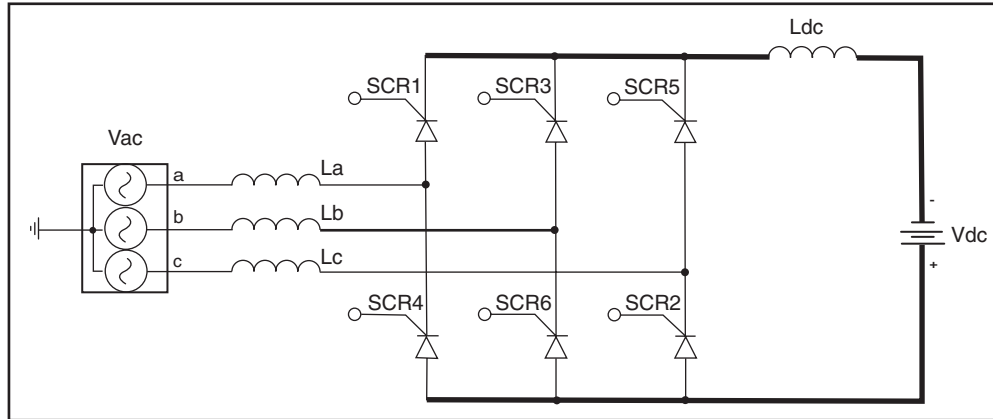


FIGURE 14.41 Line commutated converter in inverter mode.

on the IGBTs to the voltage differential between two tabs on the DC bus. Figure 14.40 shows the topology of a three-level inverter. Here, each phase leg consists of four IGBTs in series with additional antiparallel and clamping diodes. The output is again at the center-point of the phase leg. The output of each phase can be connected to the top DC bus, the center connection of the DC supply, or the negative DC bus. This amounts to three distinct voltage levels for the voltage of each phase, which explains the name of the circuit. It turns out that the resulting line-to-line voltage has five distinct levels in a three-phase inverter.

Line Commutated Inverters

Figure 14.41 shows the topology of a line commutated inverter. In Fig. 14.41 the SCRs are numbered according to their firing sequence. The circuit can operate both as a rectifier and an inverter. The mode of operation is controlled by the firing angle of the SCRs in the circuit (Ahmed, 1999; Barton, 1994; Mohan et al., 1995). The reference value for the firing angle α is the instant when the voltage across each SCR becomes positive, i.e., when an uncontrolled diode would turn on. This time corresponds to 30° past the positive going zero crossing of each phase. By delaying the turn-on angle α more than 90° past this instant, the polarity of the average DC bus voltage reverses and the circuit enters the inverter mode. The DC source in Fig. 14.41 shows the polarity of the DC voltage for inverter operation. The firing delay angle corresponds to the phase of the utility voltage. The maximum delay angle must be limited to less than 180° , to provide enough time for the next SCR in the sequence to acquire the load current. Equation (14.3) gives the value of the DC output voltage of the converter as a function of the delay angle α and the DC current I_{dc} , which is considered constant.

$$V_{dc} = \frac{3}{\pi} \cdot \left(\sqrt{2} \cdot V_{LL} \cdot \cos(\alpha) - \omega \cdot L_s \cdot I_{dc} \right) \quad (14.3)$$

V_{LL} is the rms value of the AC line-to-line voltage, ω is the radian frequency of the AC voltage, and L_s is the value of the inductors L_a , L_b , and L_c in Fig. 14.41. Line commutated inverters have a negative impact on the utility voltage and a relatively low total power factor. Equation (14.4) gives an estimate of the total power factor of the circuit shown in Fig. 14.41 for constant DC current and negligible AC line reactors.

$$PF = \frac{3}{\pi} \cdot \cos(\alpha) \quad (14.4)$$

References

- Ahmed A., *Power Electronics for Technology*, Prentice-Hall, Upper Saddle River, NJ, 1999.
- Barton, T. H., *Rectifiers, Cycloconverters, and AC Controllers*, Oxford University Press Inc., New York, 1994.
- Bird, B. M., King, K.G., Pedder, D. A. G., *An Introduction to Power Electronics*, 2nd Edition, John Wiley & Sons, Inc., New York, 1993.
- Bose, B. K., *Modern Power Electronics, Evolution, Technology, and Applications*, IEEE Press, Piscataway, NJ, 1992.
- Bose, B. K., *Microcomputer Control of Power Electronics and Drives*, IEEE Press, Piscataway, NJ, 1987.
- Bose, B. K., *Power Electronics and Variable Frequency Drives*, IEEE Press, Piscataway, NJ, 1996.
- Brumsickle, W.E., D.M. Divan, T.A. Lipo, Reduced switching stress in high-voltage IGBT inverters via a three-level structure, *IEEE-APEC* 2, 544–550, February 1998.
- Cash, M.A., and Habetler, T.G., Insulation failure prediction in induction machines using line-neutral voltages, *IEEE Trans. on Ind. Appl.*, 34, 6, 1234–1239, Nov/Dec 1998.
- De Donker, R., and Novotny, D. W., The universal field-oriented controller, in *Conf. Rec. IEEE-IAS* 1988, 450–456.
- Gottlieb, I. M., *Power Supplies, Switching Regulators, Inverters and Converters*, TAB Books, Inc., Blue Ridge Summit, PA, 1984.
- Holtz, J., Pulsewidth modulation — A survey, *IEEE Trans. on Ind. Electr.*, 39, 5, 410–420, 1992.
- Kassakian, J. G., Schlecht, M. F., Verghese, G. C., *Principles of Power Electronics*, Addison-Wesley Publishing Company, Reading, MA, 1991.
- Lorenz, R.D., and Divan, D.M., Dynamic analysis and experimental evaluation of delta modulators for field oriented induction machines, *IEEE Trans. Ind. Appl.*, 26, 2, 296–301, 1990.
- Mohan, N., Undeland, T., Robbins, W., *Power Electronics, Converters, Applications, and Design*, 2nd ed., John Wiley & Sons, New York, 1995.
- Novotny, D. W., and Lipo, T. A., *Vector Control and Dynamics of AC Drives*, Oxford Science Publications, New York, 1996.
- Rashid, M. H., *Power Electronics, Circuits, Devices, and Applications*, Prentice-Hall, Englewood Cliffs, NJ, 1993.
- Shepherd, W., and Zand, P., *Energy Flow and Power Factor in Nonsinusoidal Circuits*, Cambridge University Press, London and New York, 1979.
- Tarter, R. E., *Solid State Power Conversion Handbook*, John Wiley & Sons, Inc., New York, 1993.
- Tolbert, L.M., Peng, F.Z., and Habetler, T.G., Multilevel converters for large electric drives, *IEEE Trans. Ind. Appl.*, 35, 1, 36–44, Jan/Feb 1999.
- Trzynadlowski, A. M., *The Field Orientation Principle in Control of Induction Motors*, Kluwer Academic Publishers, Inc., Dordrecht, The Netherlands, 1994.
- Von Jouanne, A., Rendusara, D., Enjeti, P., Gray, W., Filtering techniques to minimize the effect of long motor leads on PWM inverter fed AC motor drive systems, *IEEE Trans. Ind. Appl.*, July/Aug. 1996, 919–926.

14.4 Active Filters for Power Conditioning

Hirofumi Akagi

Much research has been performed on active filters for power conditioning and their practical applications since their basic principles of compensation were proposed around 1970 (Bird et al., 1969; Gyugyi and Strycula, 1976; Kawahira et al., 1983). In particular, recent remarkable progress in the capacity and switching speed of power semiconductor devices such as insulated-gate bipolar transistors (IGBTs) has spurred interest in active filters for power conditioning. In addition, state-of-the-art power electronics technology has enabled active filters to be put into practical use. More than one thousand sets of active filters consisting of voltage-fed pulse-width-modulation (PWM) inverters using IGBTs or gate-turn-off (GTO) thyristors are operating successfully in Japan.

Active filters for power conditioning provide the following functions:

- reactive-power compensation,
- harmonic compensation, harmonic isolation, harmonic damping, and harmonic termination,
- negative-sequence current/voltage compensation,
- voltage regulation.

The term “active filters” is also used in the field of signal processing. In order to distinguish active filters in power processing from active filters in signal processing, the term “active power filters” often appears in many technical papers or literature. However, the author prefers “active filters for power conditioning” to “active power filters,” because the term “active power filters” is misleading to either “active filters for power” or “filters for active power.” Therefore, this section takes the term “active filters for power conditioning” or simply uses the term “active filters” as long as no confusion occurs.

Harmonic-Producing Loads

Identified Loads and Unidentified Loads

Nonlinear loads drawing nonsinusoidal currents from utilities are classified into identified and unidentified loads. High-power diode/thyristor rectifiers, cycloconverters, and arc furnaces are typically characterized as identified harmonic-producing loads because utilities identify the individual nonlinear loads installed by high-power consumers on power distribution systems in many cases. The utilities determine the point of common coupling with high-power consumers who install their own harmonic-producing loads on power distribution systems, and also can determine the amount of harmonic current injected from an individual consumer.

A “single” low-power diode rectifier produces a negligible amount of harmonic current. However, multiple low-power diode rectifiers can inject a large amount of harmonics into power distribution systems. A low-power diode rectifier used as a utility interface in an electric appliance is typically considered as an unidentified harmonic-producing load. Attention should be paid to unidentified harmonic-producing loads as well as identified harmonic-producing loads.

Harmonic Current Sources and Harmonic Voltage Sources

In many cases, a harmonic-producing load can be represented by either a harmonic current source or a harmonic voltage source from a practical point of view. Figure 14.42(a) shows a three-phase diode rectifier with a DC link inductor L_d . When attention is paid to voltage and current harmonics, the rectifier can be considered as a harmonic current source shown in Fig. 14.42(b). The reason is that the load impedance is much larger than the supply impedance for harmonic frequency ω_h , as follows:

$$\sqrt{R_L^2 + (\omega_h L_d)^2} \gg \omega_h L_S.$$

Here, L_S is the sum of supply inductance existing upstream of the point of common coupling (PCC) and leakage inductance of a rectifier transformer. Note that the rectifier transformer is disregarded from Fig. 14.42(a). Figure 14.42(b) suggests that the supply harmonic current i_{sh} is independent of L_S .

Figure 14.43(a) shows a three-phase diode rectifier with a DC link capacitor. The rectifier would be characterized as a harmonic voltage source shown in Fig. 14.43(b) if it is seen from its AC terminals. The reason is that the following relation exists:

$$\frac{1}{\omega_h C_d} \ll \omega_h L_S.$$

This implies that i_{sh} is strongly influenced by the inductance value of L_S .

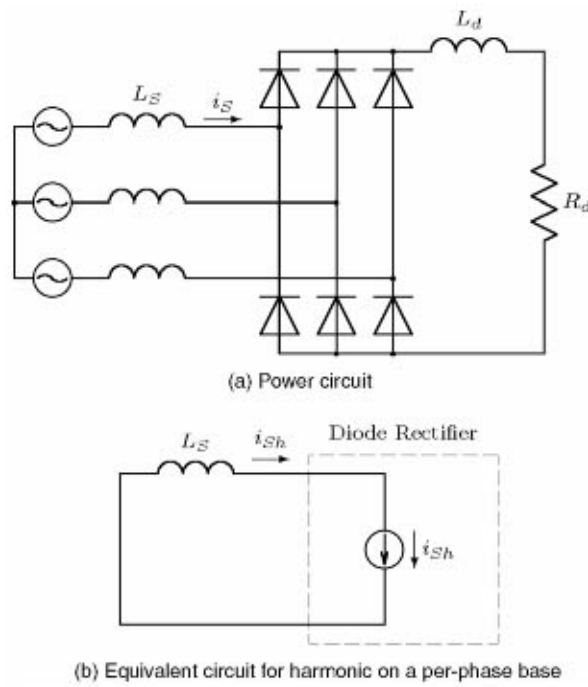


FIGURE 14.42 Diode rectifier with inductive load.

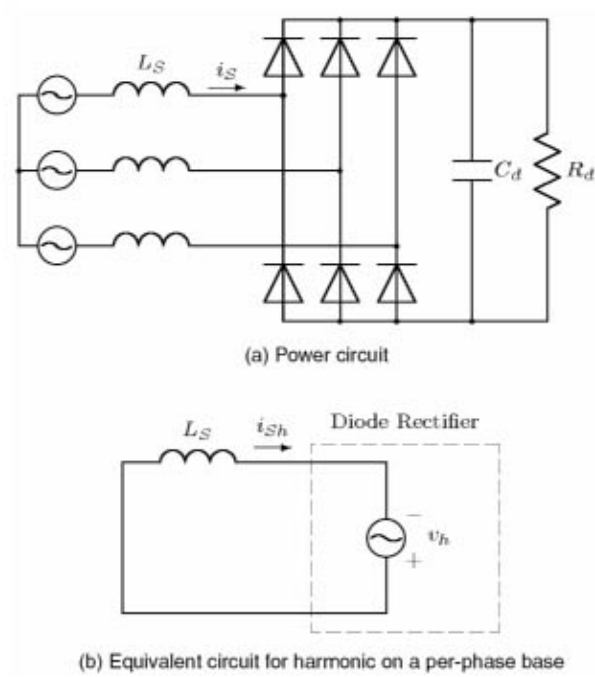


FIGURE 14.43 Diode rectifier with capacitive load.

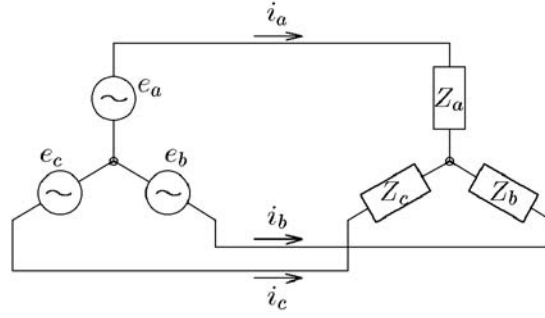


FIGURE 14.44 Three-phase three-wire system.

Theoretical Approach to Active Filters for Power Conditioning

The Akagi-Nabae Theory

The theory of instantaneous power in three-phase circuits is referred to as the “Akagi-Nabae theory” (Akagi et al., 1983; Akagi et al., 1984). Figure 14.44 shows a three-phase three-wire system on the a - b - c coordinates, where no zero-sequence voltage is included in the three-phase three-wire system. Applying the theory to Fig. 14.44 can transform the three-phase voltages and currents on the a - b - c coordinates into the two-phase voltages and currents on the α - β coordinates, as follows:

$$\begin{bmatrix} e_\alpha \\ e_\beta \end{bmatrix} = \sqrt{\frac{2}{3}} \begin{bmatrix} 1 & -1/2 & -1/2 \\ 0 & \sqrt{3}/2 & -\sqrt{3}/2 \end{bmatrix} \begin{bmatrix} e_a \\ e_b \\ e_c \end{bmatrix} \quad (14.5)$$

$$\begin{bmatrix} i_\alpha \\ i_\beta \end{bmatrix} = \sqrt{\frac{2}{3}} \begin{bmatrix} 1 & -1/2 & -1/2 \\ 0 & \sqrt{3}/2 & -\sqrt{3}/2 \end{bmatrix} \begin{bmatrix} i_a \\ i_b \\ i_c \end{bmatrix}. \quad (14.6)$$

As is well known, the instantaneous real power either on the a - b - c coordinates or on the α - β coordinates is defined by

$$p = e_a i_a + e_b i_b + e_c i_c = e_\alpha i_\alpha + e_\beta i_\beta. \quad (14.7)$$

To avoid confusion, p is referred to as three-phase instantaneous real power. According to the theory, the three-phase instantaneous imaginary power, q , is defined by

$$q = e_\alpha i_\beta - e_\beta i_\alpha. \quad (14.8)$$

The combination of the above two equations bears the following basic formulation:

$$\begin{bmatrix} p \\ q \end{bmatrix} = \begin{bmatrix} e_\alpha & e_\beta \\ -e_\beta & e_\alpha \end{bmatrix} \begin{bmatrix} i_\alpha \\ i_\beta \end{bmatrix}. \quad (14.9)$$

Here, $e_\alpha \cdot i_\alpha$ or $e_\beta \cdot i_\beta$ obviously means instantaneous power in the α -phase or the β -phase because either is defined by the product of the instantaneous voltage in one phase and the instantaneous current in the

same phase. Therefore, p has a dimension of [W]. Conversely, neither $e_\alpha \cdot i_\beta$ nor $e_\beta \cdot i_\alpha$ means instantaneous power because either is defined by the product of the instantaneous voltage in one phase and the instantaneous current in the other phase. Accordingly, q is quite different from p in dimension and electric property although q looks similar in formulation to p . A common dimension for q should be introduced from both theoretical and practical points of view. A good candidate is [IW], that is, “imaginary watt.”

Equation (14.9) is changed into the following equation:

$$\begin{bmatrix} i_\alpha \\ i_\beta \end{bmatrix} = \begin{bmatrix} e_\alpha & e_\beta \\ -e_\beta & e_\alpha \end{bmatrix} \begin{bmatrix} p \\ q \end{bmatrix} \quad (14.10)$$

Note that the determinant with respect to e_α and e_β in Eq. (14.9) is not zero. The instantaneous currents on the α - β coordinates, i_α and i_β , are divided into two kinds of instantaneous current components, respectively:

$$\begin{aligned} \begin{bmatrix} i_\alpha \\ i_\beta \end{bmatrix} &= \begin{bmatrix} e_\alpha & e_\beta \\ -e_\beta & e_\alpha \end{bmatrix}^{-1} \begin{bmatrix} p \\ 0 \end{bmatrix} + \begin{bmatrix} e_\alpha & e_\beta \\ -e_\beta & e_\alpha \end{bmatrix}^{-1} \begin{bmatrix} 0 \\ q \end{bmatrix} \\ &\equiv \begin{bmatrix} i_{\alpha p} \\ i_{\beta p} \end{bmatrix} + \begin{bmatrix} i_{\alpha q} \\ i_{\beta q} \end{bmatrix} \end{aligned} \quad (14.11)$$

Let the instantaneous powers in the α -phase and the β -phase be p_α and p_β , respectively. They are given by the conventional definition as follows:

$$\begin{bmatrix} p_\alpha \\ p_\beta \end{bmatrix} = \begin{bmatrix} e_\alpha i_\alpha \\ e_\beta i_\beta \end{bmatrix} = \begin{bmatrix} e_\alpha i_{\alpha p} \\ e_\beta i_{\beta p} \end{bmatrix} + \begin{bmatrix} e_\alpha i_{\alpha q} \\ e_\beta i_{\beta q} \end{bmatrix} \quad (14.12)$$

The three-phase instantaneous real power, p , is given as follows, by using Eqs. (14.11) and (14.12):

$$\begin{aligned} p &= p_\alpha + p_\beta = e_\alpha i_{\alpha p} + e_\beta i_{\beta p} + e_\alpha i_{\alpha q} + e_\beta i_{\beta q} \\ &= \frac{e_\alpha^2}{e_\alpha^2 + e_\beta^2} p + \frac{e_\beta^2}{e_\alpha^2 + e_\beta^2} p + \frac{-e_\alpha e_\beta}{e_\alpha^2 + e_\beta^2} q + \frac{e_\alpha e_\beta}{e_\alpha^2 + e_\beta^2} q \end{aligned} \quad (14.13)$$

The sum of the third and fourth terms on the right-hand side in Eq. (14.13) is always zero. From Eqs. (14.12) and (14.13), the following equations are obtained:

$$p = e_\alpha i_{\alpha p} + e_\beta i_{\beta p} \equiv p_{\alpha p} + p_{\beta p} \quad (14.14)$$

$$0 = e_\alpha i_{\alpha q} + e_\beta i_{\beta q} \equiv p_{\alpha q} + p_{\beta q} \quad (14.15)$$

Inspection of Eqs. (14.14) and (14.15) leads to the following essential conclusions:

- The sum of the power components, $p_{\alpha p}$ and $p_{\beta p}$, coincides with the three-phase instantaneous real power, p , which is given by Eq. (14.7). Therefore, $p_{\alpha p}$ and $p_{\beta p}$ are referred to as the α -phase and β -phase instantaneous active powers.

- The other power components, $p_{\alpha q}$ and $p_{\beta q}$, cancel each other and make no contribution to the instantaneous power flow from the source to the load. Therefore, $p_{\alpha q}$ and $p_{\beta q}$ are referred to as the α -phase and β -phase instantaneous reactive powers.
- Thus, a shunt active filter without energy storage can achieve instantaneous compensation of the current components, $i_{\alpha q}$ and $i_{\beta q}$ or the power components, $p_{\alpha q}$ and $p_{\beta q}$. In other words, the Akagi-Nabae theory based on Eq. (14.9) exactly reveals what components the active filter without energy storage can eliminate from the α -phase and β -phase instantaneous currents, i_α and i_β or the α -phase and β -phase instantaneous real powers, p_α and p_β .

Energy Storage Capacity

Figure 14.45 shows a system configuration of a shunt active filter for harmonic compensation of a diode rectifier, where the main circuit of the active filter consists of a three-phase voltage-fed PWM inverter and a DC capacitor, C_d . The active filter is controlled to draw the compensating current, i_{AF} , from the utility, so that the compensating current cancels the harmonic current flowing on the AC side of the diode rectifier with a DC link inductor.

Referring to Eq. (14.10) yields the α -phase and β -phase compensating currents,

$$\begin{bmatrix} i_{AF\alpha} \\ i_{AF\beta} \end{bmatrix} = \begin{bmatrix} e_\alpha & e_\beta \\ -e_\beta & e_\alpha \end{bmatrix}^{-1} \begin{bmatrix} p_{AF} \\ q_{AF} \end{bmatrix}. \quad (14.16)$$

Here, p_{AF} and q_{AF} are the three-phase instantaneous real and imaginary power on the AC side of the active filter, and they are usually extracted from p_L and q_L . Note that p_L and q_L are the three-phase instantaneous real and imaginary power on the AC side of a harmonic-producing load. For instance, when the active filter compensates for the harmonic current produced by the load, the following relationships exist:

$$p_{AF} = -\tilde{p}_L, \quad q_{AF} = -\tilde{q}_L. \quad (14.17)$$

Here, \tilde{p}_L and \tilde{q}_L are AC components of p_L and q_L , respectively. Note that the DC components of p_L and q_L correspond to the fundamental current present in i_L and the AC components to the harmonic current. In general, two high-pass filters in the control circuit extract \tilde{p}_L from p_L and \tilde{q}_L from q_L .

The active filter draws p_{AF} from the utility, and delivers it to the DC capacitor if no loss is dissipated in the active filter. Thus, p_{AF} induces voltage fluctuation of the DC capacitor. When the amplitude of p_{AF} is assumed to be constant, the lower the frequency of the AC component, the larger the voltage fluctuation (Akagi et al., 1984; Akagi et al., 1986). If the period of the AC component is one hour, the DC capacitor

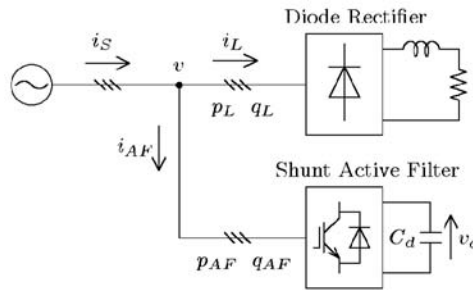


FIGURE 14.45 Shunt active filter.

has to absorb or release electric energy given by integration of p_{AF} with respect to time. Thus, the following relationship exists between the instantaneous voltage across the DC capacitor, v_d and p_{AF} :

$$\frac{1}{2} C_d v_d^2(t) = \frac{1}{2} C_d v_d^2(0) + \int_0^t p_{AF} dt. \quad (14.18)$$

This implies that the active filter needs an extremely large-capacity DC capacitor to suppress the voltage fluctuation coming from achieving “harmonic” compensation of \tilde{p}_L . Hence, the active filter is no longer a harmonic compensator, and thereby it should be referred to as a “DC capacitor-based energy storage system,” although it is impractical at present. In this case, the main purpose of the voltage-fed PWM inverter is to perform an interface between the utility and the bulky DC capacitor.

The active filter seems to “draw” q_{AF} from the utility, as shown in Fig. 14.45. However, q_{AF} makes no contribution to energy transfer in the three-phase circuit. No energy storage, therefore, is required to the active filter, independent of q_{AF} , whenever $p_{AF} = 0$.

Classification of Active Filters

Various types of active filters have been proposed in technical literature (Moran, 1989; Grady et al., 1990; Akagi, 1994; Akagi and Fujita, 1995; Fujita and Akagi, 1997; Aredes et al., 1998). Classification of active filters is made from different points of view (Akagi, 1996). Active filters are divided into AC and DC filters. Active DC filters have been designed to compensate for current and/or voltage harmonics on the DC side of thyristor converters for high-voltage DC transmission systems (Watanabe, 1990; Zhang et al., 1993) and on the DC link of a PWM rectifier/inverter for traction systems. Emphasis, however, is put on active AC filter in the following because the term “active filters” refers to active AC filters in most cases.

Classification by Objectives: Who is Responsible for Installing Active Filters?

The objective of “who is responsible for installing active filters” classifies them into the following two groups:

- Active filters installed by *individual consumers* on their own premises in the vicinity of one or more identified harmonic-producing loads.
- Active filters being installed by *electric power utilities* in substations and/or on distribution feeders.

Individual consumers should pay attention to current harmonics produced by their own harmonic-producing loads, and thereby the active filters installed by the individual consumers are aimed at compensating for current harmonics.

Utilities should concern themselves with voltage harmonics, and therefore active filters will be installed by utilities in the near future for the purpose of compensating for voltage harmonics and/or of achieving “harmonic damping” throughout power distribution systems or “harmonic termination” of a radial power distribution feeder. The section titled “Practical Applications of Active Filters for Power Conditioning” describes a shunt active filter intended for installation by electric power utilities on the end bus of a power distribution line.

Classification by System Configuration

Shunt Active Filters and Series Active Filters

A standalone shunt active filter shown in Fig. 14.45 is one of the most fundamental system configurations. The active filter is controlled to draw a compensating current, i_{AF} from the utility, so that it cancels current harmonics on the AC side of a general-purpose diode/thyristor rectifier (Akagi et al., 1990; Peng et al., 1990; Bhattacharya et al., 1998) or a PWM rectifier for traction systems (Krah and Holtz, 1994). Generally, the shunt active filter is suitable for harmonic compensation of a current harmonic source such as diode/thyristor rectifier with a DC link inductor. The shunt active filter has the capability of damping harmonic resonance between an existing passive filter and the supply impedance.

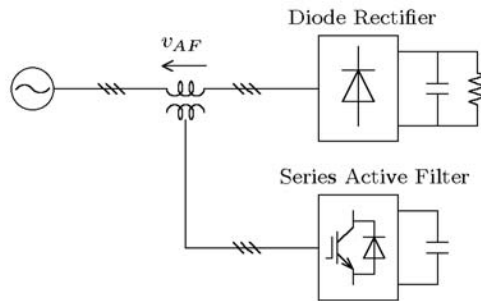


FIGURE 14.46 Series active filter.

TABLE 14.3 Comparison of Shunt Active Filters and Series Active Filters

	Shunt Active Filter	Series Active Filter
System configuration	Figure 14.45	Figure 14.46
Power circuit of active filter	Voltage-fed PWM inverter with current minor loop	Voltage-fed PWM inverter without current minor loop
Active filter acts as	Current source: i_{AF}	Voltage source: v_{AF}
Harmonic-producing load suitable	Diode/thyristor rectifiers with inductive loads, and cycloconverters	Large-capacity diode rectifiers with capacitive loads
Additional function	Reactive power compensation	AC voltage regulation
Present situation	Commercial stage	Laboratory stage

Figure 14.46 shows a system configuration of a series active filter used alone. The series active filter is connected in series with the utility through a matching transformer, so that it is suitable for harmonic compensation of a voltage harmonic source such as a large-capacity diode rectifier with a DC link capacitor. The series active filter integrated into a diode rectifier with a DC common capacitor is discussed in section V. Table 14.3 shows comparisons between the shunt and series active filters. This concludes that the series active filter has a “dual” relationship in each item with the shunt active filter (Akagi, 1996; Peng, 1998).

Hybrid Active/Passive Filters

Figures 14.47, 14.48, and 14.49 show three types of hybrid active/passive filters, the main purpose of which is to reduce initial costs and to improve efficiency. The shunt passive filter consists of one or more tuned LC filters and/or a high-pass filter. Table 14.4 shows comparisons among the three hybrid filters in which the active filters are different in function from the passive filters. Note that the hybrid filters are applicable to any current harmonic source, although a harmonic-producing load is represented by a thyristor rectifier with a DC link inductor in Figs. 14.47, 14.48, and 14.49.

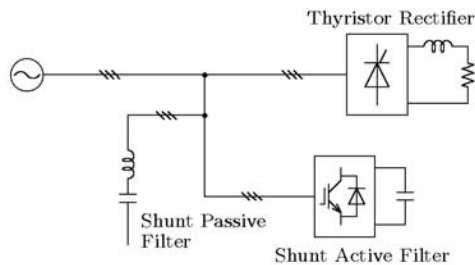


FIGURE 14.47 Combination of shunt active filter and shunt passive filter.

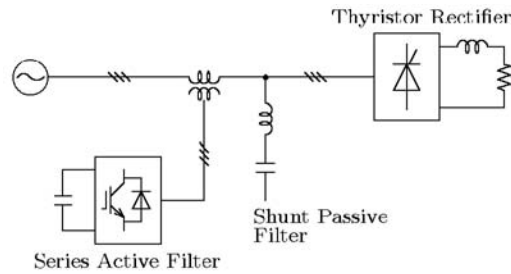


FIGURE 14.48 Combination of series active filter and shunt passive filter.

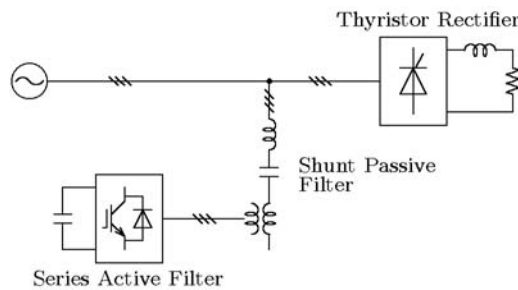


FIGURE 14.49 Series active filter connected in series with shunt passive filter.

TABLE 14.4 Comparison of Hybrid Active/Passive Filters

	Shunt Active Filter Plus Shunt Passive Filter	Series Active Filter Plus Shunt Passive Filter	Series Active Filter Connected in Series with Shunt Passive Filter
System configuration	Figure 14.47	Figure 14.48	Figure 14.49
Power circuit of active filter	• Voltage-fed PWM inverter with current minor loop	• Voltage-fed PWM inverter without current minor loop	• Voltage-fed PWM inverter with or without current minor loop
Function of active filter	• Harmonic compensation	• Harmonic isolation	• Harmonic isolation or harmonic compensation
Advantages	<ul style="list-style-type: none"> • General shunt active filters applicable • Reactive power controllable 	<ul style="list-style-type: none"> • Already existing shunt passive filters applicable • No harmonic current flowing through active filter 	<ul style="list-style-type: none"> • Already existing shunt passive filters applicable • Easy protection of active filter
Problems or issues	• Share compensation in frequency domain between active filter and passive filter	• Difficult to protect active filter against overcurrent	• No reactive power control
Present situation	• Commercial stage	• No reactive power control • A few practical applications	• Commercial stage

Such a combination of a shunt active filter and a shunt passive filter as shown in Fig. 14.47 has already been applied to harmonic compensation of naturally-commutated twelve-pulse cycloconverters for steel mill drives (Takeda et al., 1987). The passive filters absorb 11th and 13th harmonic currents while the active filter compensates for 5th and 7th harmonic currents and achieves damping of harmonic resonance between the supply and the passive filter. One of the most important considerations in system design is to avoid competition for compensation between the passive filter and the active filter.

The hybrid active filters, shown in Fig. 14.48 (Peng et al., 1990; Peng et al., 1993; Kawaguchi et al., 1997) and in Fig. 14.49 (Fujita and Akagi, 1991; Balbo et al., 1994; van Zyl et al., 1995), are right now on the commercial stage, not only for harmonic compensation but also for harmonic isolation between

supply and load, and for voltage regulation and imbalance compensation. They are considered prospective alternatives to pure active filters used alone. Other combined systems of active filters and passive filters or LC circuits have been proposed in Bhattacharya et al. (1997).

Classification by Power Circuit

There are two types of power circuits used for active filters; a voltage-fed PWM inverter (Akagi et al., 1986; Takeda et al., 1987) and a current-fed PWM inverter (Kawahira et al., 1983; van Schoor and van Wyk, 1987). These are similar to the power circuits used for AC motor drives. They are, however, different in their behavior because active filters act as nonsinusoidal current or voltage sources. The author prefers the voltage-fed to the current-fed PWM inverter because the voltage-fed PWM inverter is higher in efficiency and lower in initial costs than the current-fed PWM inverter (Akagi, 1994). In fact, almost all active filters that have been put into practical application in Japan have adopted the voltage-fed PWM inverter as the power circuit.

Classification by Control Strategy

The control strategy of active filters has a great impact not only on the compensation objective and required kVA rating of active filters, but also on the filtering characteristics in transient state as well as in steady state (Akagi et al., 1986).

Frequency-Domain and Time-Domain

There are mainly two kinds of control strategies for extracting current harmonics or voltage harmonics from the corresponding distorted current or voltage; one is based on the Fourier analysis in the frequency-domain (Grady et al., 1990), and the other is based on the Akagi-Nabae theory in the time-domain. The concept of the Akagi-Nabae theory in the time-domain has been applied to the control strategy of almost all the active filters installed by individual high-power consumers over the last ten years in Japan.

Harmonic Detection Methods

Three kinds of harmonic detection methods in the time-domain have been proposed for shunt active filters acting as a current source i_{AF} . Taking into account the polarity of the currents i_s , i_L and i_{AF} in Fig. 14.45 gives

$$\begin{aligned} \text{load-current detection:} \quad & i_{AF} = -i_{Lh} \\ \text{supply-current detection:} \quad & i_{AF} = K_S \cdot i_{Sh} \\ \text{voltage detection:} \quad & i_{AF} = K_V \cdot v_h. \end{aligned}$$

Note that load-current detection is based on feedforward control, while supply-current detection and voltage detection are based on feedback control with gains of K_S and K_V , respectively. Load-current detection and supply-current detection are suitable for shunt active filters installed in the vicinity of one or more harmonic-producing loads by individual consumers. Voltage detection is suitable for shunt active filters that will be dispersed on power distribution systems by utilities, because the shunt active filter based on voltage detection is controlled in such a way to present infinite impedance to the external circuit for the fundamental frequency, and to present a resistor with low resistance of $1/K_V$ [Ω] for harmonic frequencies (Akagi et al., 1999).

Supply-current detection is the most basic harmonic detection method for series active filters acting as a voltage source v_{AF} . Referring to Fig. 14.46 yields

$$\text{supply current detection:} \quad v_{AF} = G \cdot i_{Sh}.$$

The series active filter based on supply-current detection is controlled in such a way to present zero impedance to the external circuit for the fundamental frequency and to present a resistor with high

resistance of G [Ω] for the harmonic frequencies. The series active filters shown in Fig. 14.46 (Fujita and Akagi, 1997) and Fig. 14.48 (Peng et al., 1990) are based on supply current detection.

Integrated Series Active Filters

A small-rated series active filter integrated with a large-rated double-series diode rectifier has the following functions (Fujita and Akagi, 1997):

- harmonic compensation of the diode rectifier,
- voltage regulation of the common DC bus,
- damping of harmonic resonance between the commutation capacitors connected across individual diodes and the leakage inductors including the AC line inductors,
- reduction of current ripples flowing into the electrolytic capacitor on the common DC bus.

System Configuration

Figure 14.50 shows a harmonic current-free AC/DC power conversion system described below. It consists of a combination of a double-series diode rectifier of 5 kW and a series active filter with a peak voltage and current rating of 0.38 kVA. The AC terminals of a single-phase H-bridge voltage-fed PWM inverter are connected in “series” with a power line through a single-phase matching transformer, so that the combination of the matching transformers and the PWM inverters forms the “series” active filter. For small to medium-power systems, it is economically practical to replace the three single-phase inverters with a single three-phase inverter using six IGBTs. A small-rated high-pass filter for suppression of switching ripples is connected to the AC terminals of each inverter in the experimental system, although it is eliminated from Fig. 14.50 for the sake of simplicity.

The primary windings of the Y- Δ and Δ - Δ connected transformers are connected in “series” with each other, so that the combination of the three-phase transformers and two three-phase diode rectifiers forms the “double-series” diode rectifier, which is characterized as a three-phase twelve-pulse rectifier. The DC terminals of the diode rectifier and the active filter form a common DC bus equipped with an electrolytic capacitor. This results not only in eliminating any electrolytic capacitor from the active filter, but also in reducing current ripples flowing into the electrolytic capacitor across the common DC bus.

Connecting only a commutation capacitor C in parallel with each diode plays an essential role in reducing the required peak voltage rating of the series active filter.

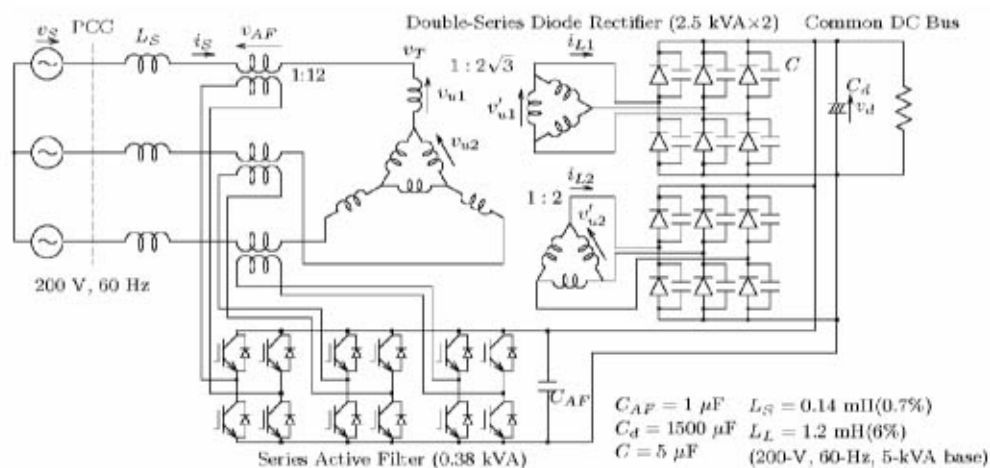


FIGURE 14.50 The harmonic current-free ac/dc power conversion system.

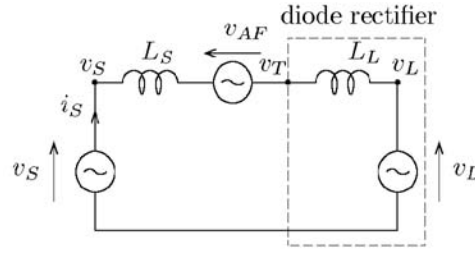


FIGURE 14.51 Single-phase equivalent circuit.

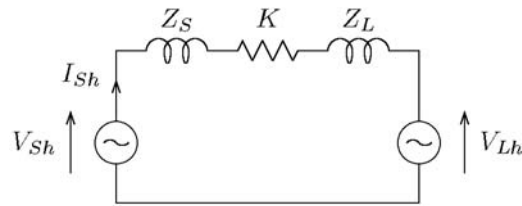


FIGURE 14.52 Single-phase equivalent circuit with respect to harmonics.

Operating Principle

Figure 14.51 shows an equivalent circuit for the power conversion system on a per-phase basis. The series active filter is represented as an AC voltage source v_{AF} , and the double-series diode rectifier as the series connection of a leakage inductor L_L of the transformers with an AC voltage source v_L . The reason for providing the AC voltage source to the equivalent model of the diode rectifier is that the electrolytic capacitor C_d is directly connected to the DC terminal of the diode rectifier, as shown in Fig. 14.50.

The active filter is controlled in such a way as to present zero impedance for the fundamental frequency and to act as a resistor with high resistance of K [Ω] for harmonic frequencies. The AC voltage of the active filter, which is applied to a power line through the matching transformer, is given by

$$v_{AF}^* = K \cdot i_{Sh} \quad (14.19)$$

where i_{Sh} is a supply harmonic current drawn from the utility. Note that v_{AF} and i_{Sh} are instantaneous values. Figure 14.52 shows an equivalent circuit with respect to current and voltage harmonics in Fig. 14.51. Referring to Fig. 14.52 enables derivation of the following basic equations:

$$I_{Sh} = \frac{V_{Sh} - V_{Lh}}{Z_S + Z_L + K} \quad (14.20)$$

$$V_{AF} = \frac{K}{Z_S + Z_L + K} (V_{Sh} - V_{Lh}) \quad (14.21)$$

where V_{AF} is equal to the harmonic voltage appearing across the resistor K in Fig. 14.51.

If $K \gg Z_S + Z_L$, Eqs. (14.20) and (14.21) are changed into the following simple equations.

$$I_{Sh} \approx 0 \quad (14.22)$$

$$V_{AF} \approx V_{Sh} - V_{Lh}. \quad (14.23)$$

Equation (14.22) implies that an almost purely sinusoidal current is drawn from the utility. As a result, each diode in the diode rectifier continues conducting during a half cycle. Equation (14.23) suggests that the harmonic voltage V_{Lh} , which is produced by the diode rectifier, appears at the primary terminals of the transformers in Fig. 14.50, although it does not appear upstream of the active filter or at the utility-consumer point of common coupling (PCC).

Control Circuit

Figure 14.53 shows a block diagram of a control circuit based on hybrid analog/digital hardware. The concept of the Akagi-Nabae theory (Akagi, 1983; Akagi, 1984) is applied to the control circuit implementation. The p-q transformation circuit executes the following calculation to convert the three-phase supply current i_{Su} , i_{Sv} , and i_{Sw} into the instantaneous active current i_p and the instantaneous reactive current i_q .

$$\begin{bmatrix} i_p \\ i_q \end{bmatrix} = \sqrt{\frac{2}{3}} \begin{bmatrix} \cos \omega t & \sin \omega t \\ -\sin \omega t & \cos \omega t \end{bmatrix} \begin{bmatrix} 1 & -1/2 & -1/2 \\ 0 & \sqrt{3}/2 & -\sqrt{3}/2 \end{bmatrix} \begin{bmatrix} i_{Su} \\ i_{Sv} \\ i_{Sw} \end{bmatrix}. \quad (14.24)$$

The fundamental components in i_{Su} , i_{Sv} , and i_{Sw} correspond to DC components in i_p and i_q , and harmonic components to AC components. Two first-order high-pass-filters (HPFs) with the same cut-off frequency of 10 Hz as each other extract the AC components \tilde{i}_p and \tilde{i}_q from i_p and i_q , respectively. Then, the p-q transformation/inverse transformation of the extracted AC components produces the following supply harmonic currents:

$$\begin{bmatrix} i_{Shu} \\ i_{Shv} \\ i_{Shw} \end{bmatrix} = \sqrt{\frac{2}{3}} \begin{bmatrix} 1 & 0 \\ -1/2 & \sqrt{3}/2 \\ -1/2 & -\sqrt{3}/2 \end{bmatrix} \begin{bmatrix} \cos \omega t & -\sin \omega t \\ \sin \omega t & \cos \omega t \end{bmatrix} \begin{bmatrix} \tilde{i}_p \\ \tilde{i}_q \end{bmatrix}. \quad (14.25)$$

Each harmonic current is amplified by a gain of K , and then it is applied to the gate control circuit of the active filter as a voltage reference v_{AF}^* in order to regulate the common DC bus voltage, v_{AF}^* is divided by the gain of K , and then it is added to \tilde{i}_p .

The PLL (phase locked loop) circuit produces phase information ωt which is a 12-bit digital signal of 60×2^{12} samples per second. Digital signals, $\sin \omega t$ and $\cos \omega t$, are generated from the phase information, and then they are applied to the p-q (inverse) transformation circuits. Multifunction in the transformation circuits is achieved by means of eight multiplying D/A converters. Each voltage reference, v_{AF}^* is compared with two repetitive triangular waveforms of 10 kHz in order to generate the gate signals for

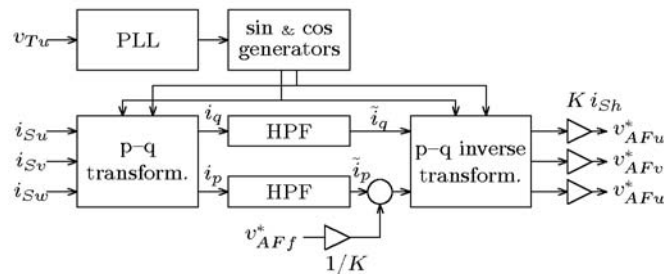


FIGURE 14.53 Control circuit for the series active filter.

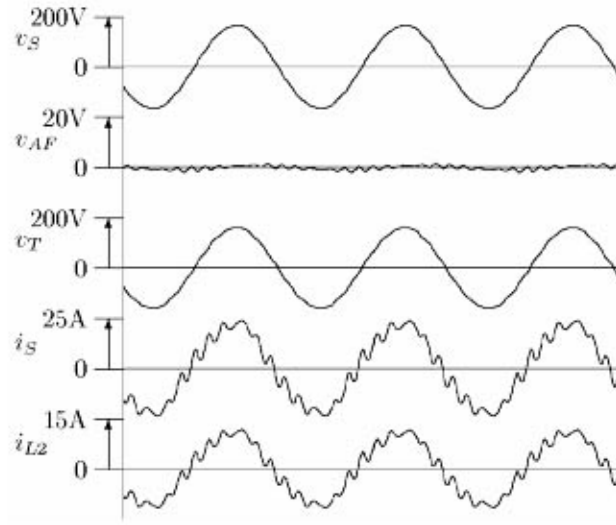


FIGURE 14.54 Experimental waveforms before starting the series active filter.

the IGBTs. The two triangular waveforms have the same frequency, but one has polarity opposite to the other, so that the equivalent switching frequency of each inverter is 20 kHz, which is twice as high as that of the triangular waveforms.

Experimental Results

In the following experiment, the control gain of the active filter, K , is set to 27Ω , which is equal to 3.3 p.u. on a 3 ϕ 200-V, 15-A, 60-Hz basis. Equation (14.20) suggests that the higher the control gain, the better the performance of the active filter. An extremely high gain, however, may make the control system unstable, and thereby a trade-off between performance and stability exists in determining an optimal control gain. A constant load resistor is connected to the common DC bus, as shown in Fig. 14.50.

Figures 14.54 and 14.55 show experimental waveforms, where a 5- μ F commutation capacitor is connected in parallel with each diode used for the double-series diode rectifier. Table 14.5 shows the THD of i_s and the ratio of each harmonic current with respect to the fundamental current contained in i_s . Before starting the active filter, the supply 11th and 13th harmonic currents in Fig. 14.54 are slightly magnified due to resonance between the commutation capacitors C and the AC line and leakage inductors, L_s and L_L . Nonnegligible amounts of 3rd, 5th, and 7th harmonic currents, which are so-called “non-characteristic current harmonics” for the three-phase twelve-pulse diode rectifier, are drawn from the utility.

Figure 14.55 shows experimental waveforms where the peak voltage of the series active filter is imposed on a limitation of ± 12 V inside the control circuit based on hybrid analog/digital hardware. Note that the limitation of ± 12 V to the peak voltage is equivalent to the use of three single-phase matching transformers with turn ratios of 1:20 under the common DC link voltage of 240 V. After starting the active filter, a sinusoidal current with a leading power factor of 0.96 is drawn because the active filter acts as a high resistor of 27Ω , having the capability of compensating for both voltage harmonics V_{sh} and V_{Lh} , as well as of damping the resonance. As shown in Fig. 14.55, the waveforms of i_s and v_T are not affected by the voltage limitation, although the peak voltage v_{AF} frequently reaches the saturation or limitation voltage of ± 12 V.

The required peak voltage and current rating of the series active filter in Fig. 14.55 is given by

$$3 \times 12^V / \sqrt{2} \times 15^A = 0.38 \text{ kVA}, \quad (14.26)$$

which is only 7.6% of the kVA-rating of the diode rectifier.

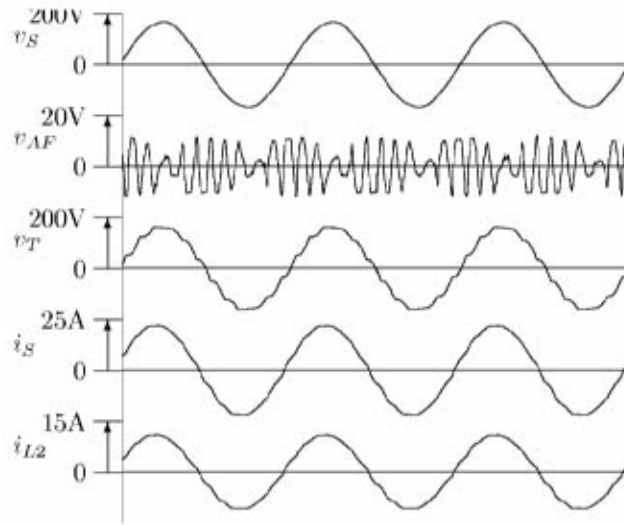


FIGURE 14.55 Experimental waveforms after starting the series active filter.

TABLE 14.5 Supply Current THD and Harmonics Expressed as the Harmonic-to-Fundamental Current Ratio [%], Where Commutation Capacitors of 5 μ F are Connected

	THD	3rd	5th	7th	11th	13th
Before (Fig. 14.54)	16.8	5.4	2.5	2.2	12.3	9.5
After (Fig. 14.55)	1.6	0.7	0.2	0.4	0.8	1.0

The harmonic current-free AC-to-DC power conversion system has both practical and economical advantages. Hence, it is expected to be used as a utility interface with large industrial inverter-based loads such as multiple adjustable speed drives and uninterruptible power supplies in the range of 1–10 MW.

Practical Applications of Active Filters for Power Conditioning

Present Status and Future Trends

Shunt active filters have been put into practical applications mainly for harmonic compensation, with or without reactive-power compensation. Table 14.6 shows ratings and application examples of shunt active filters classified by compensation objectives.

Applications of shunt active filters are expanding, not only into industry and electric power utilities but also into office buildings, hospitals, water supply utilities, and rolling stock. At present, voltage-fed

TABLE 14.6 Shunt Active Filters on Commercial Base in Japan

Objective	Rating	Switching Devices	Applications
Harmonic compensation with or without reactive/negative-sequence current compensation	10 kVA ~ 2 MVA	IGBTs	Diode/thyristor rectifiers and cycloconverters for industrial loads
Voltage flicker compensation	5 MVA ~ 50 MVA	GTO thyristors	Arc furnaces
Voltage regulation	40 MVA ~ 60 MVA	GTO thyristors	Shinkansen (Japanese “bullet” trains)

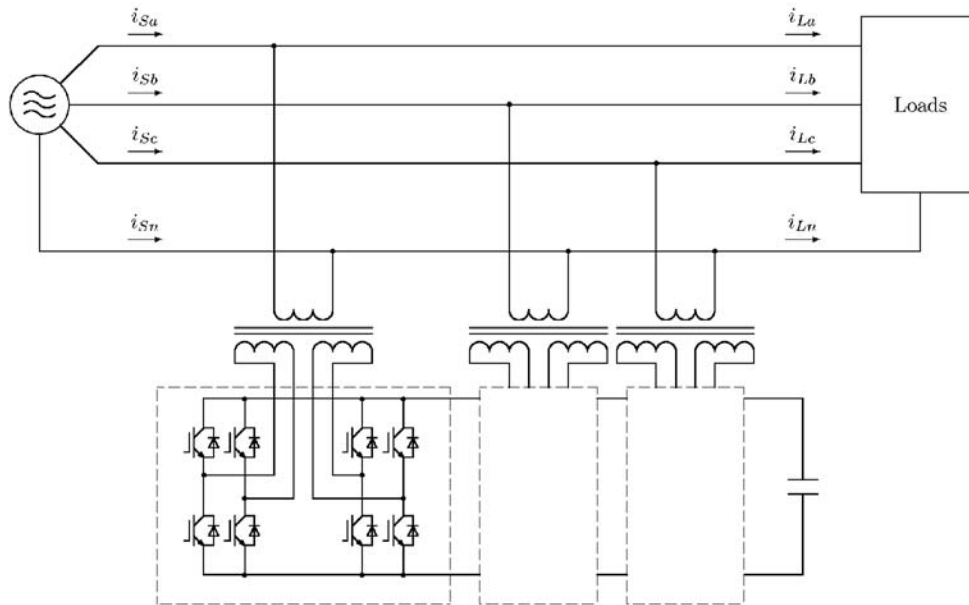


FIGURE 14.56 Shunt active filter for three-phase four-wire system.

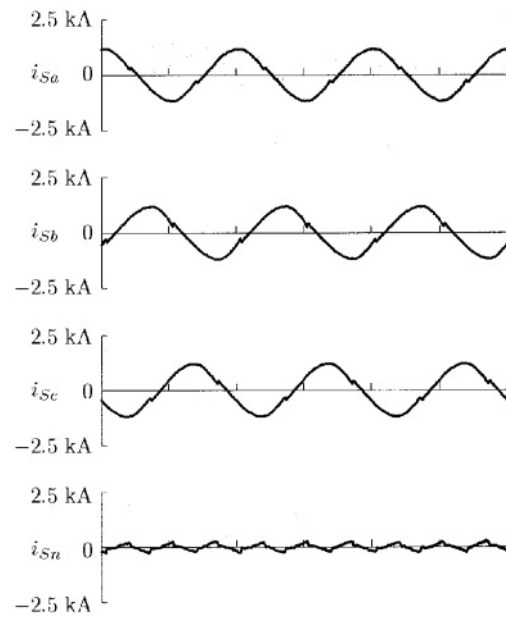
PWM inverters using IGBT modules are usually employed as the power circuits of active filters in a range of 10 kVA to 2 MVA, and DC capacitors are used as the energy storage components.

Since a combined system of a series active filter and a shunt passive filter was proposed in 1988 (Peng et al., 1990), much research has been done on hybrid active filters and their practical applications (Bhattacharya et al., 1997; Aredes et al., 1998). The reason is that hybrid active filters are attractive from both practical and economical points of view, in particular, for high-power applications. A hybrid active filter for harmonic damping has been installed at the Yamanashi test line for high-speed magnetically-levitated trains (Kawaguchi et al., 1997). The hybrid filter consists of a combination of a 5-MVA series active filter and a 25-MVA shunt passive filter. The series active filter makes a great contribution to damping of harmonic resonance between the supply inductor and the shunt passive filter.

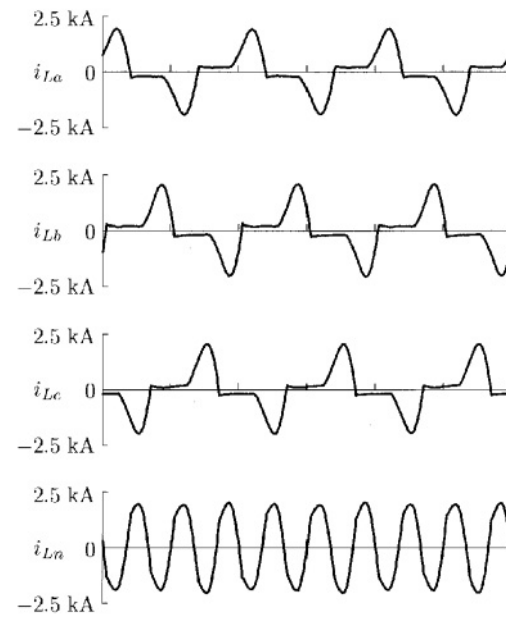
Shunt Active Filters for Three-Phase Four-Wire Systems

Figure 14.56 depicts the system configuration of a shunt active filter for a three-phase four-wire system. The 300-kVA active filter developed by Meidensha has been installed in a broadcasting station (Yoshida et al., 1998). Electronic equipment for broadcasting requires single-phase 100-V AC power supply in Japan, and therefore the phase-neutral rms voltage is 100 V in Fig. 14.56. A single-phase diode rectifier is used as an AC-to-DC power converter in an electronic device for broadcasting. The single-phase diode rectifier generates an amount of third-harmonic current that flows back to the supply through the neutral line. Unfortunately, the third-harmonic currents injected from all of the diode rectifiers are in phase, thus contributing to a large amount of third-harmonic current flowing in the neutral line. The current harmonics, which mainly contain the 3rd, 5th, and 7th harmonic frequency components, may cause voltage harmonics at the secondary of a distribution transformer. The induced harmonic voltage may produce a serious effect on other harmonic-sensitive devices connected at the secondary of the transformer.

Figure 14.57 shows actually measured current waveform in Fig. 14.56. The load currents, i_{La} , i_{Lb} , and i_{Lc} , and the neutral current flowing on the load side, i_{Ln} , are distorted waveforms including a large amount of harmonic current, while the supply currents, i_{Sa} , i_{Sb} , and i_{Sc} , and the neutral current flowing on the supply side, i_{Sn} , are almost sinusoidal waveforms with the help of the active filter.



(a) Supply currents.



(b) Load currents.

FIGURE 14.57 Actual current waveforms.

The 48-MVA Shunt Active Filter for Compensation of Voltage Impact Drop, Variation, and Imbalance

Figure 14.58 shows a power system delivering electric power to the Japanese “bullet trains” on the Tokaido Shinkansen. Three shunt active filters for compensation of fluctuating reactive current/negative-sequence current have been installed in the Shintakatsuki substation by the Central Japan Railway Company (Iizuka

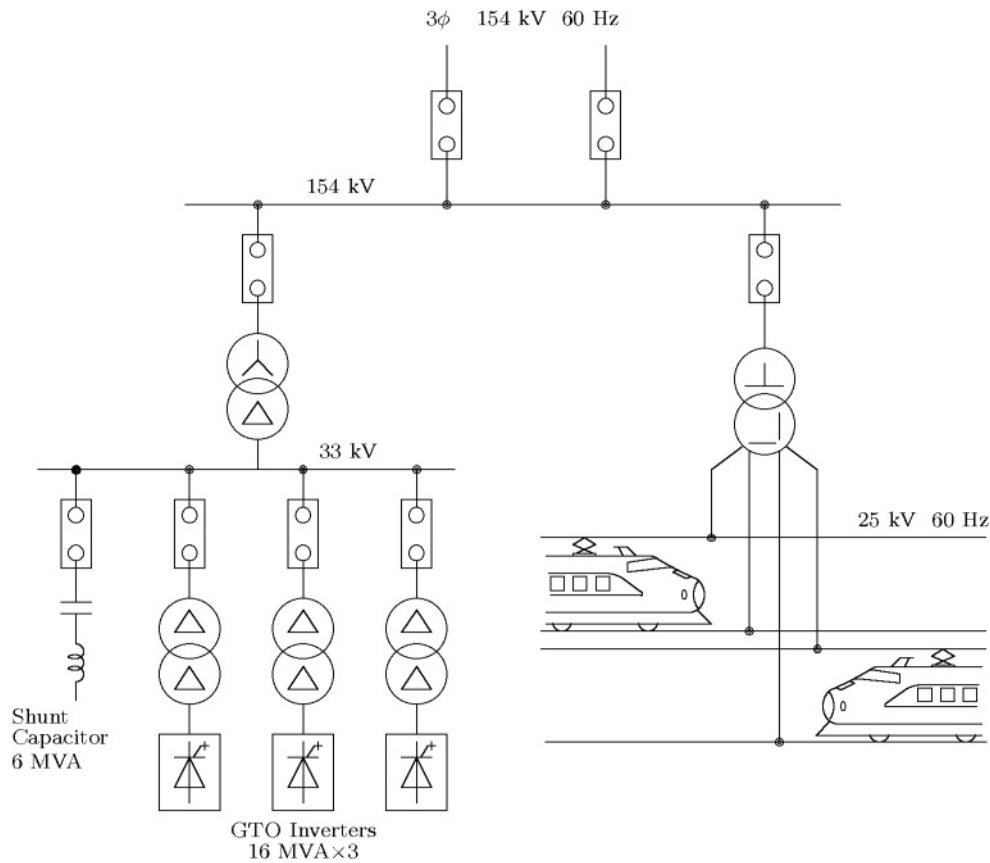


FIGURE 14.58 The 48-MVA shunt active filter installed in the Shintakatsuki substation.

et al., 1995). The shunt active filters, manufactured by Toshiba, consist of voltage-fed PWM inverters using GTO thyristors, each of which is rated at 16 MVA. A high-speed train with maximum output power of 12 MW draws unbalanced varying active and reactive power from the Scott transformer, the primary of which is connected to the 154-kV utility grid. More than twenty high-speed trains pass per hour during the daytime. This causes voltage impact drop, variation, and imbalance at the terminals of the 154-kV utility system, accompanied by a serious deterioration in the power quality of other consumers connected to the same power system. The purpose of the shunt active filters with a total rating of 48 MVA is to compensate for voltage impact drop, voltage variation, and imbalance at the terminals of the 154-kV power system, and to improve the power quality. The concept of the instantaneous power theory in the time-domain has been applied to the control strategy for the shunt active filter.

Figure 14.59 shows voltage waveforms on the 154-kV bus and the voltage imbalance factor before and after compensation, measured at 14:20–14:30 on July 27, 1994. The shunt active filters are effective not only in compensating for the voltage impact drop and variation, but also in reducing the voltage imbalance factor from 3.6 to 1%. Here, the voltage imbalance factor is the ratio of the negative to positive-sequence component in the three-phase voltages on the 154-kV bus. At present, several active filters in a range of 40 MVA to 60 MVA have been installed in substations along the Tokaido Shinkansen (Takeda et al., 1995).

Acknowledgment

The author would like to thank Meidensha Corporation and Toshiba Corporation for providing helpful and valuable information of the 300-kVA active filter and the 48-MVA active filter.

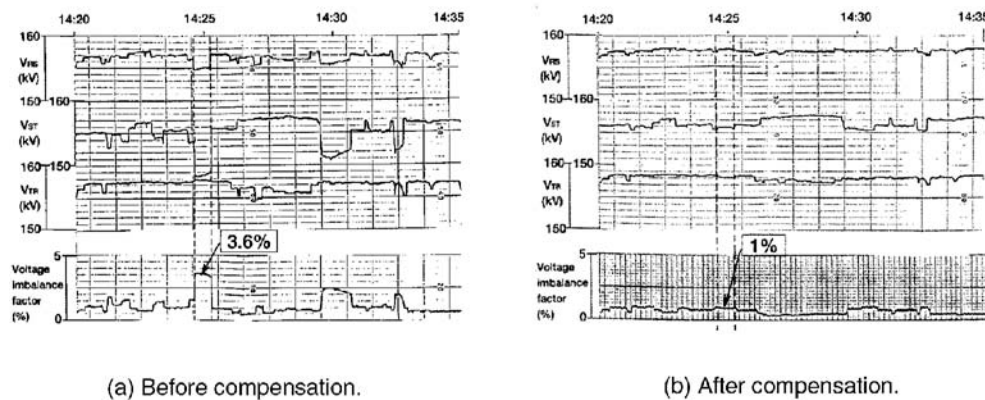


FIGURE 14.59 Installation effect.

References

- Akagi, H., New trends in active filters for power conditioning, *IEEE Trans. Ind. Appl.*, 32, 6, 1312–1322, 1996.
- Akagi, H., Trends in active power line conditioners, *IEEE Trans. Power Electronics*, 9, 3, 263–268, 1994.
- Akagi, H., and Fujita, H., A new power line conditioner for harmonic compensation in power systems, *IEEE Trans. Power Deliv.*, 10, 3, 1570–1575, 1995.
- Akagi, H., Fujita, H., and Wada, K., A shunt active filter based on voltage detection for harmonic termination of a radial power distribution line, *IEEE Trans. Ind. Appl.*, 35, 3, 638–645, 1999.
- Akagi, H., Kanazawa, Y., and Nabae, A., Generalized theory of the instantaneous reactive power in three-phase circuits, in *Proceedings of the 1983 International Power Electronics Conference*, Tokyo, Japan, 1983, 1375–1386.
- Akagi, H., Kanazawa, Y., and Nabae, A., Instantaneous reactive power compensators comprising switching devices without energy storage components, *IEEE Trans. Ind. Appl.*, 20, 3, 625–630, 1984.
- Akagi, H., Nabae, A., and Atoh, S., Control strategy of active power filters using multiple voltage-source PWM converters, *IEEE Trans. Ind. Appl.*, 22, 3, 460–465, 1986.
- Akagi, H., Tsukamoto, Y., and Nabae, A., Analysis and design of an active power filter using quad-series voltage-source PWM converters, *IEEE Trans. Ind. Appl.*, 26, 1, 93–98, 1990.
- Aredes, M., Heumann, K., and Watanabe, E. H., A universal active power line conditioner, *IEEE Trans. Power Delivery*, 13, 2, 545–551, 1998.
- Balbo, N., Penzo, R., Sella, D., Malesani, L., Mattavelli, P., and Zuccato, A., Simplified hybrid active filters for harmonic compensation in low voltage industrial applications, in *Proceedings of the 1994 IEEE/PES International Conference on Harmonics in Power Systems*, 1994, 263–269.
- Bhattacharya, S., Frank, T. M., Divan, D., and Banerjee, B., Active filter system implementation, *IEEE Industry Applications Magazine*, 4, 5, 47–63, 1998.
- Bhattacharya, S., Cheng, P., and Divan, D., Hybrid solutions for improving passive filter performance in high power applications, *IEEE Trans. Ind. Appl.*, 33, 3, 732–747, 1997.
- Bird, B. M., Marsh, J. F., and McLellan, P. R., Harmonic reduction in multiple converters by triple-frequency current injection, *IEEE Proceedings*, 116, 10, 1730–1734, 1969.
- Fujita, H., and Akagi, H., An approach to harmonic current-free AC/DC power conversion for large industrial loads: The integration of a series active filter and a double-series diode rectifier, *IEEE Trans. Ind. Appl.*, 33, 5, 1233–1240, 1997.
- Fujita, H., and Akagi, H., A practical approach to harmonic compensation in power systems—Series connection of passive and active filters, *IEEE Trans. Ind. Appl.*, 27, 6, 1020–1025, 1991.

- Fujita, H., and Akagi, H., The unified power quality conditioner: The integration of series- and shunt-active filters, *IEEE Trans. Power Electronics*, 13, 2, 315–322, 1998.
- Grady, W. M., Samotyj, M. J., and Noyola, A. H., Survey of active power line conditioning methodologies, *IEEE Trans. Power Deliv.*, 5, 3, 1536–1542, 1990.
- Gyugyi, L., and Strycula, E. C., Active AC power filters, in *Proceedings of the 1976 IEEE/IAS Annual Meeting*, 1976, 529–535.
- Iizuka, A., Kishida, M., Mochinaga, Y., Uzuka, T., Hirakawa, K., Aoyama, F., and Masuyama, T., Self-commutated static var generators at Shintakatsuki substation, in *Proceedings of the 1995 International Power Electronics Conference*, Yokohama, Japan, 1995, 609–614.
- Kawaguchi, I., Ikeda, H., Ogihara, Y., Syogaki, M., and Morita, H., Novel active filter system composed of inverter bypass circuit for suppression of harmonic resonance at the Yamanashi maglev test line, in *Proceedings of the IEEE-IEEE/IAS Power Conversion Conference*, 175–180, 1997.
- Kawahira, H., Nakamura, T., Nakazawa, S., and Nomura, M., Active power filters, in *Proceedings of the 1983 International Power Electronics Conference*, Tokyo, Japan, 1983, 981–992.
- Krah, J. O., and Holtz, J., Total compensation of line-side switching harmonics in converter-fed AC locomotives, in *Proceedings of the 1994 IEEE/IAS Annual Meeting*, 1994, 913–920.
- Lêe, T.-N., Pereira, M., Renz, K., and Vaupel, G., Active damping of resonances in power systems, *IEEE Trans. Power Deliv.*, 9, 2, 1001–1008, 1994.
- Moran, S., A line voltage regulator/conditioner for harmonic-sensitive load isolation, in *Proceedings of the 1989 IEEE/IAS Annual Meeting*, 947–951, 1989.
- Peng, F. Z., Application issues of active power filters, *IEEE Industry Application Magazine*, 4, 5, 21–30, 1998.
- Peng, F. Z., Akagi, H., and Nabae, A., Compensation characteristics of the combined system of shunt passive and series active filters, *IEEE Trans. Ind. Appl.*, 29, 1, 144–152, 1993.
- Peng, F. Z., Akagi, H., and Nabae, A., A new approach to harmonic compensation in power systems—A combined system of shunt passive and series active filters, *IEEE Trans. Ind. Appl.*, 26, 6, 983–990, 1990.
- Peng, F. Z., Akagi, H., and Nabae, A., A study of active power filters using quad-series voltage-source PWM converters for harmonic compensation, *IEEE Trans. Power Electronics*, 5, 1, 9–15, 1990.
- Van Schoor, G., and van Wyk, J., A study of a system of a current-fed converters as an active three-phase filter, in *Proceedings of the 1987 IEEE/PELS Power Electronics Specialist Conference*, 482–490, 1987.
- Takeda, M., Murakami, S., Iizuka, A., Kishida, M., Mochinaga, Y., Hase, S., and Mochinaga, H., Development of an SVG series for voltage control over three-phase unbalance caused by railway load, in *Proceedings of the 1995 International Power Electronics Conference*, Yokohama, Japan, 1995, 603–608.
- Takeda, M., Ikeda, K., and Tominaga, Y., Harmonic current compensation with active filter, in *Proceedings of the 1987 IEEE/IAS Annual Meeting*, 808–815, 1987.
- Watanabe, E. H., Series active filter for the DC side of HVDC transmission systems, in *Proceedings of the 1990 International Power Electronics Conference*, Tokyo, Japan, 1024–1030, 1990.
- Yoshida, T., Nakagawa, G., Kitamura, H., and Iwatani, K., Active filters (multi-functional harmonic suppressors) used to protect the quality of power supply from harmonics and reactive power generated in loads, *Meiden Review*, 262, 5, 13–17, 1998 (in Japanese).
- Zhang, W., Asplund, G., Åberg, A., Jonsson, U., and Löf, O., Active DC filter for HVDC system—A test installation in the Konti-Skan at Lindome converter station, *IEEE Trans. Power Deliv.*, 8, 3, 1599–1605, 1993.
- Van Zyl, A., Enslin, J. H. R., and Spée, R., Converter based solution to power quality problems on radial distribution lines, in *Proceedings of the 1995 IEEE/IAS Annual Meeting*, 2573–2580, 1995.